Prostate Specific Membrane Antigen (PSMA) Targeting Polymer-Peptide Conjugates

by

Simbarashe Jokonya

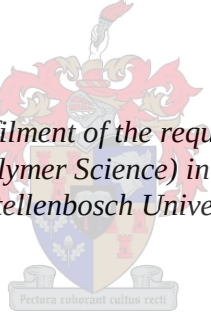

Thesis presented in fulfilment of the requirements for the degree of Master of Science (Polymer Science) in the Faculty of Science at Stellenbosch University

Supervisor: Prof. Bert Klumperman
Co-supervisor: Dr Rueben Pfukwa
Co-supervisor: Prof. Marina Rautenbach

March 2017

Declaration

By submitting this thesis electronically, I declare that the entirety of the work contained therein is my own, original work, that I am the sole author thereof (save to the extent explicitly otherwise stated), that reproduction and publication thereof by Stellenbosch University will not infringe any third party rights and that I have not previously in its entirety or in part submitted it for obtaining any qualification.

March 2017

Abstract

The primary objective of the study was the development of a polymeric drug delivery system targeting prostate specific membrane antigen (PSMA) by employing amphiphilic poly(*N*-vinylpyrrolidone) (PVP) as a drug delivery vehicle and tyrothricin as an anti-tumour agent.

Three xanthate based reversible addition-fragmentation chain-transfer (RAFT) agents were synthesised, namely: α-succinimide ω-xanthate, α-hydroxyl ω-xanthate, and α-acetal ω-xanthate. The RAFT agents were subsequently employed in the polymerisation of *N*-vinylpyrrolidone to form α- and ω-heterotelechelic PVP. The α-acetal ω-xanthate heterotelechelic PVP system was selected because of its ability to form aldehyde and thiol/disulphide functionalities on the α- and ω-chain ends respectively in a one pot deprotection strategy. The deprotected PVP was conjugated to a model ligand through Schiff base and reductive animation via the *N*-terminus and a model drug via thiol-ene Michael addition.

Successful conjugation of model compounds was followed by a five stage synthesis of a glutamate urea based PSMA targeting small molecule ligand starting with L-lysine. The targeting ligand was subsequently conjugate to the α-chain end of PVP via the *N*-terminus. Tyrothricin was purified to remove erythrocyte haemolytic linear gramicidin and modified to introduce acrylate on the L-lysine and L-ornithine residues. Conjugation to PVP via an acid labile β-thiopropionamide was achieved through thiol-ene Michael addition. The resultant drug delivery construct was self-assembled into micellar structures and particle diameter was determined by dynamic light scattering (DLS); z average 151 d.nm and confirmed by scanning transmission electron microscopy (STEM). The release studies were done by dissolving the conjugates in formic acid solutions of pH = 5.5 and 3.0. Real time analysis on an ultra-performance liquid chromatography coupled to a mass spectrometer detector (UPLC-MS) was done by monitoring tyrothricin release over 24 hours. Tyrothrin was not detected after 24 hours leading to the conclusion that the amide bond was too strong to be destabilised by the β-thio ether in a similar way to the ester.

Opsomming

Die primêre doel van die studie was om 'n polimeriese dwelmvervoerstelsel te ontwikkel wat fokus op ‘n prostaatspesifieke membraanantigeen (PSMA) deur die amfifiliese polivinielpirrolidoon as die dwelmafleweringsvoertuig en tirotrisien as die anti-kankermiddel te gebruik.

Drie xantaat-gebaseerde omkeerbare addisie-fragmentasie kettingoordrag (OAFO) agente is gesintetiseer; α- succinimide ω- xantaat, α- hidroksiel ω- xantaat, en α- asetaal ω- xantaat. Die OAFO agente is daarna gebruik in die polimerisasie van *N*-Vinielpirrolidoon om α- en ω-heterotelecheliese polivinielpirrolidoon (PVP) te vorm. Die α- asetaal ω- xantaat heterotelecheliese PVP stelsel is gekies omdat dit onderskeidelik aldehiede en tiol/disulfied funksionelegroepe op die α- en ω- eindkettings vorm in 'n een-pot-sintese om die beskermings groepe te verwyder. Die beskermde PVP was gekonjugeerd aan ‘n modelligand deur Schiff basis en reduktiewe aminasie via die *N*-terminus en aan 'n modeldwelm via tiol-een Michael addisie.

Suksesvolle konjugasie van die modelverbindings was gevolg deur 'n vyf stap sintese van 'n glutamaat ureum gebaseerde PSMA wat kleinmolekuul ligande teiken. Die ligand wat ‘n teiken sal bereik is daarna gekonjugeerd aan die α-eindketting van PVP via die *N*-terminus. Tirotrisien is gesuiwer om eritrosiet-hemolitiese-lineêre-gramisidien te verwyder en is daarna gemodifiseer om akrielaat funksionelegroepe aan die L-Lisien en L-ornitien te heg. Konjugasie aan die PVP via 'n suurlabiele β-tiopropionaatamied is bereik deur ‘n tiol-een Michael addisie. Die gevolglike geneesmiddelafleweringssisteem het miselstrukure gevorm tydens selfaddisie en deeltjiegrootte is bepaal deur skanderingtransmissie-elektronmikroskopie (STEM) en dinamieseligverspreiding (DLV); z gemiddelde 151 d.nm. Die vrystellingsstudies is gedoen deur die gekonjugeerdesisteem op te los in mieresuuroplossings van pH = 5.5 en 3.0. Regstreeksetydanalise op ‘n ultra-prestasie-vloeistofchromatograaf wat gekoppel is aan 'n massaspektrometerdetektor (UPLC-MS) is gedoen om tirotrisienvrylating oor ‘n tydperk van 24 uur te bestudeer. Tirotrisienvrylating is nie waargeneem na 24 uur nie. Dit lei tot die gevolgtrekking dat die amiedbinding te sterk was om gedestabiliseer te word deur die tiol.

Acknowledgements

Firstly, I would like to thank God the Father of my Lord Jesus Christ for the wonderful opportunity to study towards this degree.

I want to take this opportunity to thank and acknowledge the National Research Foundation (NRF) for the funding that was channelled towards this study. I am grateful to my supervisor, Prof. Bert Klumperman for granting me the opportunity to work in his group, for the funding as well as his invaluable guidance during the course of the study. I would also want to thank my co-supervisors, Dr. Rueben Pfukwa for his guidance and encouragement that kept the optimism even in the darkest periods. I would like to extent my gratitude to my co-supervisor from biochemistry, Prof. Marina Rautenbach for her advice, dedication towards my work and the hours she spent with me in the lab as well as working through the data.

I extent my gratitude to past and present free radical colleagues with special mention to Anna Kargaard, Paul Reader, Nusrat Begum for the help they afforded me as I was still trying to find my feet and throughout the period of my study. I would also like to thank the staff and support staff of Polymer Science as well as the Biopep Peptide group in Biochemistry.

I would like to thank the Central Analytical Facilities staff particularly Elsa Malherbe and Jaco Brand for NMR analysis, Malcolm Taylor and Marietjie Stander for assistance with the UPLC-MS analysis

On a personal level, I would like to thank my family for the support and encouragement as well as my friends and girlfriend, Tapiwa. Above all I want to thank and dedicate the work and effort to my late father, Charles Jokonya, who succumbed to colon cancer in October 2015.

Table of Contents

List of figures

List of schemes

List of tables

List of acronyms

ACP	Anticancer peptides
AIBN	2,2'-Azobis(isobutyronitrile)
AMP	Antimicrobial peptides
ATRP	Atom transfer radical polymerisation
BHT	2,6-Di-*tert*-butyl-4-methylphenol
CRP	Controlled radical polymerisation
CSIRO	Common Wealth Scientific and Industrial Research Organisation
CTA	Chain-transfer agent
CuAAC	Copper-catalysed alkyne azide 1,3-dipolar cycloaddition
DLS	Dynamic light scattering
DMAc	*N*,*N*-Dimethylacetamide
DP	Degree of polymerisation
DRI	Differential refractive index
EPR	Enhanced permeability and retention
FDA	Food and drug administration
L-Lys	L-lysine
L-Orn	L-ornithine
L-Tyr	L-tyrosine
LCST	Lower critical solution temperature
MaxEnt	Maximum Entropy
MWCO	Molecular weight cut-off
NMR	Nuclear magnetic resonance
*N*VP	*N*-Vinylpyrrolidone
ODN	Oligodeoxynucleotide

PAAc	Polyacrylic acid
PAAm	Polyacrylamide
PEG	Polyethylenegylcol
PS	Phospholipid phosphatidylserine
PSMA	Prostate specific membrane antigen
PVP	Polyvinylpyrrolidone
r.t	Room temperature
RAFT	Reversible addition-fragmentation chain-transfer
RDRP	Reversible deactivation radical polymerisation
SEC	Size exclusion chromatography
STEM	Scanning transmission electron microscope
TCEP	Tris(2-carboxyethyl)phosphine hydrochloride
TLC	Thin layer chromatography
Trc	Tyrocidine
Tpc	Tryptocidine
UPLC-MS	Ultra performance liquid chromatography linked to electrospray mass spectrometry
ESIMS	Electrospray ionisation mass spectroscopy
VGA	Val-gramicidin A

1 Prologue

1.1 Introduction

Cancer is known to kill more people than malaria, tuberculosis and HIV combined.[1] Despite recent advances in treatment strategies, as high as 10 million people are thought to be diagnosed with cancer every year, and it is estimated that over half live in the developed world. In these parts of the world, cancer incidence has been able to reach pandemic proportions.[1] According to Balmain *et al.*, all forms of cancer are characterised by abnormal cell growth resulting from small numbers of environmentally induced and inherited gene mutations.[2] This results in cells that have the ability to generate their own growth signals and respond to weak signals that are ignored by healthy cells. Other important traits include; insensitivity to anti-proliferative signals, resistance to apoptosis, capacity to replicate exponentially, ability to form new blood vessels allowing for tumour growth and crucially, the capacity to invade tissues.[3]

Many treatment options have been explored in the fight against cancer for example surgical removal, radiation therapy with combination chemotherapy normally employed as a secondary treatment option.[4-5] The increased incidence of many cancers including colon, breast, skin, kidney and prostate coupled by the limitations of chemotherapy has led to a pressing need to develop new drug delivery mechanisms. Chemotherapy is known to be effective for relatively short periods of times. In most cases, not exceeding two years. Moreover, it is highly non-selective with deleterious side effects and the drugs are poorly soluble in the physiological environment.[4, 6]

The key to improving the chances of survival for cancer patients rests on the cancer being detected early. In the case of prostate cancer, patients with early stage disease have encouraging 5 year prognoses of almost 100 percent survival. However, patients in which the disease has metastasised show significant reductions of survival rates that drop to as low as 30 percent.[6-9]

Active targeting entails the employing of conjugated targeting ligands that enhance the specific delivery of polymeric drug delivery systems. The increase in the site specificity as well as internalisation can subsequently improve the activity whilst decreasing the chances of the occurrence of side effects that are normally associated with cancer therapy.[10,11] In the case of prostate cancer, prostate specific membrane antigen (PSMA) has long been established to be a viable target. It is a highly prostate restricted type II transmembrane glycoprotein (also called carboxypeptidase glutamate II) that is overexpressed in prostate cancer cells, about 100 to 1000-fold higher than in

moderately expressed normal tissues; and numerous studies have reported that normal prostate tissue predominantly expresses a splice variant that does not contain the transmembrane domain (PSM).[4, 6, 12] Most importantly, it has been shown that PSMA is not present on normal vasculature.[12-13] The incorporation of targeting moieties and therapeutic payloads orthogonally onto biocompatible polymer chains has led to supramolecular drug delivery systems normally referred to as polymer-protein and polymer-drug conjugates.[14] Such systems have the ability to shield the drug from the immune system and physiological environment until it reaches the target after which a physiological stimulus can trigger the release of the therapeutic payload.[15]

One *in vivo* stimulus that has been employed to trigger responsive release of drugs is the low pH of endosomal compartments in cells (pH = 5.5). This has normally been exploited by having therapeutic agents bonded to the polymer system by acid labile linkers. Active targeting normally results in binding at cell membrane of the target which allows the drug delivery construct to enter the cell and then the endosome via receptor mediated endocytosis. In the endosome rapid degradation of the acid labile linkages within the low pH environment results in the consequent site specific release of the therapeutic agent.[16] This thesis focusses on the development of a targeted polymeric drug delivery system for prostate cancer, comprising of a hydrophilic poly(*N*-vinylpyrrolidone) (PVP) segment conjugated to tyrothricin through an acid labile linker, self-assembled in water to form micellar structures. The construct is sparsely decorated with a PSMA targeted ligand.

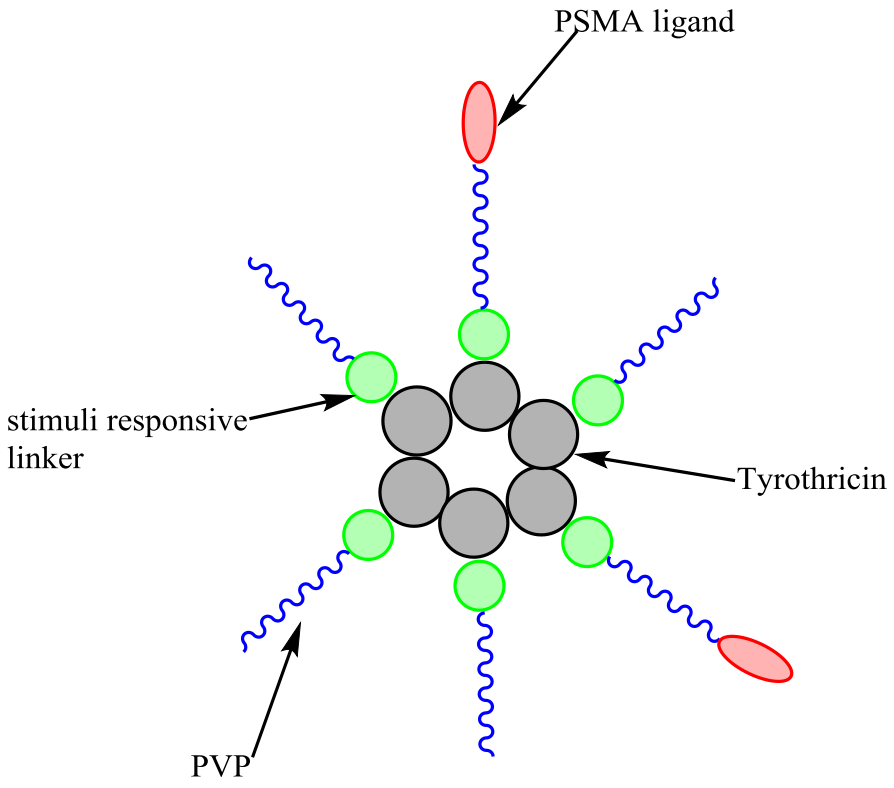

Figure 1.1: Schematic representation of a self-assembled PVP-tyrothrin-PSMA ligand drug delivery system.

1.2 Aims and objectives

1. To synthesize α- and, ω heterotelechelic PVP via reversible addition fragmentation chain transfer (RAFT) mediated polymerisation.
2. To develop robust, efficient and orthogonal facile post polymerisation modification techniques and conjugate the α- and ω-chain end functionalities to a model drug and model ligand.
3. To synthesise a glutamate urea, PSMA targeting ligand and conjugate it to the α-chain end of the PVP via the *N*-terminus along with a fluorescent marker.
4. To modify the tyrothricin mixture and conjugate it to the ω-chain end of PVP and subsequently self-assemble the construct into micelles
5. To study the ease of release of the tyrothricin under a pH stimulus and subsequently study the targeting efficiency and activity of the drug delivery construct.

1.3 Outline of thesis

Chapter 1 – Prologue

The chapter gives a brief introduction to cancer and briefly discusses the shortcomings of the current treatment strategies. It offers an insight into the alternative active targeting polymeric drug delivery systems that form the basis of this study. The aims and objectives of the study are outlined.

Chapter 2 – Literature review

Chapter 2 gives an in-depth theoretical background in which history and developments in reversible deactivation radical polymerisation (RDRP) are critically discussed. The robust, efficient and orthogonal chemistries that result in facile introduction of functional handles post polymerisation are also assessed. The final part of the review focuses on polymeric drug delivery systems' specificity and mechanisms of drug release.

Chapter 3 – Synthesis and characterisation of poly(*N*-vinylpyrrolidone)

This chapter addresses the role of the chain transfer agents in not only the control of polymerisation, but also the subsequent post polymerisation reactions. The importance of polymer characterisation in determining the retention of α- and ω-chain end functionalities is highlighted.

Chapter 4 – PVP chain end functionalisation, target ligand synthesis and ligand conjugation

The chapter addresses the different strategies necessary to introduce the aldehyde functionality to the α-chain end of heterotelechelic PVP. Additionally the synthesis of the PSMA ligand is discussed followed by reductive amination conjugation to the *N*-terminus.

Chapter 5 - Tyrocidine PVP PSMA targeting conjugates

The chapter describes model drug conjugation with the view of optimising the conditions for conjugation to the expensive therapeutic agent. PVP – tyrocidine conjugates are synthesised and subsequently self-assembled into micelles. The particle size of the conjugates was determined after which the release studies were done.

Chapter 6 – Epilogue

The chapter gives conclusions of the as well as gives recommendations for future work.

1.4 References

(1) Moten, A.; Schafer, D.; Ferrari, M., *J.Glob.Health* **2014**, 4, 010304.

(2) Balmain, A.; Barrett, J. C.; Moses, H.; Renan, M. J., *Mol. Carcinog.* **1993**, 7, 139.

(3) Hanahan, D.; Weinberg, R. A., *Cell* **2000**, 100, 57.

(4) Huang, B.; Otis, J.; Joice, M.; Kotlyar, A.; Thomas, T. P., *Biomacromolecules* **2014**, 15, 915.

(5) Karan, D.; Holzbeierlein, J. M.; Van Veldhuizen, P.; Thrasher, J. B., *Nat. Rev. Urol.* **2012**, 9, 376.

(6) Pearce, A. K.; Rolfe, B. E.; Russell, P. J.; Tse, B. W. C.; Whittaker, A. K.; Fuchs, A. V.; Thurecht, K. J., *Polym. Chem.* **2014**, 5, 6932.

(7) Crawford, E. D.; Eisenberger, M. A.; McLeod, D. G.; Spaulding, J. T.; Benson, R.; Dorr, F. A.; Blumenstein, B. A.; Davis, M. A.; Goodman, P. J., *N. Engl. J. Med.* **1989**, 321, 419.

(8) Eisenberger, M. A.; Blumenstein, B. A.; Crawford, E. D.; Miller, G.; McLeod, D. G.; Loehrer, P. J.; Wilding, G.; Sears, K.; Culkin, D. J.; Thompson Jr, I. M., *N. Engl. J. Med.* **1998**, 339, 1036.

(9) Ferlay, J.; Autier, P.; Boniol, M.; Heanue, M.; Colombet, M.; Boyle, P., *Ann. Oncol.* **2007**, 18, 581.

(10) Byrne, J. D.; Betancourt, T.; Brannon-Peppas, L., *Adv. Drug Deliv. Rev.* **2008**, 60, 1615.

(11) Wang, M.; Thanou, M., *Pharmacol. Res.* **2010**, 62, 90.

(12) Ghosh, A.; Heston, W. D., *J. Cell. Biochem.* **2004**, 91, 528.

(13) Silver, D. A.; Pellicer, I.; Fair, W. R.; Heston, W.; Cordon-Cardo, C., *Clin. Cancer. Res.* **1997**, 3, 81.

(14) Haag, R.; Kratz, F., *Angew. Chem. Int. Ed.* **2006**, 45, 1198.

(15) Schmaljohann, D., *Adv. Drug Deliv. Rev.* **2006**, 58, 1655.

(16) Binauld, S.; Stenzel, M. H., *J. Chem. Soc., Chem. Commun.* **2013**, 49, 2082.

2 Literature review

2.1 Introduction

A good number of therapeutic drugs currently used, particularly in cancer therapy, are poorly soluble in the aqueous, physiological environment. This poor solubility results in a low concentration of drug reaching the internalised target sites. This results in poor bioavailability and poor pharmacokinetics. Apart from that, there are drug toxicity issues that arise as a result from off target release, as higher doses need to be administered to circumvent the solubility problems. The versatility of biocompatible, aqueous soluble polymers synthesised via reversible deactivation radical polymerisation allows for conjugation to the drugs, imaging modalities and target ligands, post polymerisation, through facile chain end modification that results in polymeric drug delivery constructs with improved pharmacokinetics and reduced drug toxicity. More importantly, it also lowers the drug dose that has to be administered to the patients. The challenge, however, lies in careful design of these conjugated systems, whereby the overall goal is optimum therapeutic efficiency with minimal side effects.

2.2 Controlled Radical Polymerisation

Living anionic polymerisation was discovered in the mid-twentieth century by Michael Szwarc. Since then it has contributed significantly to polymer chemistry.[1] Controlled radical polymerisation, which has been termed living radical polymerisation, and more recently reversible deactivation radical polymerisation, was developed to address the short comings of conventional free radical polymerisations. However, authors have tended to come up with different terminologies.[2] According to the IUPAC recommendations of 2010, controlled radical or living radical polymerisation has been termed reversible deactivation radical polymerisation (RDRP).[2] These techniques are characterised by fast initiation, propagating species and dormant species with the overall goal of minimising chain breaking events. Chain breaking events, e.g. transfer and termination, lead to the loss of the living character resulting in the broadening of molecular weight distributions.[3]

Many authors have demonstrated that certain additives are capable of reversibly reacting with the chain carriers. Because of the reversibility of the reaction, the period that an individual propagating chain grows can be extended to the time frame of the experiment. However, for most of the time, the chains remain inactive and are not able to take part in chain growth or chain termination. Consequently, polymerisation conditions are chosen such that the majority of the chains are living.[4] It is important to note that chain breaking events are inherent to all radical polymerisation processes,

however, with the careful selection of reagents and reaction conditions, chain termination and reversible chain transfer can be significantly minimised.[5]

When classifying the different RDRP techniques, a distinction is made between systems that are based on a persistent radical effect (PRE),[6-8] and systems based on degenerative transfer.[8] The generic name, stable free radical polymerisation, was coined for systems based on the persistent radical effect.[9] In systems based on the PRE, a steady state of growing radicals is set up via the activation–deactivation process rather than initiation–termination, as is the case in conventional radical polymerisation. These systems comprise of nitroxide mediated polymerisation (NMP),[10] and cobalt mediated radical polymerisation.[11] Atom transfer radical polymerisation (ATRP)[12-13] is also based on the PRE, but it is a catalytic process. The systems based on degenerative transfer are iodine transfer,[14] reversible addition fragmentation chain transfer (RAFT),[15-16] organotellurium[17] and organostibine mediated polymerisation.[18] In this study emphasis will be placed on RAFT.

2.2.1 RAFT Mediated Polymerisation

Reversible addition fragmentation chain transfer (RAFT) process is based on degenerative chain transfer. It was first reported in Melbourne Australia, by a team researchers in 1998. These researchers were part of the Common Wealth Scientific and Industrial Research Organisation (CSIRO) group. It is controlled by a reversible chain transfer mechanism.[19] Since it was first reported it has grown to become a powerful tool in the construction of complex macromolecular structures.[20]

According to Coote *et al.*, RAFT relies upon a kinetic grand design in determining controlled architectures and molecular weights of resultant polymers. Since the radical terminations cannot be entirely eliminated, their frequency is instead significantly reduced with respect to the number of growing chains by trapping the polymeric radical reversibly as a dormant species.[21] In RAFT mediated polymerisation, this is accomplished by employing thiocarbonyl thio compounds that are termed RAFT agents.[22] The addition of the propagating radical to the thiocarbonyl sulphur centre of the RAFT agent produces an intermediate carbon centred radical. The carbon centred radical readily undergoes β scission to either reform the propagating radical or to liberate a new carbon centred radical (the leaving group). The RAFT mechanism in Schemes 2.1 and 2.2 was described in a scheme by Coote *et al.*[21]

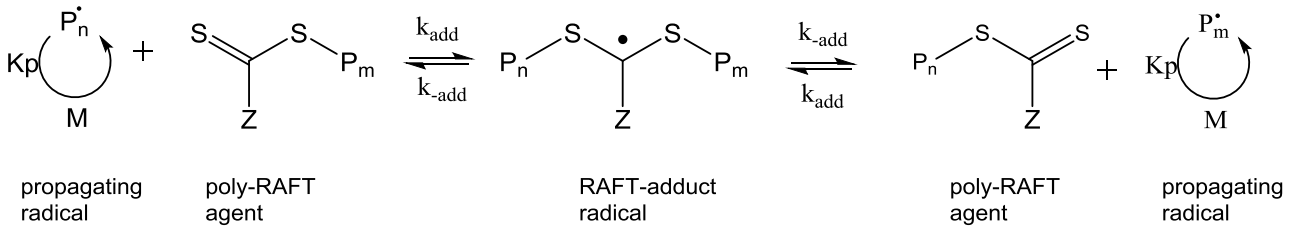

Scheme 2.1: RAFT polymerisation mechanism (I)

The selection of the R group of the RAFT agent is such that it undergoes β scission from the RAFT adduct radical in preference to the propagating species, but is still capable of reinitiating polymerisation.[21] As a result, there is swift conversion of the initial RAFT agent (**S=C (Z) SR)** to more propagating species until, there is a symmetrical equilibrium established between the propagating radical and the dormant poly-RAFT (Scheme 2.2).

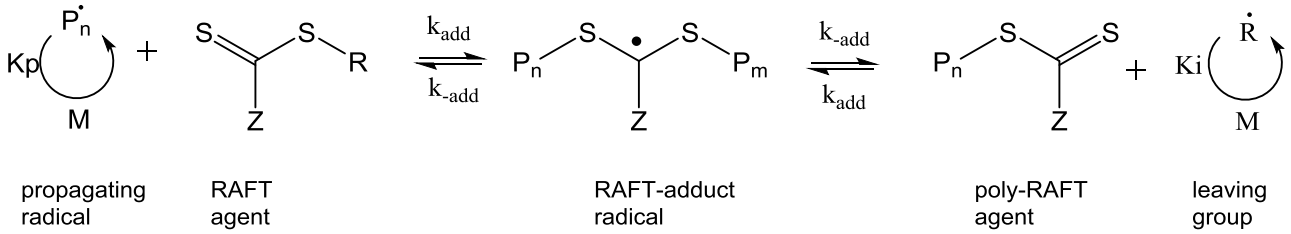

Scheme 2.2: RAFT polymerisation mechanism (II)

The CSIRO group concluded that through this mechanism, polymers with predictable molecular weights and low dispersities could be synthesised for a wide range of monomers [1.05 < dispersity (*Đ*) <1.40). Furthermore, the end groups are kept active at the end of the reaction and are accessible for further chain extension or block copolymer formation.[23] Polymers synthesized from RAFT mediated polymerisation of *N*-vinylpyrrolidone (*N*VP) were used in this study.

2.3 Polymers of *N*VP

With increasing complexity of drug delivery systems, protein and peptide based drugs are now being used successfully as therapeutic agents. The challenge, however, lies in the ease with which these molecules degrade when exposed to proteolytic enzymes, as well as their poor solubility in aqueous media.[24] PEGylation refers to the modification of protein, peptides and even non peptide molecules by linking one or more polyethylene glycol (PEG) chains. PEG offers advantages in that it is neither toxic, nor immunogenic. It is also not antigenic and has good aqueous solubility properties. PEG-drug conjugates are known to offer longer residence times in the body and are relatively non-susceptible to degradation by metabolic enzymes.[25] Crucially, PEG is FDA approved. Since PEGylation was introduced, other drug delivery systems have been used and studied e.g. cellulose

derivatives, hydroxypropylmethyl cellulose[26] and poly(*N*-vinylpyrrolidone) (PVP),[9] only to mention a few.

PVP is known to exhibit most of the characteristics that are common to PEG, and more. Apart from having good adhesion characteristics, resistance to hydrolysis in aqueous media, biocompatibility and low toxicity[27-30], PVP conjugates have been shown to have a longer plasma half-lives compared to PEG conjugates. Sun *et al.* evaluated the effect of grafting PVP onto PMMA-based lucitone denture materials, which resulted in increased water solubility, as well as a decreased contact angle. The capacity of the new denture resins to bind to the drug also increased with the increase in PVP grafting yield [28]. This makes PVP conjugation a viable route, coupled with the benefits that come with RDRP of *N*VP, such as chain end fidelity and low dispersities. The former is of great importance in post polymerisation modifications. It is, however, important to state that ATRP and NMP have been shown to be relatively ineffective in controlling the polymerisation of *N*VP [31-32]. This makes RAFT mediated polymerisation the most viable route in the polymerisation of *N*VP.

2.4 Post polymerisation modification of chain ends

Achieving successful synthesis of macromolecular architectures with precise reactivity, domain size and functionality, to mention a few, in RDRP, is largely dependent on chain end fidelity. The use of RAFT agents allows for the incorporation of functional handles post polymerisation[33]. This results in what have been termed heterotelechelic polymers[34]. The complexity of functional groups that can be introduced at the chain ends through RAFT mediated polymerisation is enormous, ranging from the incorporation of small functional moieties that are used in subsequent reactions such as organic azides[35], to subsequently bigger groups such as peptides in bio-conjugation chemistry.[13] RAFT agents generally contain two important substituents namely the Z and R groups[36]. Post polymerisation, the R group becomes the α-chain end and the Z group becomes the ω-chain end.

2.4.1 Z group manipulation

There have been disadvantages in employing the ω-functionalisation approach in some applications owing to the influence of the labile C–S bond in the RAFT end-group.[15] However, lability of the thiocarbonyl thio moiety, and its proximity to the Z group, means that functionality can be built into the Z group post polymerisation to yield ω-chain end functional polymers.[37] A number of strategies have been used for the ω-chain end transformation as shown in Scheme 2.3.[38]

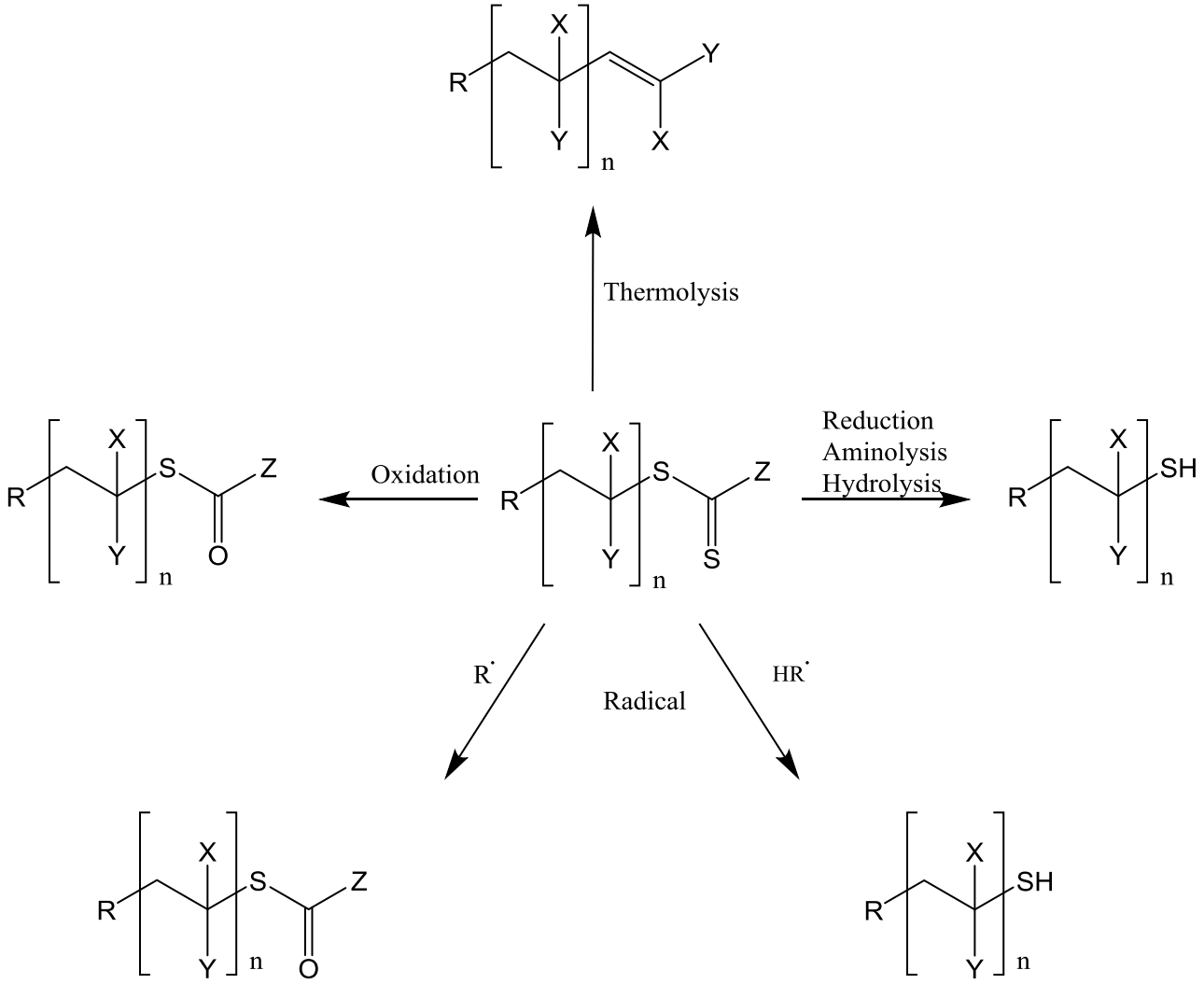

Scheme 2.3: Modification of thiocarbonyl thio end group of a RAFT synthesised polymer chain.[38]

2.4.1.1 Thermolysis

The studies of thermal decomposition show that different RAFT agents decompose at varying temperatures yielding unsaturated chain ends. The cumyl dithiobenzoate RAFT agent was employed in the polymerisation of MMA. At temperatures above 120 °C, it was converted into a polymeric dithiobenzoate which yielded an unsaturated group at the polymeric chain end and dibenzoic acid.[38] When *N*VP polymerisation is facilitated by xanthates, loss of the end groups starts far below 100 °C. This can be deduced from the presence of the unsaturated product of monomolecular elimination of the xanthate,[39] verified using NMR spectroscopy. Interestingly Liu *et al*., demonstrated that the high temperature (120, 150, 180 °C) polymerisation of styrene facilitated by cumyl dithiobenzoate at high temperatures (120, 150, 180 °C) was not affected by thermal decomposition of the CTA.[40] It was concluded that this was a result of the initial CTA being swiftly converted into a polymeric CTA that was more stable.

2.4.1.2 Hydrolysis

Aqueous RAFT polymerisations, or simply the presence of water, brings a dimension of complexity. It promotes the hydrolysis of the CTA, resulting in diminished control of polymerisations.[41-42] This happens because thiocarbonyl thio compounds are known to be thermodynamically unstable under hydrolysis conditions. The energy difference that exists between the C=O and C=S functionalities has been determined to be 180 kJ·mol^{-1}.[43] However, a kinetic barrier to hydrolysis exists, hence there is a strong dependence on temperature also observed in the hydrolysis of dithioesters.[44] More recently Pound *et al*.[39] described the process of modifying PVP xanthate chains into hydroxyl and aldehyde end groups. This was illustrated in a scheme by Thomas *et al.* in Fig 2.4.[41]

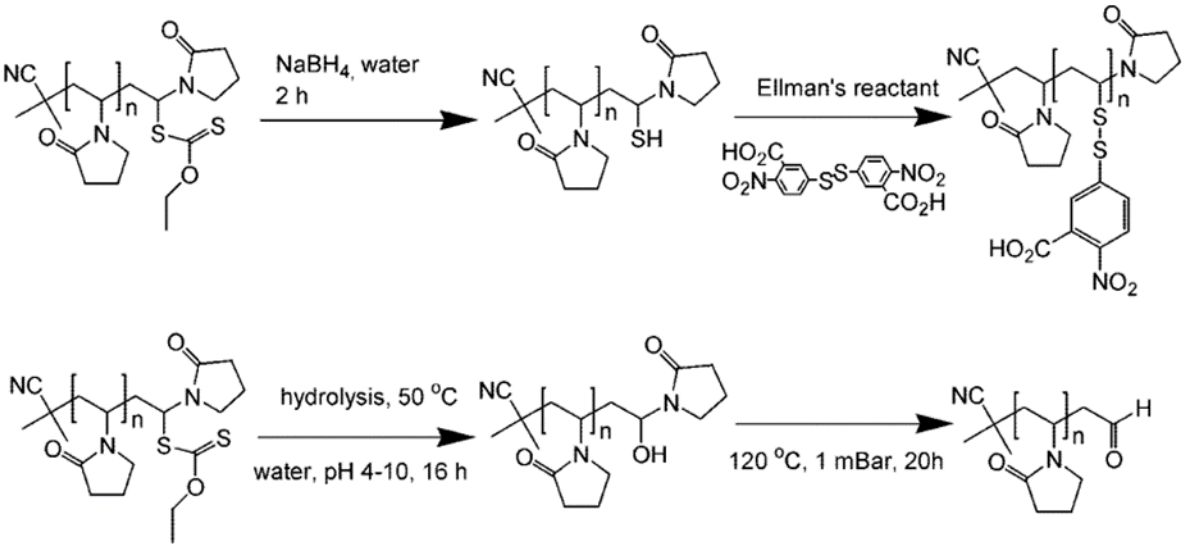

Scheme 2.4: Hydrolysis of the xanthate chain end functionality.[41]

It was established that the hydrolysis was strongly influenced by the pH. At pH values higher than 10, notable fractions of thiol/disulphide chain end functionalities were observed.[45] Zelikin *et al*. transformed the xanthate moieties of PVP chains to thiol end groups that formed disulphide bridges upon reacting with Ellman's reagent.[46] The latter approach is crucial as it facilitates flexible chemistries that are based on thiol, such as thiol maleimide, thiol-ene Michael addition or thiol disulphide exchange that leads to the introduction of specific end groups such as fluorescent markers and peptides.

2.4.1.3 Aminolysis

Aminolysis is a deleterious reaction that transforms the thiocarbonylthio termini of RAFT polymers to thiol through the nucleophilic action of primary and secondary amines.[38, 47-48] The reaction has been determined to be first order with respect to dithioester concentration, and it has low activation energies. However, since amines also catalyse the reaction, it results in a second-order dependence

on amine concentration.[49] Furthermore, only unprotonated amines are capable of reacting with dithioesters. Consequently, the rate of aminolysis becomes a strong function of solution pH. This means that when the pH is above 7 primary and secondary amines readily react rapidly with dithioesters, but are in essence unreactive below a pH of 7.[41, 49-50]

2.4.2 R group manipulation

As mentioned previously, the R group has a role of initiating the growth of polymeric chains. Although the Z is principally responsible for stabilisation of the radical intermediate in RAFT, the R group also shares that responsibility to a lesser extent. During the pre-equilibrium stage, at which a polymeric radical with **n** number of monomer units reacts with the RAFT agent to form the RAFT adduct radical,[21] the R group stabilises the radical intermediate. Parameters such as polarity, steric hindrance, and generated radical stability are often considered when it comes to choosing the R group.[51] More importantly, the R group has been used to introduce functionality both pre and post-polymerisation. This is made possible because the aforementioned roles of the R group only need to be met adjacent to the thiocarbonyl thio moiety. This means that an array of functionalities can be built into the R group further away from the thiocarbonyl thio moiety. Akeroyd *et al.*[52] demonstrated the use of a RAFT agent leaving group that was versatile enough for linkage to a variety of entities, such as small molecule organic substrates, polymers and compounds that occur naturally such as proteins. This was achieved via copper catalysed alkyne azide cycloaddition to yield a triazole based R-leaving group (Scheme.2.5). The pseudo-aromatic nature of the triazole imparts stability on the R-group.[52]

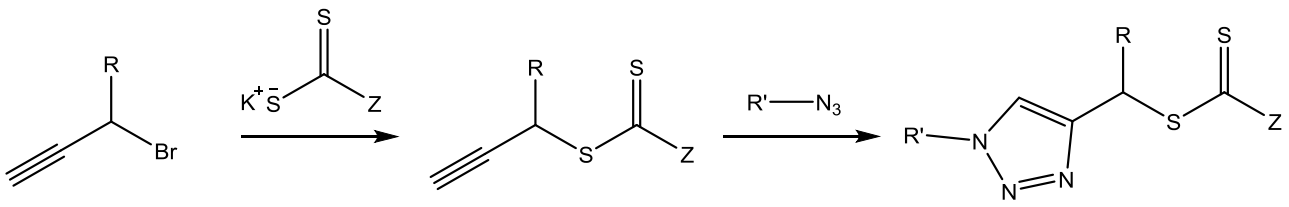

Scheme 2.5: Synthesis of triazole-based R leaving group[52]

Pearce *et al.* developed a hyper-branched polymeric drug carrier of polyethylene glycol monomethyl-methacrylate, with ethylene glycol dimethacrylate as the branching agent synthesised via RAFT mediated polymerisation. The RAFT agent was synthesised by attaching a targeting ligand for prostate specific membrane antigen (PSMA) to the leaving group of the RAFT agent.[53]

2.5 Polymer drug delivery systems

Conventional therapeutic approaches present many shortcomings arising from premature *in vivo* drug degradation, poor aqueous solubility, short circulating half-lives, non-specific drug delivery and high dosage. All of these phenomena result in high toxicity and low bio-availability.[26, 54-55] This leads to poor pharmacokinetics and a seemingly inevitable occurrence of side effects. These challenges have led to what has been termed "polymer therapeutics", which refers to any polymer that is employed as a building block of a therapeutic product for the purpose of eliciting or altering therapeutic action.[56] Polymer therapeutics can be divided into 5 subclasses: polymeric micelles, polymeric drugs, polymer–protein conjugates, polyplexes (complexes of polymers and poly(nucleic acids)) and polymer-drug conjugates.[57] The idea of polymer conjugation, which has since revolutionized drug delivery systems, was envisioned by Helmut Ringsdorf in 1975. According to his model, a drug delivery system should have a bio-compatible, water soluble macromolecular backbone, a therapeutic drug, a spacer, separating the drug from the backbone and a targeting ligand to selectively find the target site [58] leading to an increased efficiency of chemical entity (Fig 2.1) .

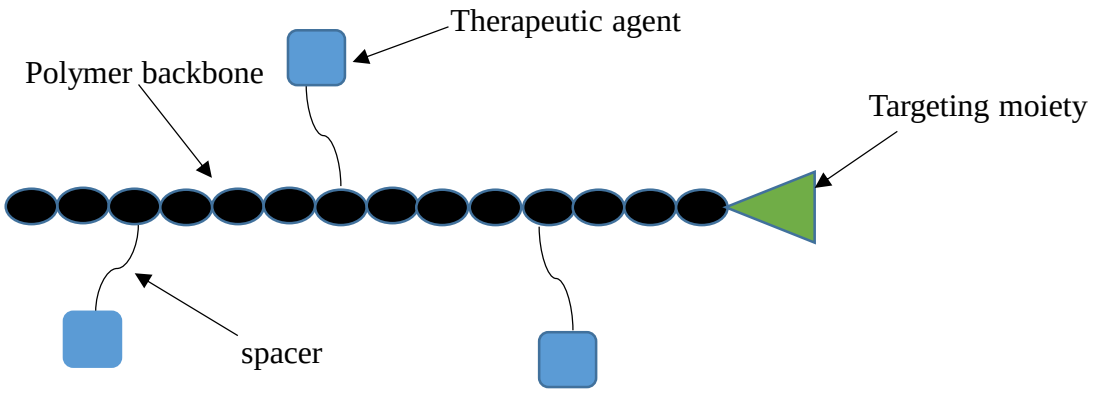

Figure 2.1: Ringsdorf's drug delivery model

Two methods have generally been used to deliver therapeutic agents either passively or through active targeting, namely:

i. Encapsulation of the drug within a three-dimensional amphiphilic polymeric construct, and
ii. Conjugation of the drug to the polymeric system as described by Ringsdorf.

In this study, however, most of the examples are based on conjugated polymeric systems since the focus is on polymer-peptide conjugates.

2.5.1 Theranostics

Based on Ringsdorf model, the idea of theranostics, which is based on combining therapeutics and diagnostics, was developed, and it has gained great interest particularly in the field of oncology. Although the concept is fairly new, major inroads in research have been made in designing theranostic devices that are capable of locating infection at specific areas within the host. Additionally, they have a unique ability to deliver the therapeutic agent directly to the target.[53] This has been achieved by the careful designing of theranostic devices into an imaging modality, a targeting moiety, or signal emitter, and a therapeutic payload. The construct would be completed with a mechanism that ensures safe release of the therapeutic agent at a precise location. The payload is normally carried by a matrix comprising of a polymer system synthesised from RDRP techniques, with functional handles on which fluorescent markers or therapeutic agents can be conjugated. The targeting moiety is selected for binding and complexation with specific cell markers on the target. This facilitates transportation of the theranostic device to the site of interest leading to specific interactions that result in internalisation.[59] Pearce *et al.* developed hyper-branched polymers through RAFT polymerisation that were designed to include a high degree of functional end groups.[53] The authors, however did not specify on how they managed to retain the xanthate end groups in their construct after post polymerisation modifications, considering that the targeting ligand had an amine functionality. In the study described in this thesis, heterotelechelic polymer constructs of PVP with a glutamate urea targeting ligand, a fluorescent marker and a peptide based therapeutic payload make up the theranostic device, actively targeting prostate specific membrane antigen (PSMA).

2.6 Targeted drug delivery

The major challenges with conventional chemotherapeutic agents are the deleterious side effects of toxicity that result from lack of selectivity.[60] They accumulate both in normal and tumour cells. The main goals of cancer therapy include reduction of systemic toxicity, pain and improved prognoses. The compromised selectivity of conventional chemotherapy drugs for tumour cells has a detrimental effect on the body because it results in side effects. Apart from that, it results in lower therapeutic indices of the regiments due to the restrictions of sub-optimal dosage being important for safety. This has led to intensive investigations with the overall goal being to improve the drugs selectivity for tumour tissues. The idea of targeted drug delivery was introduced by Dr. Paul Ehrlich at the turn of the twentieth century. He envisioned a therapy for infectious diseases in which the declared paradigm would be the design of ‘personalised and tailored drugs’ that have the capacity to target specific anomalies of cancerous cells. This idea was referred to as the magic bullet concept,[61] and it optimises

the drug delivery systems' pharmacodynamics and pharmacokinetics with the goal of achieving increased localisation and release of a payload at a specific site.[62-63] As this study focuses on cancer, the drug delivery systems examples will mostly be focused on targeting tumours.

2.6.1 Passive Targeting

Targeted drug delivery systems are normally classified as passive targeting and active targeting. Passive targeting is based on the enhanced permeability and retention effect (EPR).[64] Tumours are known to become diffusion-limited at a volume of 2 mm^3 or above. This limitation has an impact on uptake of nutrients, excretion of waste and the delivery of oxygen. Tumours are capable of overcoming the limitation in diffusion by a process termed angiogenesis in which the surrounding vasculature is increased.[65] This results in most solid tumours possessing pathological characteristics that are unique to cancerous tissues and are not observed in normal tissues or organs. These include; hyper-vascularisation; aberrant vascular architecture; and extensive production of vascular permeability factors stimulating extravasation within tumour tissues. The incomplete and poorly formed vasculature of tumour tissues results in leaky vessels with pore sizes that range from 100 – 2000 nm, depending on the tumour type. [66-69] Synthesised nanoparticles that have diameters smaller than the pores but larger than the diameters of normal vascular tight junctions (usually 2 nm) are capable of penetrating the tumour tissue.[63] On the other hand, the tight junctions of normal tissue vasculature prevent this phenomenon. In addition, a non-functional lymphatic system or its absence within tumour tissue means that the clearance of accumulated nanoparticles is prevented. Thus, selective accumulation of polymeric drug nanoparticles is encouraged, leading to increased localisation.[64] EPR-effect is not by any means momentary, but it results in prolonged drug retention that can exceed several weeks.[70] In addition to that, tumour-to-normal tissue background ratios (T/B), which are a measure of the drug concentration in the tumour compared to that of the blood, have been found to be as high as 10–30, and this points to significant tumour localisation of polymeric conjugates.[60] Furthermore, passive targeting is known to employ additional natural characteristics of polymeric nanoparticles that can improve targeting to the tumour such as charge. Cationic liposomes and amphipathic anti-microbial peptides bind via electrostatic association with phospholipid head groups that are negatively charged and expressed preferentially on tumour endothelial cells.[71-74]

In as much as the EPR effect has been exploited to selectively deliver therapeutic agents with some degree of success, some shortcomings of the method associated with heterogeneity within and among tumour types are known. Apart from different tumour types having different dimensions with respect to pores, the maximum pore size is known to vary with location for any given type of tumour. For instance the maximum pore sizes for primary tumours might be differ from those of metastases.[75]

Furthermore, vessel structures in a given tumour type may differ. In addition to this, the extent of macrophage tumour infiltration and the activity of the mono-nuclear phagocytic system (MPS) can vary between and within tumour types, as well as in patient characteristics (e.g. age, gender, tumour type, body composition, treatment). These factors can lead to the accumulation of polymeric nanoparticles carrying potent payloads in both normal tissue and in different sections of the tumour, for example, in the periphery, viable tumour, and necrotic sections.[75] Despite the widespread and successful application of the EPR effect, these shortcomings have generally led to its limited impact.

2.6.2 Active targeting

Active targeting entails the employment of conjugated targeting ligands that enhance the specific delivery of polymeric drug delivery systems. The increase in the site specificity as well as internalisation can subsequently improve the activity whilst decreasing the chances of the occurrence of side effects that are normally associated with cancer therapy.[76] Active targeting, can be applied using peripherally, covalently bonded small molecule ligands, antibodies or peptides. These molecules are known to lead to enhanced uptake of polymeric devices at specified locations resulting in an increase in internalisation.[53] It goes a long way towards addressing some of the challenges that come with the EPR, although Kirpotin *et al*. have argued that it results in decreased localisation.[77] However, there is little to dispute the fact that the internalization of nanoparticle drug delivery systems result in increased therapeutic effect. An illustration of an active targeting nanoparticle construct is shown in Figure.2.2.

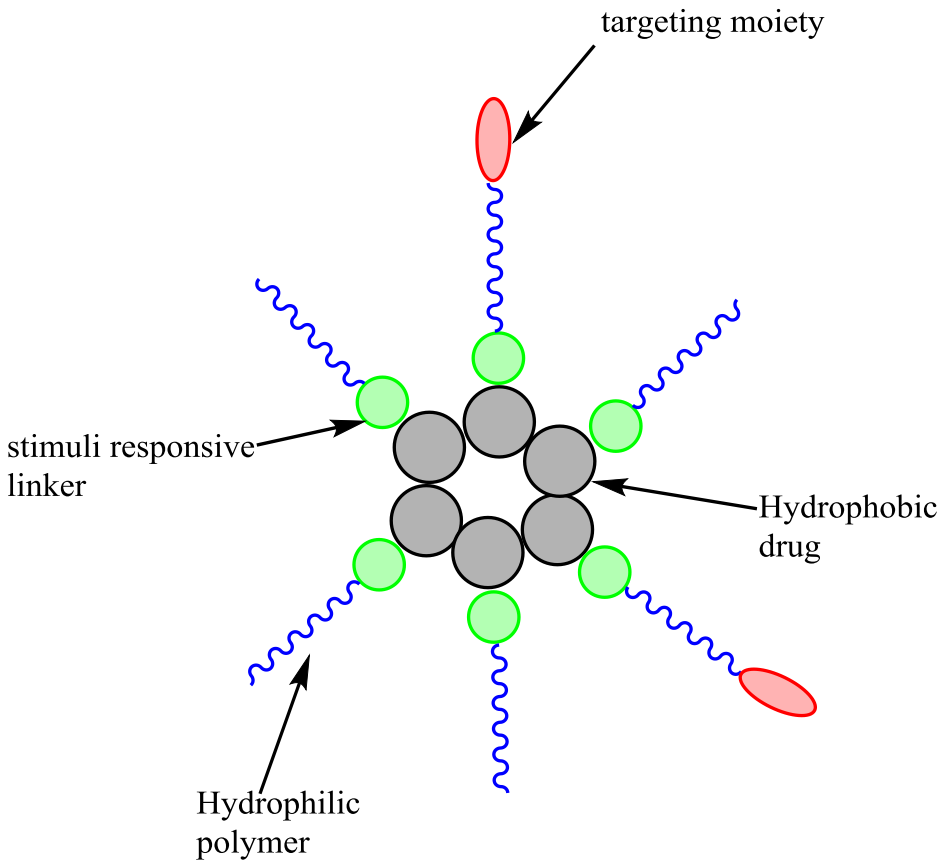

Figure 2.2: Drug delivery design of nanoparticle systems.

One challenge that is usually encountered in the targeting of tumours is that some of the aberrant cells possess similar characteristics to those of their surrounding tissue. To overcome this problem, and differentiate between the cells, there is a need to design ligands that can specifically target receptors that show over-expression on tumour tissue, but being moderately expressed on healthy tissue.[78] In the case of prostate cancer, prostate specific membrane antigen (PSMA) has long been established to be a viable target. It is a highly prostate restricted type II transmembrane glycoprotein (also called carboxypeptidase glutamate II) that is overexpressed in prostate cancer cells, about 100 to 1000-fold higher than in moderately expressed normal tissues; and numerous studies have reported that normal prostate tissue principally expresses a splice variant that does not contain the transmembrane domain (PSM).[53, 79-80] Most importantly, it has been shown that PSMA is not present on normal vasculature.[81-82]

The feasibility and efficiency of drug delivery into prostate and other cancerous cells through the PSMA, and other cell markers, has recently been explored using a variety of cell marker directed ligands, such as antibodies, aptamers, and small molecules, that bind to the cell surface. The preference is that these molecules should have high affinity to their cognate receptors and have the natural ability to trigger receptor-mediated endocytosis.[78] As far as antibodies are concerned, other

crucial design parameters in the development of antibody-conjugated polymeric systems must be carefully considered, for instance, steric hindrance effects as a result of the size, the disposition of the antibodies, the origin of the antibodies, and the mode in which these are attached to the nanoparticles. All these phenomena will influence the *in vivo* tolerability and overall activity of the system.[76] Furthermore antibodies are known to present challenges with site-specific conjugation and they normally show reduction in affinity towards the cognate receptors after they have been conjugated. This inevitably leads to poor bioavailability, poor pharmacokinetics and a compromised drug delivery system.[80] To counter the shortcomings, fragments of antibodies that contain only variable regions of the antibody have become more relevant for active targeting of theranostics. This is because they have a higher tendency to retain the specificity for their target. In addition, they lack the constant Fc effector region that results in complement activation or unfavourable interaction with other cells. This could potentially lead to premature phagocytosis of the nanoparticle construct.[76, 83]

Even though antibody fragments have been used successfully compared to full antibody molecules, there are still a number of concerns and limitations associated with them. One of the most important factors in the use of antibodies in therapeutic applications is their immunogenicity. The recognition of antibodies derived from animals as foreign, causes strong immune responses. This problem has been circumvented to some extent by the use of chimeric antibodies (combining human constant regions and mouse variable regions). This has been shown to significantly reduce the immune responses even though they are not completely prevented.[84-85] Reductions in immunogenicity have been reported when humanised antibodies that contained only binding regions of antibodies derived from mice were fused with human antibodies. However, these still compromise the affinity for the target. In the case of humanised antibodies which contain only the binding regions of the mouse antibodies fused with a human antibody, reductions in immunogenicity have been reported, but sometimes these come at the expense of affinity for the target.[84]

Although antibodies and fragments of antibodies have often been successfully employed as targeting moieties in polymeric drug delivery systems, there are natural problems that are associated with them. Receptor affinity is often decreased depending on the methods of conjugation that are employed. This problem can be exacerbated by free antigen in circulation, inadequate tumour penetration as well as the tendency of antibodies to bind to non-specific Fc receptors. There is also a possibility of the antigen changing over time. Owing to these factors research has been focused on other targeting systems that include, small molecule ligands, short peptide sequences and RNA.[76] A common example of peptide based targeting moieties is the RGD (arginylglycylaspartic acid) peptide. Through phage display, it has been identified to have a high affinity for α5β3 integrin receptors that are over-

expressed on vasculatures of angiogenesis.[86-87] Anisamide is a small molecule ligand that has been employed to target sigma receptors that show over-expression on prostate cancer cells.[88] Folic acid is specific for the folate receptors that are found on ovarian cells,[89] and glutamate ureas are specific for PSMA. Folic acid and glutamate urea are shown in Figure 2.3.

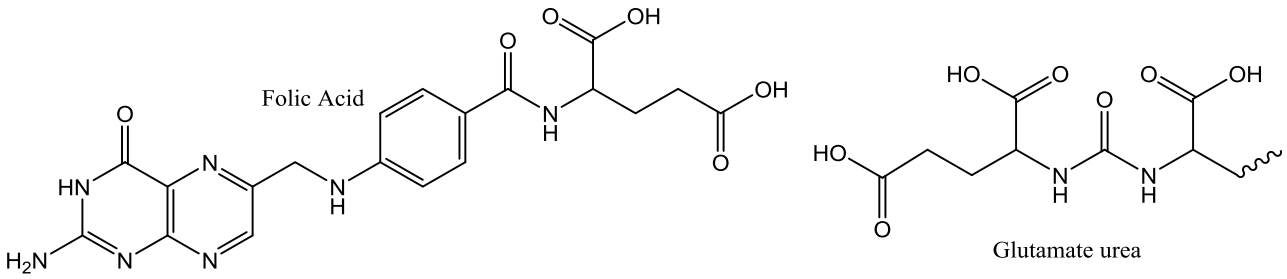

Figure 2.3: Structures of ligands commonly used to functionalise nanoparticle surfaces.

As was aforementioned, the ligands that are selected for the purpose of targeting receptors should be capable of inducing receptor-mediated endocytosis. The rate of cellular internalisation differs depending on the interactions between the ligands and the receptors. This is a crucial factor as the internalisation rates tend to affect the accumulation of nanoparticles on the relevant tumour sites. Folate, for instance and other ligand species are known to exhibit swift internalisation. Furthermore the rates of cell surface recycling are relatively fast in cancerous cells.[90]

2.7 Antimicrobial Peptides

Widespread use of antibiotics has resulted in an unprecedented occurrence and fast spreading of resistant microorganisms.[91] In recent years, knowledge of biological and biomedical relevance of antimicrobial peptides has been regarded as an advance toward new and resistance-free therapies for infectious diseases.[91] Naturally occurring antimicrobial peptides (AMPs) could probably be one of the first successful forms of evolved chemical defence of eukaryotes against viruses, protozoa, fungi and bacteria.[92] Lipopolysaccharides are a major component of the outer membrane of Gram-negative bacteria which has a role of serving as a physical barrier that provides the bacteria with protection from its surrounding environment. It is well known to elicit strong immune responses in animals.[93] Some of the AMPs have been found to have the ability to neutralise lipopolysaccharide while at the same time being capable of recruiting adaptive immune responses.[74, 93] Recent studies have shown that some (but not all) of the AMPs are potent against cancerous cells, and it has led to them being termed anticancer peptides (ACPs). This has been attributed to the negative charge on the surface of the cancer cell membranes. Interestingly, it is a characteristic also shared by the bacterial cells.[74, 94] Although this has been proven to be the case, it is important that the ACPs are classified into two broad categories. The first category being ACPs that are antagonistic against bacteria and cancer cells

and crucially not against normal mammalian cells, and the second being those that show a broad spectrum of cytotoxic activity against cancer cells, bacteria and normal mammalian cells.[74]

2.7.1 Structure and modes of action of AMPs

From a structural information that has been reported, most AMPs have either α-helical or β-sheet conformation but some extended structures are known to exist.[74, 95] AMPs are generally small and amphipathic molecules, and most of them contain cationic (i.e. net charge at neutral pH ranges from + 2 to + 9) and hydrophobic sections. The positive charge facilitates the interaction of the peptides with the lipid membranes, leading to their disruption.[74, 96] The mechanism and selectivity criteria by which AMPs or ACPs kill cells is not yet clear and has so far been a theme of major debate at controversy. According to Harris and co-workers, ACPs oncolytic activities generally occur by membranolytic mechanisms although there is growing evidence of additional/alternative non-membranolytic mechanisms.[97-99]

2.7.1.1 Membranolytic Mechanism

ACPs tend to differ in their mechanisms depending on the characteristics of the peptides as well as the features on the target membranes. The latter tends to modulate the toxicity and selectivity of the peptides.[91] It has been shown that cancerous cells and normal mammalian cells have a number of significant differences and these go a long way towards explaining the selectivity of some of the ACPs. Certain molecules that are present in the malignant tumour cell membranes are known to be responsible for imparting negative surface charge.[100] These molecules include, sialylated gangliosides, phospholipid phosphatidylserine (PS), *O*-glycosylated mucans, and heparin sulphate. This differs from normal tissue cell membranes that are normally zwitterionic in nature.[74, 100] According to Dobrzynska *et al.*, in their work on colorectal cancer, it was concluded that the tendency to metastasise is facilitated by the differences in the phospholipid contents of the cell membranes.[101] High ratios of phosphatidylcholine/ phosphatidyl ethanolamine (PC/PE) are normally associated with malignant neoplasm cells that have a large number of metastases while low (PC/PE) ratios are associated with malignant neoplasm cells low numbers of metastases.[101]

In addition to the zwitterionic lipids, normal cells are known to have elevated levels of cholesterol. It has been proposed that cholesterol acts to protect the membrane by denying cationic peptides entry into the cell. It also acts as a fluidity modulator for the cell.[100] On the other hand the membranes of most cancerous cells are generally more fluid when compared to normal cells. This allows for the

destabilisation of the membranes by ACPs.[91] However, it is important to note that other types of cancerous cells still present elevated proportions of cholesterol in their cell membranes. Typical examples are breast cancer and prostate cancer.[102]

The feasibility of solid tumour targeting using ACPs has been explored, however, conclusions about the structural requisites for targeting these tumour cells selectively remain unknown. The information that is available on these tumours that are characterised by solid masses of tissue that lack cysts or areas of liquid have led to the conclusion that ACPs target by a number of mechanisms.[91] When skin cancer is not taken into account, the cancers that are mostly diagnosed in men and women are prostate cancer and breast cancer respectively.[91, 103] Moreover, according to Papo *et al*., prostate cancer has a tendency of not responding sufficiently to single and even multiple drug regiments.[104] The targeted cancers in the development of ACPs have been cancers of the breast,[77] prostate[53], uterine,[105], liver[106] and lung[107]. Some of the ACPs have been known to defy the malignant cells by apoptotic and necrotic mechanisms after damaging cell membranes, others by intracellular targets,[91] the former being facilitated by receptor mediated endocytosis. There is also a great possibility that many anticancer activities could be presented by one single peptide.

A lot of research effort has gone into understanding what actually happens after the ACPs are engaged to the cell membrane. The peptides might penetrate into intracellular tissue, and this would inevitably lead to the disruption of the cell membrane accompanied by the formation of pores and or changes to the cell membrane charge.[108] To add on to this, it will result in the interference with the necrotic and apoptotic pathways.

2.7.1.2 Diversified modes of action and targets

The ACP's are known to have diverse modes of action that are not limited to membranolytic mechanisms that rely on disruption of the plasma and mitochondrial membranes.[91] Other mechanisms are best described by Gasper *et al.* in a scheme that summarises the different modes of action shown in Figure 2.4. These include mediated immunity[109], hormonal receptors[110], DNA synthesis inhibition[111], and anti-angiogenic effects[112].

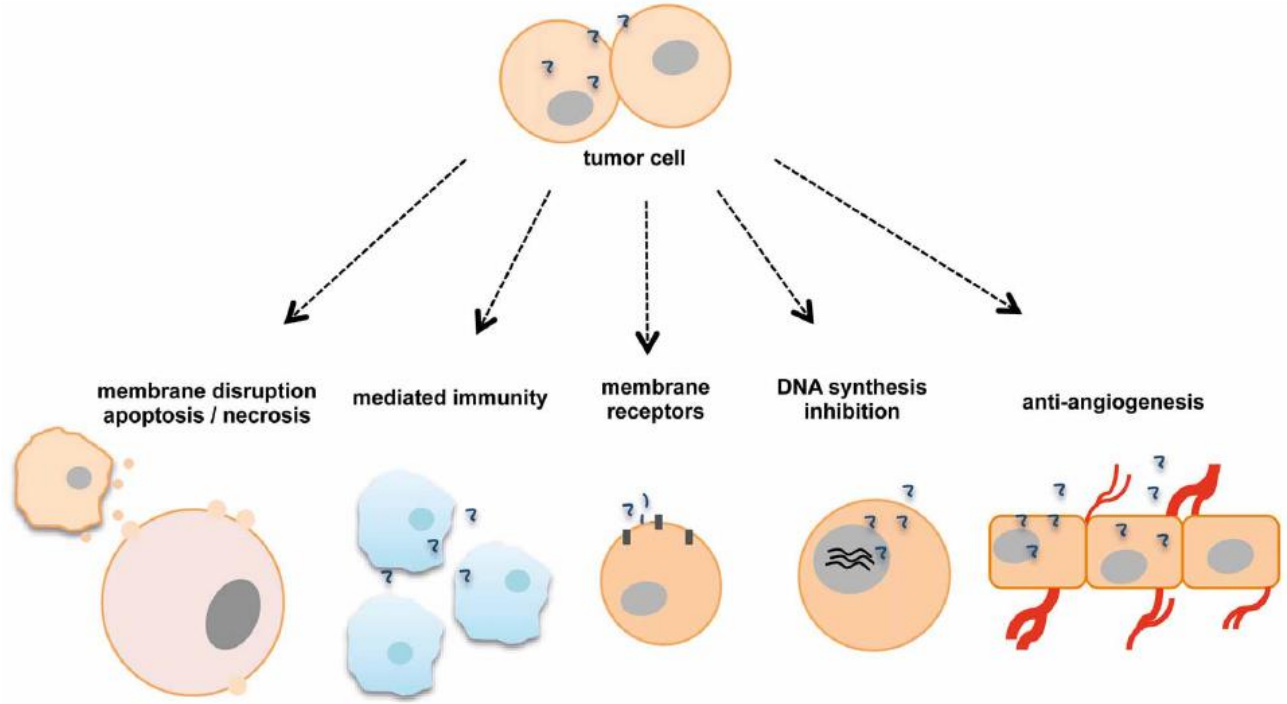

Figure 2.4:Different membranolytic and non-membranolytic modes of action shown by AMPs and ACPs[91]

2.8 Drug release triggering mechanisms

Stimuli-responsive polymers, which have also been referred to as 'smart' or 'intelligent'[113] polymers are known to mimic biological systems, and rapid changes in properties are observed at the slightest or modest change in environmental condition, *e.g.* pH, concentration salt, temperature, or light.[114] They have proven to be extremely vital in the design of drug release triggering mechanisms. Stimuli-responsive linkers, that have the ability to cleave under certain physiological stimuli, can facilitate the release of drugs from conjugates. Despite there being many stimuli (Fig 2.5), the majority of studies, by far, have used temperature or pH to facilitate drug release.

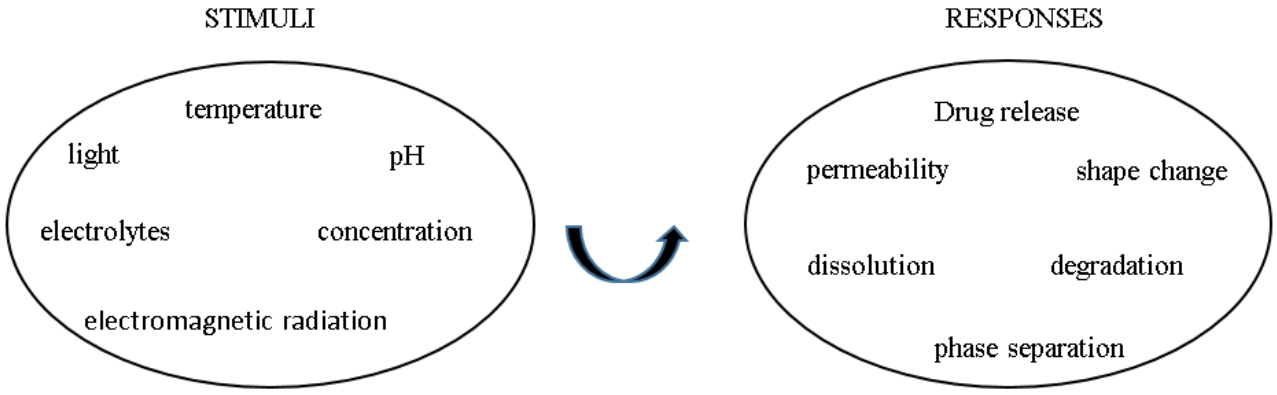

Figure 2.5: Potential stimuli and corresponding responses in 'smart' polymers

2.8.1 Thermo-responsive polymers

According to Schmaljohann, volume phase transitions at specific temperature ranges, that are accompanied by sudden changes in solvation states are associated with thermo-responsive polymers.[114] In general, the phase transitions, with respect to biologically relevant intermolecular forces, rely on a number of different interactions namely, hydrogen bonding, hydrophobic interactions, van der Waals, and attractive ionic interactions. Certain polymers, which when heated become insoluble, have what is termed a lower critical solution temperature (LCST), while those that tend to be soluble on heating exhibit an upper critical solution temperature (UCST).[114] Schilid described PNIPAAM behaviour of inverse solubility upon heating, *i.e*. macromolecular transition from a hydrophilic to a hydrophobic structure that occurs abruptly. It undergoes a sharp coil-globule transition in water at 32 °C, shifting from a hydrophilic state below this temperature (LCST), to a hydrophobic state.[115] The origin of the 'intelligent' behaviour, comes about as a result of a gain in entropy when water molecules that are associated with isopropyl side chain moieties are released into the bulk phase. This takes place as the temperature increase passes a critical point.[116] Aoki *et al.* described what they termed positive temperature-dependent sigmodal transitions as well as changes in swelling that are within specified ranges of temperature for interpenetrating polymer networks (IPN).[117] The IPN hydrogel they described was composed of polyacrylamide (PAAm) and poly(acry1ic acid) (PAAc), forming inter-polymer complexes via hydrogen bonding at lower temperatures that dissociate at elevated temperatures.

2.8.2 pH responsive polymers

The change in pH has been widely used as a physiological stimulus. pH responsive polymeric drug delivery systems are extremely important in the treatment of low pH targets, such as tumours and inflammatory tissues. A number of acid-labile linkers have been employed in the design of polymer-peptide conjugates, polymeric micelles as well as nanogels to deliver therapeutic payloads in acidic pH environments.[118] Most of these linkers are destabilised in acidic media resulting in enhanced degradation or hydrolysis while they are stable at neutral pH. Their mechanism of action takes advantage of the differences in the physiological pH (7.4), and the extracellular pH in tumours and infected tissue (6.5 or less). In the case of micellar systems, acid-degradable linkages cause structural changes that result in the loss of micellar integrity. Oishi *et al.* synthesised PEG conjugated to an oligodeoxynucleotide (ODN), through a β-thiopropionate ester linkage. It was shown that the acid labile ester destabilised by the thiol cleaved at endosomal pH (5.5) over 24 hours but was stable at physiological pH (7.4).[119] Table 2.1 summarises common pH-responsive linkers found in drug delivery systems.[120]

Table 2.1: Acid labile linkers commonly found in drug delivery systems

Name	Structure	Degradation Products
Acetal/Ketal	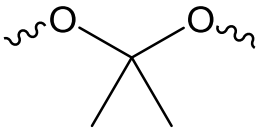	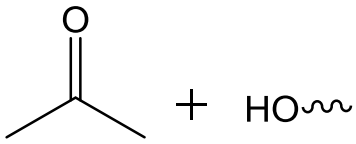
Imine	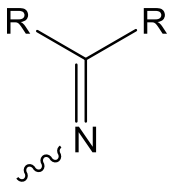	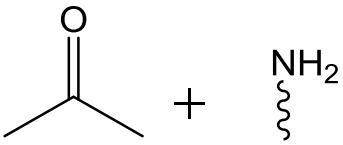
Hydrazone	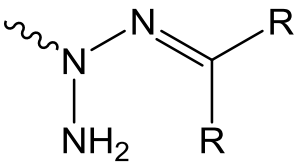	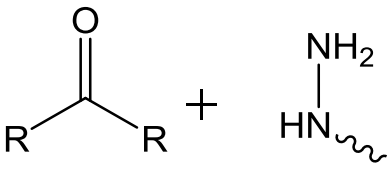
Orthoester	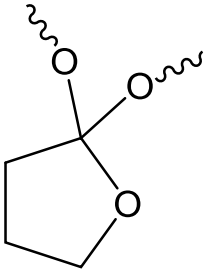	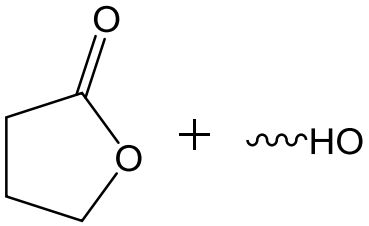

Pearce and co-workers described a hyper-branched polymer carrier targeting PSMA that incorporated a hydrazone linkage. The authors argued that hydrazones are superior to esters as they do not lead to localised acidosis upon degradation;[53] however, esters have still been used successfully in drug delivery systems.[119] Giles *et al.* developed a system in which PEO with a dendritic end-functionality was peripherally functionalised with hydrophobic groups using pH labile acetal linkages. Hydrolysis resulted in loss of the hydrophobic groups which led to blocks that formed the core to become hydrophilic. This destabilised the micelle and facilitated the release of the drug from the micelles.[121]

2.9 Conclusion

The development of RDRP techniques has resulted in precisely engineered properties and functional groups being imparted into polymeric systems. This has led to multifunctional materials being synthesised by simple covalent chemistry in tandem with biology and bio-conjugation chemistry. The development of polymer-peptide conjugates synthesized from robust, efficient and orthogonal (REO) chemistries[122] remains an area with gaps, and further research is key. Through REO chemistry it has been shown to be possible to conjugate therapeutic drugs through stimuli responsive linkers to polymer systems. Imaging modalities and targeting moieties can also be orthogonally introduced resulting in heterotelechelic systems that often self-assemble into micelles resulting in “smart” drug delivery systems.

2.10 References

(1) Szwarc, M.; Levy, M.; Milkovich, R., *J. Am. Chem. Soc.* **1956**, 78, 2656.

(2) Jenkins A, D.; Jones R, G.; Moad, G., *Pure Appl. Chem* **2009**, 82, 483.

(3) Braunecker, W. A.; Matyjaszewski, K., *Prog. Polym. Sci* **2007**, 32, 93.

(4) Greszta, D.; Mardare, D.; Matyjaszewski, K., *Macromolecules* **1994**, 27, 638.

(5) Darling, T. R.; Davis, T. P.; Fryd, M.; Gridnev, A. A.; Haddleton, D. M.; Ittel, S. D.; Matheson, R. R.; Moad, G.; Rizzardo, E., *J. Polym. Sci. A Polym. Chem.* **2000**, 38, 1706.

(6) Fischer, H., *Chem. Rev.* **2001**, 101, 3581.

(7) Tang, W.; Tsarevsky, N. V.; Matyjaszewski, K., *J. Am. Chem. Soc.* **2006**, 128, 1598.

(8) Braunecker, W. A.; Matyjaszewski, K., *Prog. Polym. Sci.* **2007**, 32, 93.

(9) Pound, G., PhD thesis, University of Stellenbosch, **2008**.

(10) Grubbs, R. B., *Polym. Rev. (Phila Pa).* **2011**, 51, 104.

(11) Debuigne, A.; Jérôme, R.; Jérôme, C.; Detrembleur, C., *J.Mater.Sci.Technol* **2012**.

(12) Keng, P. Y.; Shim, I.; Korth, B. D.; Douglas, J. F.; Pyun, J., *ACS Nano* **2007**, 1, 279.

(13) Feldman, K. E.; Kade, M. J.; de Greef, T. F. A.; Meijer, E. W.; Kramer, E. J.; Hawker, C. J., *Macromolecules* **2008**, 41, 4694.

(14) Matyjaszewski, K.; Gaynor, S.; Wang, J.-S., *Macromolecules* **1995**, 28, 2093.

(15) Moad, G.; Chong, Y. K.; Postma, A.; Rizzardo, E.; Thang, S. H., *Polymer* **2005**, 46, 8458.

(16) D'Agosto, F.; Hughes, R.; Charreyre, M.-T.; Pichot, C.; Gilbert, R. G., *Macromolecules* **2003**, 36, 621.

(17) Yamago, S.; Iida, K.; Yoshida, J.-i., *J. Am. Chem. Soc.* **2002**, 124, 13666.

(18) Yamago, S.; Ray, B.; Iida, K.; Yoshida, J.-i.; Tada, T.; Yoshizawa, K.; Kwak, Y.; Goto, A.; Fukuda, T., *J. Am. Chem. Soc.* **2004**, 126, 13908.

(19) Chiefari, J.; Chong, Y.; Ercole, F.; Krstina, J.; Jeffery, J.; Le, T. P.; Mayadunne, R. T.; Meijs, G. F.; Moad, C. L.; Moad, G., *Macromolecules* **1998**, 31, 5559.

(20) Barner-Kowollik, C., John Wiley & Sons: **2008**; p 1.

(21) Coote, M. L.; Krenske, E. H.; Izgorodina, E. I., In *Handbook of RAFT Polymerization*,(Barner-Kowollik, C., Ed. WILEY-VCH Verlag GmbH & Co. KGaA,: **2008**; p 5.

(22) Zard, S. Z., *Aust. J. Chem* **2006**, 59, 663.

(23) Perrier, S.; Takolpuckdee, P., *J. Polym. Sci. A Polym. Chem.* **2005**, 43, 5347.

(24) Harris, J. M.; Chess, R. B., *Nat. Rev. Drug. Discov.* **2003**, 2, 214.

(25) Veronese, F. M.; Pasut, G., *Drug. Discov. Today* **2005**, 10, 1451.

(26) Leuner, C.; Dressman, J., *Eur. J. Pharm. Biopharm.* **2000**, 50, 47.

(27) Kang, N.; Leroux, J.-C., *Polymer* **2004**, 45, 8967.

(28) Sun, X.; Cao, Z.; Yeh, C.-K.; Sun, Y., *Colloids. Surf. B. Biointerfaces.* **2013**, 110, 96.

(29) Stace, S. J.; Moad, G.; Fellows, C. M.; Keddie, D. J., *Polym. Chem.* **2015**, 6, 7119.

(30) Bailly, N.; Pound-Lana, G.; Klumperman, B., *Aust. J. Chem.* **2012**, 65, 1124.

(31) Lu, X.; Gong, S.; Meng, L.; Li, C.; Yang, S.; Zhang, L., *Polymer* **2007**, 48, 2835.

(32) Bilalis, P.; Pitsikalis, M.; Hadjichristidis, N., *J. Polym. Sci. A Polym. Chem.* **2006**, 44, 659.

(33) Mayadunne, R. T. A.; Rizzardo, E.; Chiefari, J.; Chong, Y. K.; Moad, G.; Thang, S. H., *Macromolecules* **1999**, 32, 6977.

(34) Tasdelen, M. A.; Kahveci, M. U.; Yagci, Y., *Prog. Polym. Sci.* **2011**, 36, 455.

(35) Mantovani, G.; Ladmiral, V.; Tao, L.; Haddleton, D. M., *Chem. Commun (Camb).* **2005**, 2089.

(36) Chong, Y. K.; Krstina, J.; Le, T. P. T.; Moad, G.; Postma, A.; Rizzardo, E.; Thang, S. H., *Macromolecules* **2003**, 36, 2256.

(37) Pfukwa, R., MSc thesis, Stellenbosch University, **2008**.

(38) Barner, L.; Perrier, S., In *Handbook of RAFT polymerisation*,(Barner-Kowollik, C., Ed. John Wiley & Sons: **2008**; p 445.

(39) Pound, G.; Eksteen, Z.; Pfukwa, R.; McKenzie, J. M.; Lange, R. F. M.; Klumperman, B., *J. Polym. Sci. A Polym. Chem.* **2008**, 46, 6575.

(40) Liu, Y.; He, J.; Xu, J.; Fan, D.; Tang, W.; Yang, Y., *Macromolecules* **2005**, 38, 10332.

(41) Thomas, D. B.; Convertine, A. J.; Hester, R. D.; Lowe, A. B.; McCormick, C. L., *Macromolecules* **2004**, 37, 1735.

(42) Thomas, D. B.; Sumerlin, B. S.; Lowe, A. B.; McCormick, C. L., *Macromolecules* **2003**, 36, 1436.

(43) Bonnans-Plaisance, C.; Levesque, G., *Macromol. Chem. Phys.* **1986**, 187, 2841.

(44) Levesque, G.; Arsène, P.; Fanneau-Bellenger, V.; Pham, T.-N., *Biomacromolecules* **2000**, 1, 400.

(45) Pound, G.; McKenzie, J. M.; Lange, R. F. M.; Klumperman, B., *J. Chem. Soc., Chem. Commun.* **2008**, 3193.

(46) Zelikin, A. N.; Such, G. K.; Postma, A.; Caruso, F., *Biomacromolecules* **2007**, 8, 2950.

(47) Kjaer, A., *Acta. Chem. Scand* **1952**, 6, 327.

(48) Kjaer, A., *Acta. Chem. Scand* **1950**, 4, 1347.

(49) Deletre, M.; Levesque, G., *Macromolecules* **1990**, 23, 4733.

(50) Scheithauer, S.; Mayer, R., *Thio-and dithiocarboxylic acids and their derivatives*. Georg Thieme Verlag: **1979**.

(51) Perrier, S.; Takolpuckdee, P.; Westwood, J.; Lewis, D. M., *Macromolecules* **2004**, 37, 2709.

(52) Akeroyd, N.; Pfukwa, R.; Klumperman, B., *Macromolecules* **2009**, 42, 3014.

(53) Pearce, A. K.; Rolfe, B. E.; Russell, P. J.; Tse, B. W. C.; Whittaker, A. K.; Fuchs, A. V.; Thurecht, K. J., *Polym. Chem.* **2014**, 5, 6932.

(54) Karan, D.; Holzbeierlein, J. M.; Van Veldhuizen, P.; Thrasher, J. B., *Nat. Rev. Urol.* **2012**, 9, 376.

(55) Mills, J. K.; Needham, D., *Expert. Opin. Ther. Pat.* **1999**, 9, 1499.

(56) Kabanov, A. V.; Batrakova, E. V.; Alakhov, V. Y., *J. Control. Release* **2002**, 82, 189.

(57) Duncan, R., *Nat Rev Drug Discov.* **2003**, 2, 347.

(58) Ringsdorf, H., *J.polym.sci.,Polym.symp* **1975**, 51, 135.

(59) Fang, C.; Zhang, M., *J. Control. Release* **2010**, 146, 2.

(60) Maeda, H.; Bharate, G. Y.; Daruwalla, J., *Eur. J. Pharm. Biopharm.* **2009**, 71, 409.

(61) Strebhardt, K.; Ullrich, A., *Nat. Rev. Cancer.* **2008**, 8, 473.

(62) Wang, B.; Siahaan, T. J.; Soltero, R. A., *Drug delivery: principles and applications*. John Wiley & Sons: **2005**, p 443.

(63) Kratz, F.; Senter, P.; Steinhagen, H., *Drug Delivery in Oncology: From Basic Research to Cancer Therapy, 3 Volume Set*. John Wiley & Sons: **2013**, p 227.

(64) Maeda, H.; Wu, J.; Sawa, T.; Matsumura, Y.; Hori, K., *J. Control. Release* **2000**, 65, 271.

(65) Jones, A.; Harris, A. L., *Cancer. J. Sci. Am.* **1998**, 4, 209.

(66) Folkman, J.; Merler, E.; Abernathy, C.; Williams, G., *J. Exp. Med.* **1971**, 133, 275.

(67) Shubik, P., *J. Cancer Res. Clin. Oncol.* **1982**, 103, 211.

(68) Rubin, P.; Casarett, G., *Clin. Radiol.* **1966**, 17, 346.

(69) Hobbs, S. K.; Monsky, W. L.; Yuan, F.; Roberts, W. G.; Griffith, L.; Torchilin, V. P.; Jain, R. K., *Proc. Natl. Acad. Sci. U.S.A.* **1998**, 95, 4607.

(70) Fang, J.; Nakamura, H.; Maeda, H., *Adv. Drug Deliv. Rev.* **2011**, 63, 136.

(71) Ran, S.; Downes, A.; Thorpe, P. E., *Cancer Res.* **2002**, 62, 6132.

(72) Kunstfeld, R.; Wickenhauser, G.; Michaelis, U.; Teifel, M.; Umek, W.; Naujoks, K.; Wolff, K.; Petzelbauer, P., *J. Invest. Dermatol* **2003**, 120, 476.

(73) Krasnici, S.; Werner, A.; Eichhorn, M. E.; Schmitt-Sody, M.; Pahernik, S. A.; Sauer, B.; Schulze, B.; Teifel, M.; Michaelis, U.; Naujoks, K., *Int. J. Cancer* **2003**, 105, 561.

(74) Hoskin, D. W.; Ramamoorthy, A., *Biochim. Biophys. Acta* **2008**, 1778, 357.

(75) Prabhakar, U.; Maeda, H.; Jain, R. K.; Sevick-Muraca, E. M.; Zamboni, W.; Farokhzad, O. C.; Barry, S. T.; Gabizon, A.; Grodzinski, P.; Blakey, D. C., *Cancer Res.* **2013**, 73, 2412.

(76) Byrne, J. D.; Betancourt, T.; Brannon-Peppas, L., *Adv. Drug Deliv. Rev.* **2008**, 60, 1615.

(77) Kirpotin, D. B.; Drummond, D. C.; Shao, Y.; Shalaby, M. R.; Hong, K.; Nielsen, U. B.; Marks, J. D.; Benz, C. C.; Park, J. W., *Cancer Res.* **2006**, 66, 6732.

(78) Wang, M.; Thanou, M., *Pharmacol. Res.* **2010**, 62, 90.

(79) Ghosh, A.; Heston, W. D., *J. Cell. Biochem.* **2004**, 91, 528.

(80) Huang, B.; Otis, J.; Joice, M.; Kotlyar, A.; Thomas, T. P., *Biomacromolecules* **2014**, 15, 915.

(81) Silver, D. A.; Pellicer, I.; Fair, W. R.; Heston, W.; Cordon-Cardo, C., *Clin. Cancer. Res.* **1997**, 3, 81.

(82) Liu, H.; Moy, P.; Kim, S.; Xia, Y.; Rajasekaran, A.; Navarro, V.; Knudsen, B.; Bander, N. H., *Cancer Res.* **1997**, 57, 3629.

(83) Chapman, A. P., *Adv. Drug Deliv. Rev.* **2002**, 54, 531.

(84) Stacy, K. M., *The Scientist* **2005**, 19, 17.

(85) Holliger, P.; Hudson, P. J., *Nat. Biotechnol.* **2005**, 23, 1126.

(86) Schiffelers, R. M.; Koning, G. A.; ten Hagen, T. L.; Fens, M. H.; Schraa, A. J.; Janssen, A. P.; Kok, R. J.; Molema, G.; Storm, G., *J. Control. Release* **2003**, 91, 115.

(87) Pasqualini, R.; Koivunen, E.; Ruoslahti, E., *Nat. Biotechnol.* **1997**, 15, 542.

(88) Banerjee, R.; Tyagi, P.; Li, S.; Huang, L., *Int. J. Cancer* **2004**, 112, 693.

(89) Pan, X.; Lee, R. J., *Expert Opin. Drug Deliv.* **2004**, 1, 7.

(90) Caraglia, M.; Marra, M.; Misso, G.; Lamberti, M.; Salzano, G.; De Rosa, G.; Abbruzzese, A., *Tumour-specific uptake of anti-cancer drugs: the future is here*. Bentham Science Publishers: **2012**, p 4.

(91) Gaspar, D.; Veiga, A. S.; Castanho, M. A., *From antimicrobial to anticancer peptides. A review*. Frontiers in Microbiology: **2014**, p 24.

(92) Zasloff, M., *Nature* **2002**, 415, 389.

(93) Rosenfeld, Y.; Shai, Y., *Biochim. Biophys. Acta* **2006**, 1758, 1513.

(94) Mader, J. S.; Hoskin, D. W., *Expert. Opin. Investig. Drugs.* **2006**, 15, 933.

(95) Munyuki, G.; Jackson, G. E.; Venter, G. A.; Kövér, K. E.; Szilágyi, L.; Rautenbach, M.; Spathelf, B. M.; Bhattacharya, B.; van der Spoel, D., *Biochem. J.* **2013**, 52, 7798.

(96) Liu, L.; Xu, K.; Wang, H.; Tan, P. J.; Fan, W.; Venkatraman, S. S.; Li, L.; Yang, Y.-Y., *Nat. Nanotechnol.* **2009**, 4, 457.

(97) Harris, F.; Dennison, S. R.; Singh, J.; Phoenix, D. A., *Med. Res. Rev.* **2013**, 33, 190.

(98) Andreu, D.; Rivas, L., *J. Pept. Sci.* **1998**, 47, 415.

(99) Toke, O., *J. Pept. Sci.* **2005**, 80, 717.

(100) Schweizer, F., *Eur. J. Pharmacol.* **2009**, 625, 190.

(101) Dobrzyńska, I.; Szachowicz-Petelska, B.; Sulkowski, S.; Figaszewski, Z., *Mol. Cell. Biochem* **2005**, 276, 113.

(102) Li, Y. C.; Park, M. J.; Ye, S.-K.; Kim, C.-W.; Kim, Y.-N., *Am. J. Pathol* **2006**, 168, 1107.

(103) Jemal, A.; Siegel, R.; Ward, E.; Murray, T.; Xu, J.; Smigal, C.; Thun, M. J.,

CA .Cancer. J. Clin. **2006**, 56, 106.

(104) Papo, N.; Braunstein, A.; Eshhar, Z.; Shai, Y., *Cancer Res.* **2004**, 64, 5779.

(105) Peer, D.; Karp, J. M.; Hong, S.; Farokhzad, O. C.; Margalit, R.; Langer, R., *Nat. Nanotechnol.* **2007**, 2, 751.

(106) Cheng, C.; Wei, H.; Zhu, J.; Chang, C.; Cheng, H.; Li, C.; Cheng, S.; Zhang, X.; Zhuo, R., *'Bioconjugate Chem.'* **2008**, 19, 1194.

(107) Danhier, F.; Feron, O.; Préat, V., *J. Control. Release* **2010**, 148, 135.

(108) Janek, T.; Krasowska, A.; Radwańska, A.; Łukaszewicz, M., *PloS one* **2013**, 8, 57991.

(109) Wang, Y.; Li, D.; Shi, H.; Wen, Y.; Yang, L.; Xu, N.; Chen, X.; Chen, X.; Chen, P.; Li, J., *Clin. Cancer. Res.* **2009**, 15, 6901.

(110) Leuschner, C.; Hansel, W., *Biol. Reprod.* **2005**, 73, 860.

(111) Ourth, D. D., *Biomed. Pharmacother.* **2011**, 65, 271.

(112) Koskimaki, J. E.; Karagiannis, E. D.; Rosca, E. V.; Vesuna, F.; Winnard, P. T.; Raman, V.; Bhujwalla, Z. M.; Popel, A. S., *Neoplasia* **2009**, 11, 1285.

(113) Hoffman, A. S., *Macromol. Symp.* **1995**, 98, 645.

(114) Schmaljohann, D., *Adv. Drug Deliv. Rev.* **2006**, 58, 1655.

(115) Schild, H. G., *Prog. Polym. Sci.* **1992**, 17, 163.

(116) de las Heras Alarcón, C.; Pennadam, S.; Alexander, C., *Chem. Soc. Rev.* **2005**, 34, 276.

(117) Aoki, T.; Kawashima, M.; Katono, H.; Sanui, K.; Ogata, N.; Okano, T.; Sakurai, Y., *Macromolecules* **1994**, 27, 947.

(118) Liu, R.; Zhang, Y.; Zhao, X.; Agarwal, A.; Mueller, L. J.; Feng, P., *J. Am. Chem. Soc.* **2010**, 132, 1500.

(119) Oishi, M.; Sasaki, S.; Nagasaki, Y.; Kataoka, K., *Biomacromolecules* **2003**, 4, 1426.

(120) Binauld, S.; Stenzel, M. H., *J. Chem. Soc., Chem. Commun.* **2013**, 49, 2082.

(121) Gillies, E. R.; Jonsson, T. B.; Fréchet, J. M. J., *J. Am. Chem. Soc.* **2004**, 126, 11936.

(122) Iha, R. K.; Wooley, K. L.; Nyström, A. M.; Burke, D. J.; Kade, M. J.; Hawker, C. J., *Chem. Rev.* **2009**, 109, 5620.

3 Synthesis and characterisation of poly(*N*-vinylpyrrolidone)

3.1 Introduction

The importance of polymers of *N*-vinylpyrrolidone (*N*VP) has gained momentum as a result of their characteristics like biocompatibility, good aqueous solubility and low toxicity,[1] to mention a few. Extensive research and development in the past few decades has resulted in the emergence of techniques for implementing reversible deactivation radical polymerisation (RDRP). These techniques have resulted in unprecedented benefits that include imparting living characteristics to radical processes, narrow molecular weight distributions and high chain end fidelity.[2-3] Various RDRP approaches have been studied, one of them being RAFT mediated polymerisation. The key to effective RAFT mediated polymerization lies in the choice of the RAFT agent and appropriate pairing to a particular monomer. This is because the process is heavily reliant on the reactivity of the monomer as well as on the homolytic leaving group ability of the propagating species formed upon radical addition.[1] Thus the so-called **Z** and **R** groups (Scheme 3.1) both play significant roles that ultimately determine the outcome of polymerisation.

Monomer species where double bonds are conjugated to unsaturated systems such as carbonyls, aromatic rings or nitriles are termed more activated monomers (MAMs), with typical examples being (meth)acrylates, styrene and acrylonitrile. These monomers generally undergo facile reaction with radicals.[4] Radicals that are derived from MAMs tend to be good homolytic leaving groups owing to their resonance stabilization. As a result, more reactive RAFT agents are most effective in controlling polymerisation of these type of monomers.

On the other hand, monomers whose structure consists of a double bond that bears a saturated carbon atom or is conjugated to a lone pair on either oxygen or nitrogen (e.g. *N*VP) are referred to as less activated monomers (LAMs). The radicals that are generated from polymerisation of these monomers tend to be poor homolytic leaving groups. Thus, the polymerisation of *N*VP and other LAMs can best be controlled by dithiocarbamate or xanthate RAFT agents (Scheme 3.1) in which the connecting atom of **Z** is nitrogen or oxygen, respectively.[5-6]

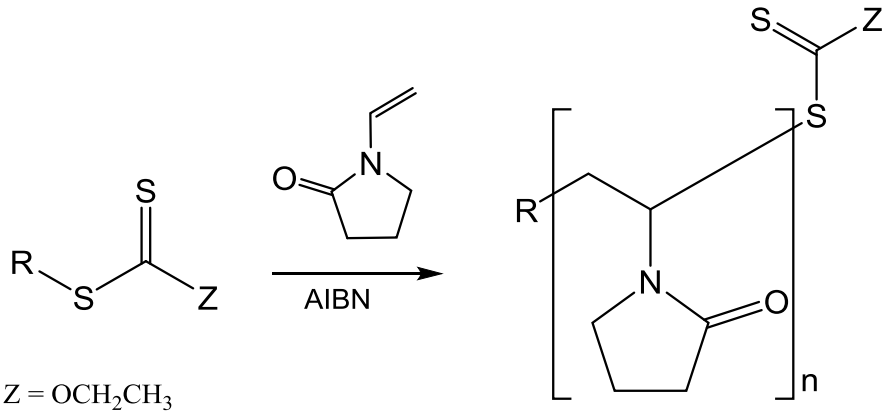

Scheme 3.1: Xanthate mediated polymerisation of *N*VP

In 2005, Wan *et al.* reported the use of benzyl (CH_2Ph) and 1-ethylphenyl (CH_3CHPh) **R** groups in xanthate mediated polymerization of *N*VP achieving simultaneous control of tacticity and molecular weight in the process.[7] As a follow up to that work a number of studies have been conducted showing great success in *N*VP polymerisation using the xanthate moiety with a vast array of R-functionalities. This has recently been reviewed by Mori and Nakahayashi.[8]

3.2 Choice of RAFT agents

The choice of the RAFT agent, particularly the R group is not only dependent on how well the R group stabilises the propagating radical, but also on the post polymerisation modifications that are intended. With the growth in the design of nano drug delivery systems, the challenge becomes having to introduce multiple functional moieties into a single entity, requiring complementary, orthogonal and facile synthetic procedures.[9] In the case of *N*VP polymerisation mediated by xanthate based RAFT agents, the xanthate moiety allows for the introduction of protected ω-chain end functionalities. These can be manipulated into an array of functionalities post polymerisation via thermolysis, oxidation, and reduction to thiols to mention a few.[10] Thiols in particular, are useful moieties that can react in thiol Michael addition reactions [11] in a robust, efficient and orthogonal fashion necessary in the building of complex nanostructures. Moreover, thiols can form disulphide bridges which are valuable functional groups owing to their potential reactivity and biological applications.[12]

As much as the R group has a role of stabilizing the radical generated during the fragmentation step of the intermediate radical, careful choice of this group allows for post-polymerisation functionalisation. Functionalised alkynes and azides have been used to introduce triazole based R leaving groups through CuAAC.[13] These types of R groups have been shown to offer good control over molar mass and molar mass distributions for vinyl acetate, styrene, *n*-butyl acrylate and *N*VP.[14]

For the purposes of polymer conjugation to biomolecules, particularly proteins and peptides, aldehyde end-functional polymers have been used to react with the *N*-terminus of peptides through Schiff base formation,[15] usually followed by reduction to a secondary amine. The aldehyde functionalities can be introduced by conversion of hydroxyls or acetals present in the R group post polymerisation.[16-17]

3.3 Synthesis and characterization of RAFT systems

Three RAFT systems were used in this study. The α-NHS ester, ω-xanthate, α-acetal ω-xanthate and α-hydroxyl, ω-xanthate were synthesised and subsequently employed in mediating the polymerisation of *N*VP to yield α,ω-heterotelechelic PVP.

3.3.1 Synthesis of α-NHS ester, ω-xanthate RAFT agent (2)

As has been mentioned earlier, a xanthate-based RAFT agent is well known to be able to control the polymerisation of *N*VP. The *N*-hydroxysuccinimide ester (NHS-ester; activated ester) functional group has also been shown through several studies to have a stabilising effect on the R group.[18] The other advantage of having these two groups on the α-and ω-chain ends is their reactivity. This allows for an array of functionalities to be introduced post-polymerisation resulting in functional handles that become useful post-polymerisation in the synthesis of complex multifunctional nanostructures like drug delivery systems. Synthesis of the α-NHS ester, ω-xanthate RAFT (**2**) is shown in Scheme 3.2. The first step was to react 2-bromopropionic acid with potassium ethyl xanthate as described by Pound *et al*. in 2008.[19]

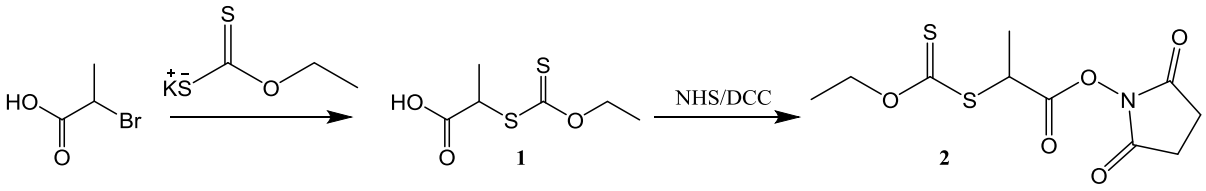

Scheme 3.2: Synthesis α-NHS ester, ω-xanthate RAFT agent

After confirmation of the successful synthesis of compound **2**, it was employed to facilitate the RAFT mediated polymerisation of *N*VP to α-NHS ester, ω-xanthate heterotelechelic. The best results were obtained with solution polymerisation in dioxane targeting a molecular weight of 8333 g/mol at 100 % conversion. The RAFT agent/thermal initiator (AIBN) ratio was 5:1 and the results are summarised in Table 3.1.

Table 3.1: Polymerisation conditions and results for PVP polymerised using RAFT agent 2

α^a (%)	Reaction time (h)	Reaction temp (°C)	$M_{n\ Theo}$ (g/mol)	$M_{n\ NMR}{}^b$ (g/mol)	$M_{n\ SEC}{}^c$ (g/mol)	Đ
60 %	**20**	**60**	**5000**	**5657**	**4762**	**1.16**

[a] Conversion

[b] $M_{n\ NMR}$ (determined by integrating the xanthate signal versus the PVP backbone signal)

[c] $M_{n\ SEC}$ (based on PMMA standards)

In general for RDRP, 1.05 < dispersity (*Đ*) < 1.40 is the acceptable range depending on the targeted molecular weight. RAFT agent **2** was able to control the polymerisation of *N*VP. The molecular weights obtained from SEC and ^{1}H NMR were relatively close to the theoretical molecular weight and the molecular weight distribution was narrow as indicated by the 1.16 dispersity value. Apart from the control of molecular weight and molecular weight distribution, it was also important to ensure that the end groups were retained post polymerisation, particularly the Z group. The temperature that was used for the *N*VP polymerisation was 60 °C and several studies have shown that long reaction times at this temperature could lead to the formation of the unsaturated product of monomolecular elimination of the xanthate.[19] End group analysis was done by ^{1}H NMR as shown in Figure 3.1.

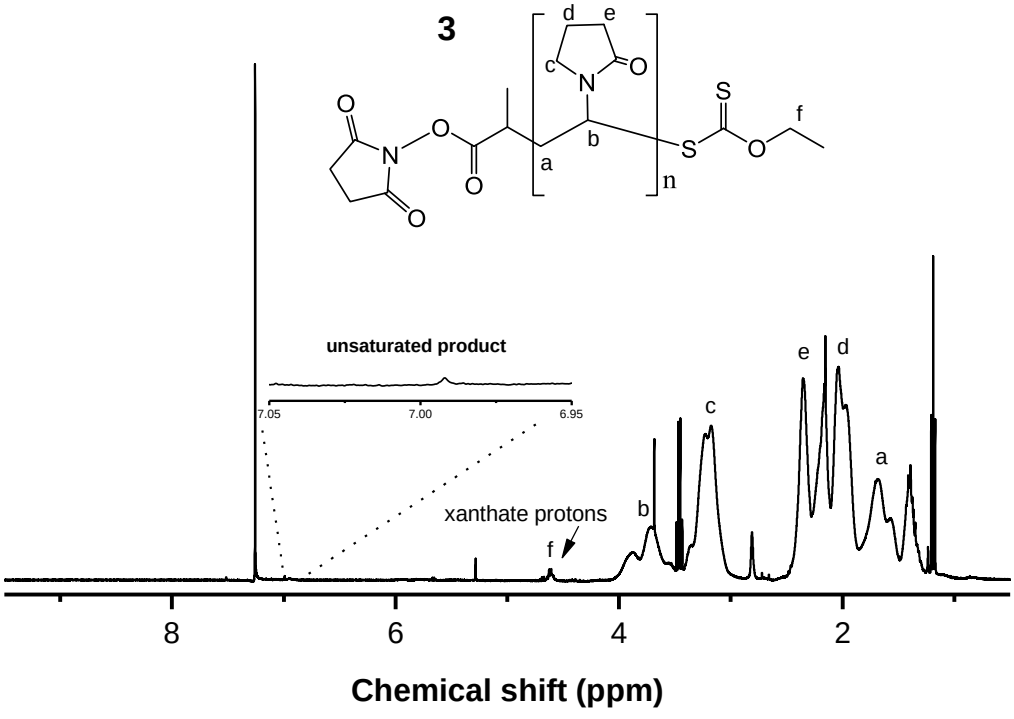

Figure 3.1: Representative ^{1}H NMR spectrum of PVP synthesised using α-NHS ester, ω-xanthate RAFT (2)

From the ^{1}H NMR data, all the PVP peaks could be accounted for and there was little saturation integrating at 1:0.08 relative to the xanthate protons peak. This was attributed to the unsaturated product of monomolecular elimination of the xanthate. The unsaturation was, however, deemed negligible relative to the retained xanthate chain ends.

3.3.1.1 Orthogonality determination of the heterotelechelic system

After having successfully synthesized PVP and retained the chain ends, it was important to determine the orthogonality of ω- and α-chain ends with respect to aminolysis. This was important because both the activated ester (NHS ester) and the xanthate moiety are known to be reactive towards amines. Lack of selectivity of this reaction would make it very difficult to introduce the multiple functionalities into the polymer system. Different molar equivalents of polymer end groups to benzyl amine were used ranging from 1:0.5 to 5 times excess of the amine. From the ^{1}H NMR data (Figure 3.2), it was clear that in all cases both end groups reacted, leading to the conclusion that there was no selectivity.

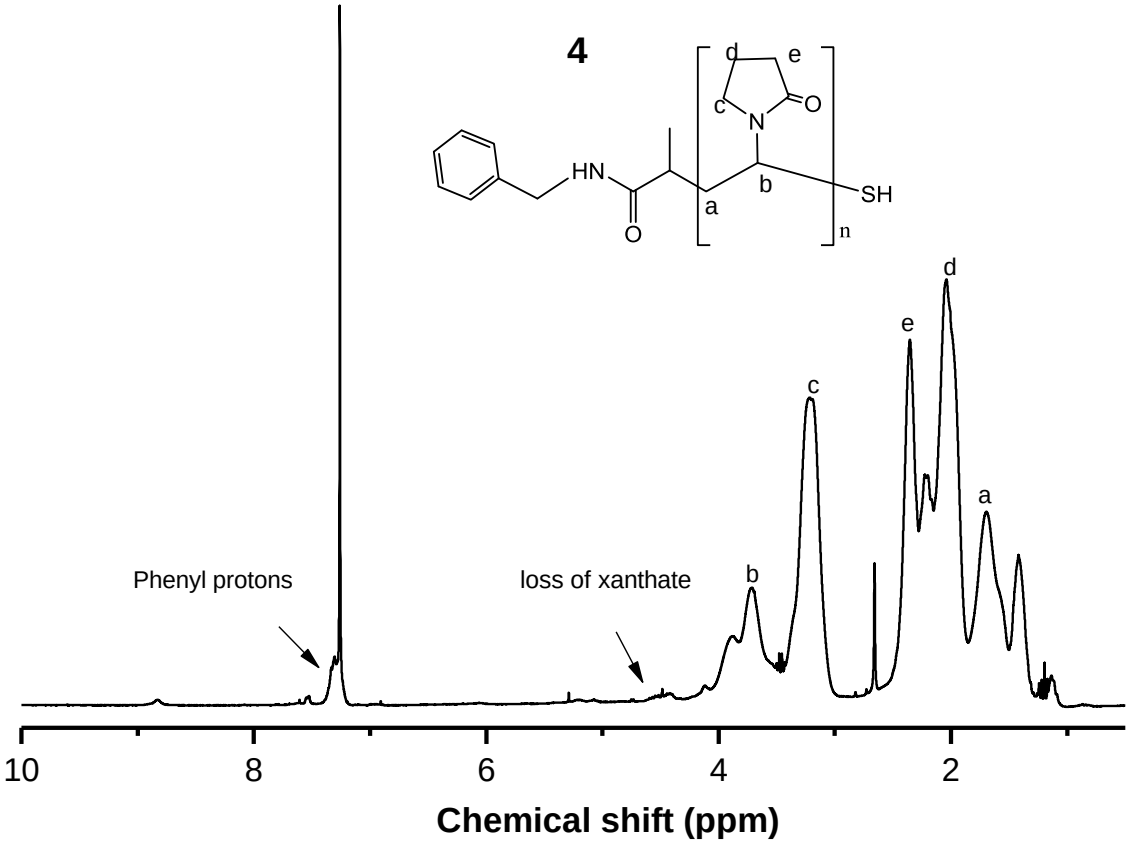

Figure 3.2: Representative ^{1}H NMR spectrum of PVP after aminolysis: PVP end groups: benzyl amine ratio (1:1).

The xanthate end group was lost and at the same time, phenyl proton peaks appeared around 7.1 ppm consistent with the introduction of the benzyl amine on the alfa chain end (Scheme 3.3). This meant

that the α-NHS ester, ω-xanthate RAFT system would not be suited for the post polymerization modifications necessary to construct a PSMA targeted theranostic device.

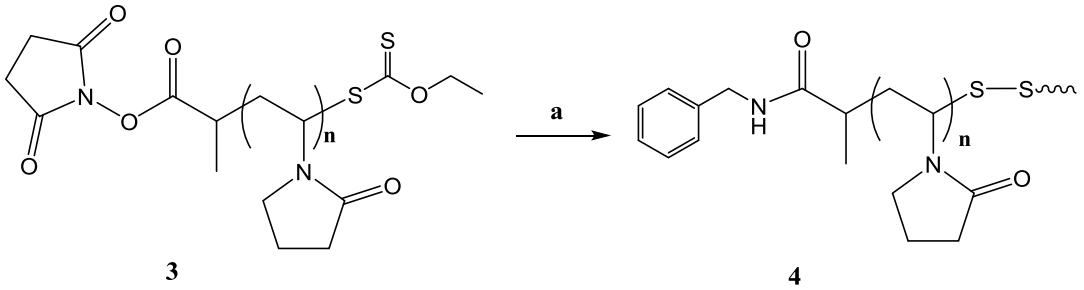

Scheme 3.3: Aminolysis of PVP (3); (a) Benzyl amine, DCM, 40 °C, 14 h.

3.3.2 Synthesis of α-hydroxyl, ω-xanthate RAFT (5)

Due to the challenges that were associated with RAFT system **2**, it was necessary to synthesise an alternative RAFT agent that would overcome the problems associated with the end group modifications. Attention switched to an α-hydroxyl, ω-xanthate RAFT system (**5**). This RAFT agent was synthesised from intermediate **1** by DCC coupling with ethylene glycol yielding an ester based, α-hydroxyl end functional R group (Scheme 3.4). Formation of the product was confirmed by ^{1}H NMR and ^{13}C NMR.

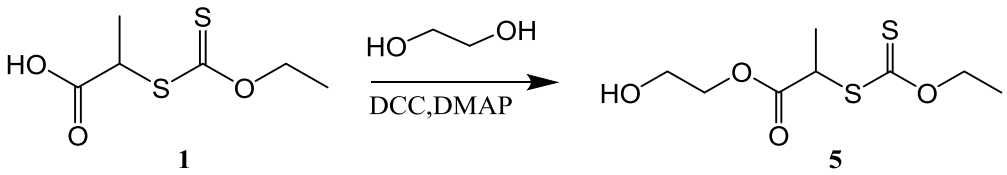

Scheme 3.4: Synthesis of α-hydroxyl, ω-xanthate RAFT

α-Hydroxyl, ω-xanthate heterotelechelic PVP (**6)** was synthesised via RAFT mediated polymerisation using RAFT agent (**5**) in dioxane targeting a molecular weight of 6666 g/mol at 100 percent conversion. The RAFT agent/thermal initiator (AIBN) ratio was kept at 5:1 and the results are summarised in Table 3.2.

Table 3.2 : Polymerisation conditions and data for PVP polymerised using RAFT agent 5

α[a] (%)	Reaction time (h)	Reaction temp (°C)	$M_{n\ (Theo)}$ (g/mol)	$M_{n\ (SEC)}$[b] (g/mol)	Đ
60 %	20	60	4000	2774	1.14

[a] Conversion

[b] M_n SEC (based on PMMA standards)

RAFT **5** was successfully used to mediate the polymerisation of NVP to form α-hydroxyl, ω-xanthate, heterotelechelic PVP with a narrow molecular weight distribution i.e. dispersity of 1.14. There was a difference in the theoretical M_n compared to the M_n obtained from SEC. This was not a surprise because the SEC molecular weight data was derived from hydrodynamic volume on a GPC system calibrated with PMMA standards. End group analysis was done by ^{1}H NMR (Figure 3.3).

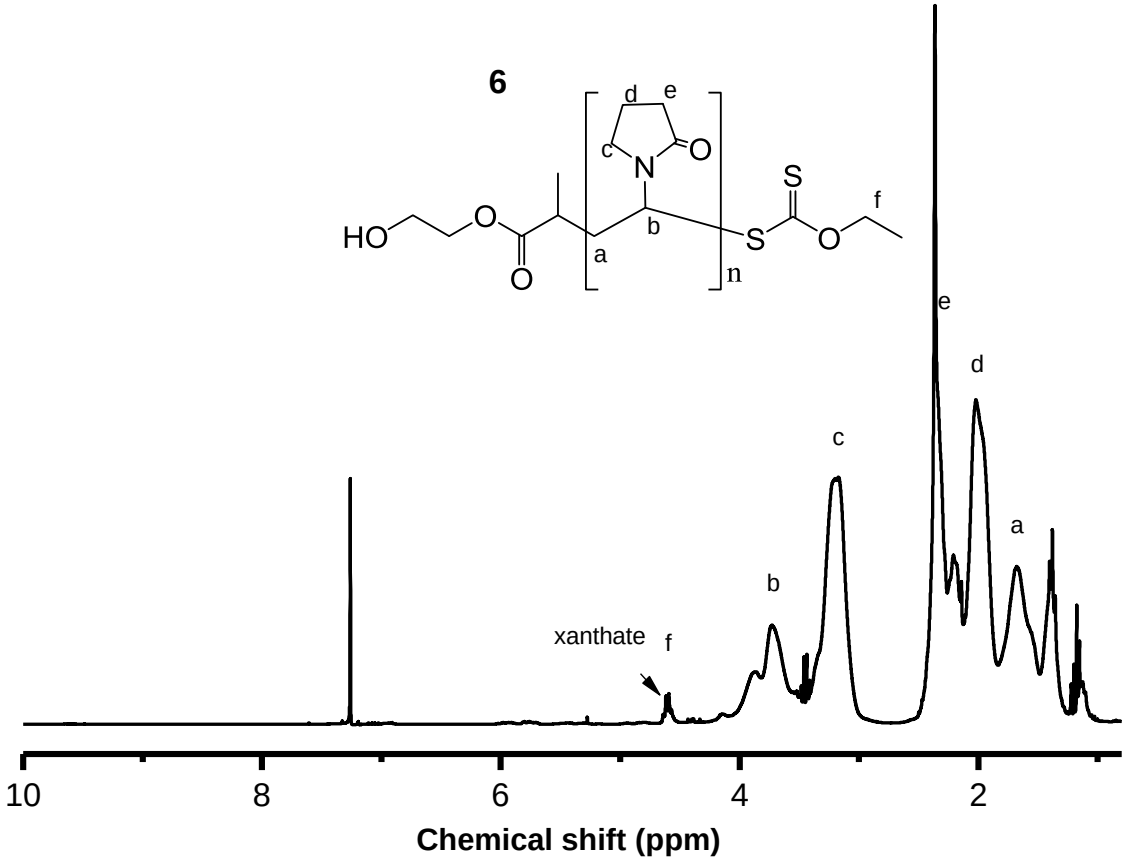

Figure 3.3: Representative ^{1}H NMR spectrum of PVP synthesised using α-hydroxyl, ω-xanthate RAFT (5)

3.3.2.1 Aminolysis

It was important that post-polymerisation, the ω-chain end be reduced to thiol. In most instances this also leads to formation of disulphide bridges accompanied by doubling of molecular weight. However, it was important that reaction with the amine be limited to the ω-chain end making sure that the hydroxyl group on the α-chain end was retained for further post polymerisation modifications. This was done by using ethanolamine as the aminolysis agent. In the event that the amine group on the aminolysis agent reacts on the R group, the potential reaction would be a transamidation with the ester in the R-group which would lead to an amide, but still bearing a hydroxyl-functional end group. Aminolysis was done as shown in Scheme 3.5.

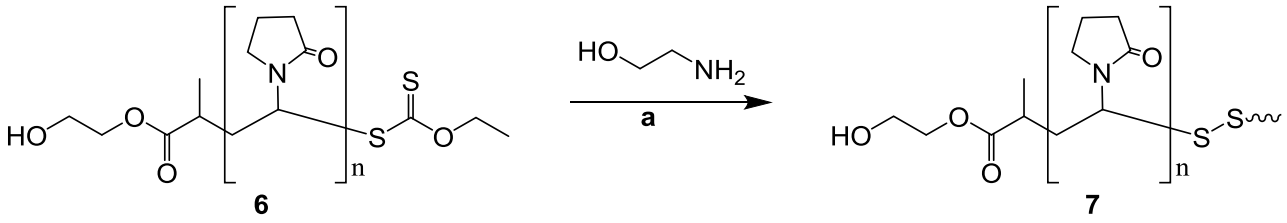

Scheme 3.5: Aminolysis of α-hydroxyl, ω-xanthate functional heterotelechelic PVP; (a) DCM, r.t, 14 h.

Modification of RAFT polymers by aminolysis normally leads to the loss of the xanthate group followed by the subsequent formation of thiol and this was observed by ^{1}H NMR. To ensure that the thiol was converted to disulphide, the aminolysis reaction was performed under oxidising conditions. SEC data showed a shift towards higher molecular weight indicated by lower elution volume, which was attributed to disulphide bridge formation. In the case of total conversion of thiol to disulphide, the M_n would be expected to double. However, free thiols were still expected.

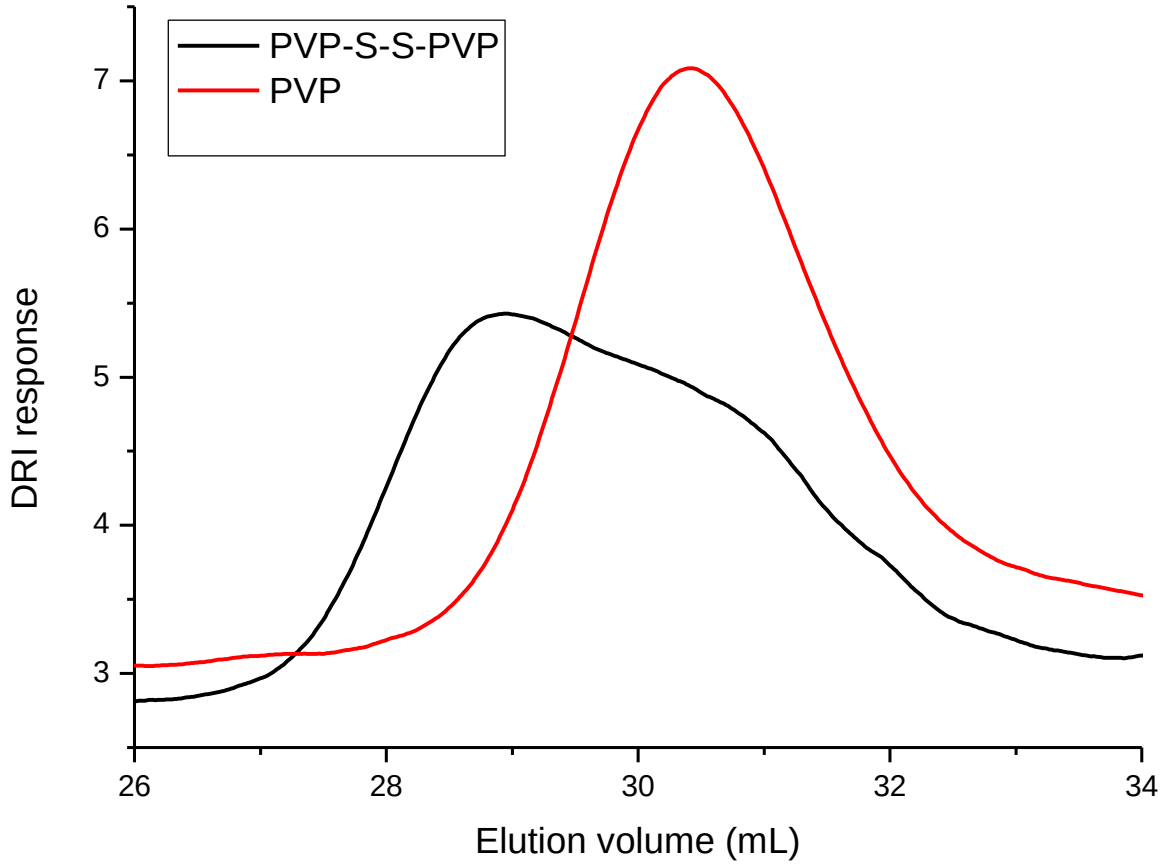

Figure 3.4: Representative SEC chromatogram of PVP synthesised from RAFT agent 5, before and after aminolysis.

PVP synthesised from α-hydroxyl, ω-xanthate RAFT agent (**6**) was kept for further post polymerisation modifications leading to conjugation studies.

3.3.3 Synthesis of α-acetal, ω-xanthate RAFT agent (8)

As was mentioned in the case of the synthesis of α-hydroxyl, ω-functional RAFT agent (**5**), the end goal was to introduce an aldehyde functionality at the α-chain end of the polymer to facilitate Schiff-base formation with the *N* terminus of the ligand during the conjugation studies. Linear acetals can also be converted into aldehydes. In work that was done in our group, Reader *et al.* concluded that linear acetals were more favourable compared to cyclic acetals when employed as part of a triazole based R-leaving group.[17] The sp_2 hybridised nitrogen on the triazole ring complicates the acid catalysed deprotection of the cyclic system by donating an electron pair to the acid at the expense of the oxygen on the cyclic acetal. Having taken that into consideration, it was necessary to synthesise α-linear acetal, ω-xanthate functional RAFT agent by a method described by Reader *et al*. as shown in Scheme 3.6.

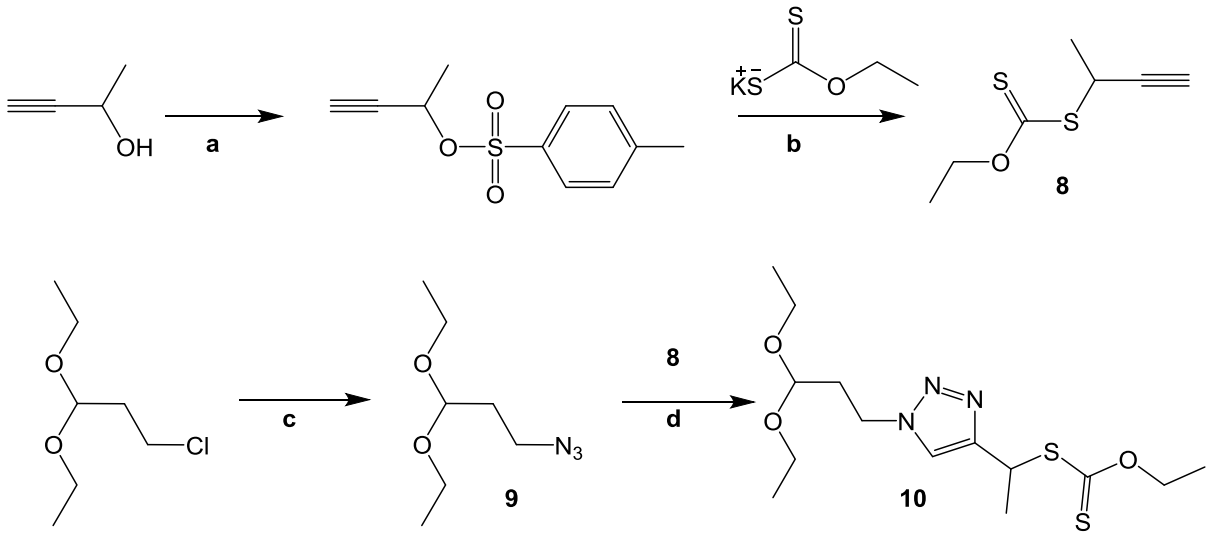

Scheme 3.6: Synthesis of α-acetal, ω-xanthate RAFT agent (10); (a) Tosyl chloride, KOH, diethyl ether, 0 °C to r.t; (b) THF, r.t; (c) sodium azide, DMSO, 50 °C, 16 h, (d) $CuSO_4$, sodium ascorbate, DMF, r.t.

But-3-yn-2ol was reacted with tosyl chloride to form an activated alcohol before addition of potassium ethyl xanthate in THF to yield an alkyne terminated xanthate derivative. Chloro-acetal was converted into an azide terminated acetal by reacting with NaN_3. The alkyne terminated xanthate derivative and the azide functional acetal were reacted via copper catalysed alkyne-azide cycloaddition (CuAAC) to yield **10** with a triazole based R leaving group. ^{1}H NMR confirmed the successful synthesis **10**. All the peaks of interest could be accounted for. The characteristic triazole proton peak was visible around 7.5 ppm was clearly visible. The methyl and methylene proton peaks on the xanthate moiety were also visible at 1.27 ppm and 4.61 ppm respectively (Figure 3.5).

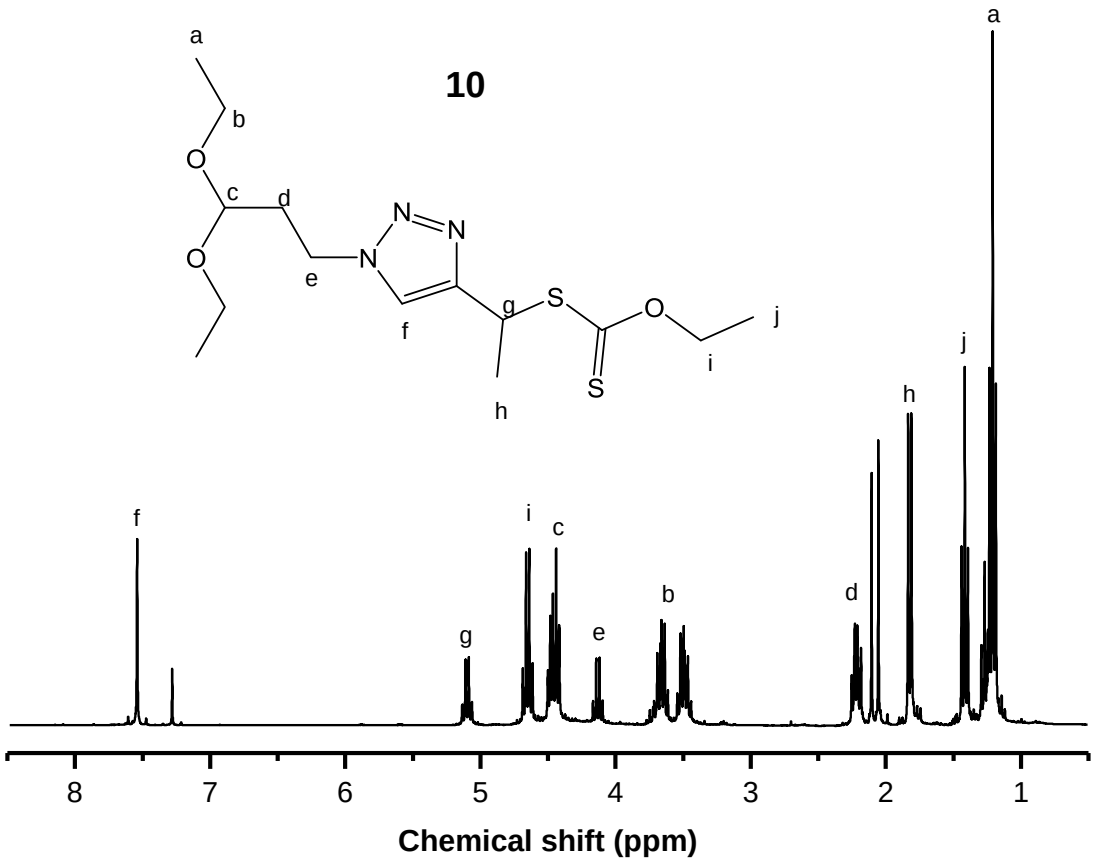

Figure 3.5: Representative ^{1}H NMR spectrum of RAFT agent 10

3.3.3.1 Polymerisation of *N*VP

*N*VP polymerisation was mediated using **10** for 20 hours at 60 °C. A theoretical molar masses of 3000 g/mol and 5000mg/mol were calculated at 60 % conversion. Table 3.3 summarises the data that was collected.

Table 3.3: Polymerisation conditions and data for PVP synthesised from 10

α[a] (%)	Reaction time (h)	Reaction temp (°C)	$M_{n\ (Theo)}$ (g/mol)	$M_{n\ (SEC)}$[b] (g/mol)	Đ
60 %	20	60	3000	2344	1.13
60 %	20	60	5000	4320	1.21

[a] Conversion

[b] $M_{n\ SEC}$ (based on PMMA standards)

The molar mass and dispersity of the polymer system were determined using SEC calibrated with PMMA standards. End group analysis was done by ^{1}H NMR. This was important to ascertain the 'living' character of the polymerisation (Figure 3.6). As was the case in the polymerisation mediated

by **5** the M_n (SEC) was significantly lower than the theoretical M_n. The discrepancies could be attributed to SEC data being derived from the hydrodynamic volume of the polymer chains based on PMMA standards due to the unavailability of PVP standards. On the other hand, good control in terms of molecular weight distribution was attained as indicated by the dispersity of 1.13. Both the R and Z group chain end functionalities were retained as indicated by the peaks at 4.03 and 4.6 ppm (Figure 3.6) corresponding to the methylene protons next to the triazole ring (*g*) and the xanthate peak (*f*) respectively. The two peaks integrated at 1:1.

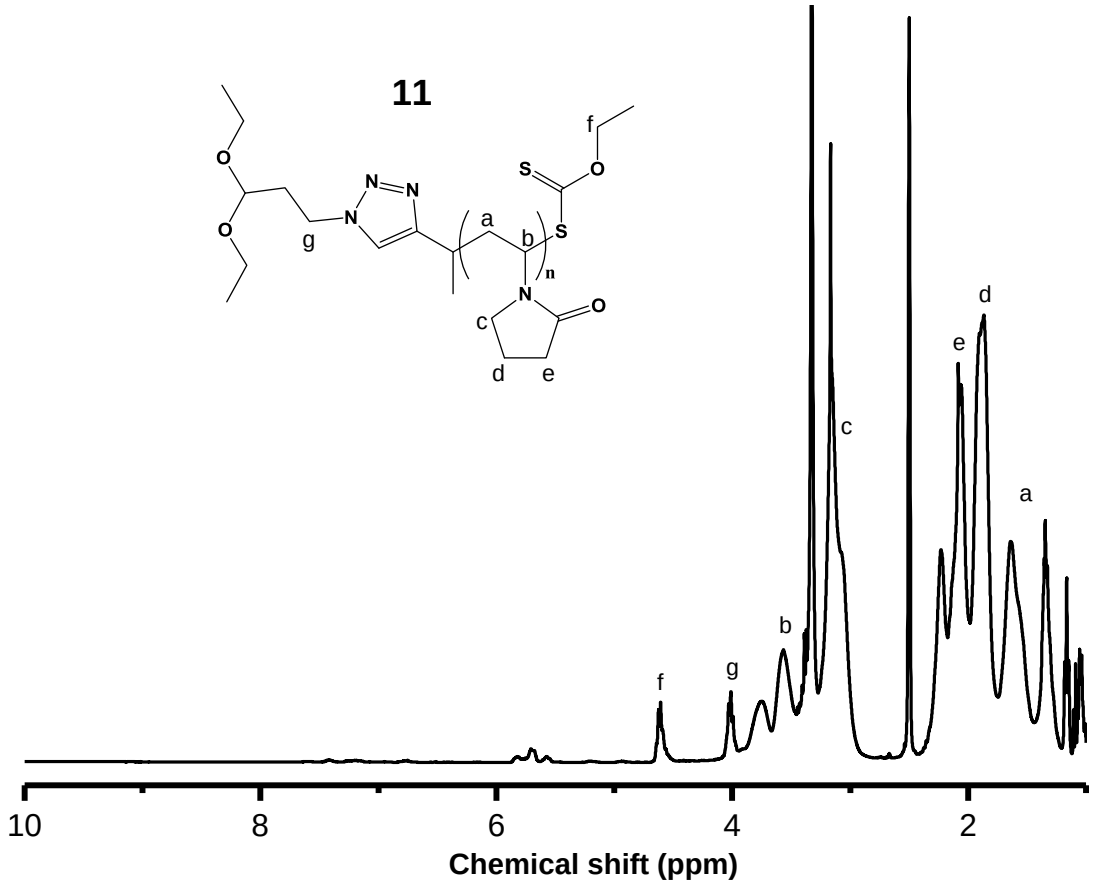

Figure 3.6: Representative ^{1}H NMR spectrum of PVP (11)

3.4 Conclusions

Three ω-xanthate based RAFT systems (α-NHS ester, α-hydroxyl and α-acetal) were employed in the polymerisation of *N*VP to investigate their suitability with respect to chain end retention and to orthogonal post-polymerisation modification. The NHS ester RAFT agent offered good control of polymerisation yielding M_n values relatively close to the predicted theoretical molecular weights, narrow molecular weight distributions as well as good retention of chain ends. However, this system fell short when it was subjected to aminolysis post polymerisation. The respective α- and ω-chain ends were transformed simultaneously in the presence of primary amines and lowering the molar equivalence of amine with respect to the polymer end groups did not improve the selectivity of the system.

The other two xanthate based RAFT systems namely, α-hydroxyl and α-acetal were also able to control the polymerisation of *N*VP and the dispersities were well within the acceptable range. These two systems showed that during aminolysis, only the xanthate functionality was transformed. Furthermore the respective α-chain ends had functional groups capable of transformation to aldehyde functionalities (hydroxyl and acetal). This was important for the later stages in which the aldehyde functionality would be necessary for conjugation reactions via the *N*-terminus of our intended PSMA ligand. Based on the aforementioned reasons, PVP **6** and **10** were selected as the candidates for the post-polymerisation reactions that followed.

3.5 Experimental

3.5.1 General experimental details

Chemicals and solvents used were bought from commercial sources and were generally used without further purification, unless in cases where it was mentioned. Recrystallization of 2,2'-Azobis(isobutyronitrile) (AIBN) (Riedel-de Haën) was done from methanol followed by drying under reduced pressure at ambient temperature. *N*VP was dried and distilled before polymerisations. The monitoring of Reactions was done using thin layer chromatography (TLC), which utilised Machery-Nagel Silica gel 60 plates with a UV 254 fluorescent indicator. An inert argon atmosphere was used for all moisture and oxygen sensitive reactions. ^{1}H-NMR and ^{13}C-NMR spectra were recorded on a Varian VXR-Unity (400 MHz) spectrometer. Samples preparation was done in deuterated solvents obtained from Cambridge Isotope labs. NMR spectra chemicals shifts were reported in parts-per-million (ppm) referenced to the residual solvent protons. Size exclusion chromatography (SEC) was used to measure the molecular weight of polymers. The SEC system comprised of a Shimadzu LC-10AT isocratic pump, a Waters 717+ autosampler, a column system fitted with a PSS guard column (50×8 mm) in series with three PSS GRAM columns (300×8 mm, 10 µm, 2 × 3000 Å and 1 × 100 Å) kept at 40 °C, a Waters 2487 dual wavelength UV detector and a Waters 2414 differential refractive index (DRI) detector. Dimethylacetamide (DMAc) was used as the eluent.The stabilising agents were 0.05 % BHT (*w/v*) and 0.03 % LiCl (*w/v*), at a flow rate of 1 mL·min^{-1}. GHP filters of 0.45 µm pore size were used to filter the polymer samples to facilitate removal of impurities prior to analysis. PMMA standard sets ranging from 690 to 1.2 × 10^{6} g·mol^{-1} obtained from Polymer Laboratories were used to carry out calibration. Data was acquired fromMillennium[32] software, version 4.

3.5.2 Synthetic procedures

2-((Ethoxycarbonothioyl)thio)propanoic acid (1): 1 was synthesised as described by Pound *et al*.[19] 30 g of distilled water was used to dissolve potassium-*O*-ethyl xanthate (10.08 g, 6.25×10^{-2} mol). As the reaction was stirring, 3.3 M sodium hydroxide (15 mL) was added to the mixture at 0 °C. This was followed by dropwise addition of 2-bromopropionic acid (7.6 g, 5.0×10^{-2} mol). The reaction was left to stir overnight at room temperature, after which the pH of the solution was adjusted from pH 7 to pH 1 using using 2 M HCl. Extraction of the product, was achieved with diethyl ether (2 × 200 mL). Sodium hydroxide solution was used to extract product from diethyl ether (25 g in 25 mL H_2O, 2 × 50 mL). 1 M HCl was used to adjust the pH to 3. Diethyl ether was used to extract the product from the acidic solution (200 mL). The organic phase was dried over anhydrous magnesium sulphate and the solvent was removed under reduced pressure. The product was recrystallized from hexane.

White crystals were obtained. The yield was 78 %.^{1}H NMR (400 MHz, $CDCl_3$) δ 4.69 – 4.58 (q, 2H), 4.42 (q, *J* = 7.4 Hz, 2H), 1.60 (d, *J* = 7.5 Hz, 2H), 1.42 (t, *J* = 7.1 Hz, 3H).

2,5-Dioxopyrrolidin-1-yl 2-((ethoxycarbonothioyl)thio)propanoate (2): 1 (2.09 g, 0.011 mol) was dissolved in 200 mL chloroform. The reaction mixture was cooled to 0 °C and argon was flushed for 30 minutes. This was followed by portion wise addition of DCC (2.27 g, 0.011 mol) and NHS (1.27 g, 0.011 mol). The reaction was left to proceed at room temperature for 24 hours. The reaction mixture was filtered and the solvent removed under reduced pressure. A minimal amount of ethyl acetate was added to the reaction flask. The mixture was filtered and the solvent removed under reduced pressure. A yield of 56 % was obtained. ^{1}H NMR (400 MHz, $CDCl_3$) δ 4.72 – 4.65 (q, 2H), 4.64 – 4.58 (q, 1H), 2.82 (s, *J* = 8.5 Hz, 4H), 1.70 (d, *J* = 7.4 Hz, 3H), 1.42 (t, *J* = 9.2, 5.1 Hz, 3H). ^{13}C NMR (101 MHz, $CDCl_3$) δ 209.77, 167.43, 77.24, 76.92, 76.60, 70.80, 44.08, 25.50, 16.39, 13.41.

2-hydroxyethyl 2-((ethoxycarbonothioyl)thio)propanoate (5): **1** (3.0 g, 0.015 mol), ethylene glycol (4.79 g, 0.077 mol) and DMAP (0.094 g, 7.72×10^{-4} mol) were added to distilled DCM and cooled to 0 °C. DCC was added portion wise while stirring. The reaction was allowed to warm to room temperature on its own accord and left to stir for 24 hours. The reaction mixture was passed through an aluminium oxide column to remove the formed DCU. The filtrate was washed with water (3 × 50 mL), dried over magnesium sulphate, filtered and concentrated. Minimal amount of ethyl acetate was added to the product before it was left in the freezer overnight. The product was purified via column chromatography, pentane: ethyl acetate (2:1) to yield a yellow oil. ^{1}H NMR (600 MHz, $CDCl_3$) δ 4.61 (q, *J* = 7.1 Hz, 2H), 4.39 (q, *J* = 7.4 Hz, 1H), 4.29 – 4.21 (t, 2H), 1.56 (d, *J* = 7.4 Hz, 3H), 1.39 (t, *J* = 7.1 Hz, 3H). ^{13}C NMR (100 MHz, $CDCl_3$) δ 212.23, 171.68, 70.40,

***S*-(But-3-yn-2-yl) *O*-ethyl carbonodithioate (8). 8** was prepared as described by Reader *et al*.[17] But-3-yn-2-ol (10.0 g, 142 mmol), tosyl chloride (32.6 g, 171 mmol) and THF (100 mL) were introduced into a 250 mL round bottom flask and the mixture was cooled to 0 °C in a sodium chloride/ice bath. Potassium hydroxide (20.2 g, 360 mmol) was portion wise over 20 minutes after which the suspension was stirred for 3 hours, warming to room temperature on its own accord. The mixture was filtered washed with water (2 × 50 mL), dried over magnesium sulphate and concentrated to yield a white crystalline solid that was used immediately in the next step.

Potassium ethyl xanthate (20.6 g, 129 mmol) and THF (80 mL) were added to the crude activated alcohol (24.0 g. 107 mmol) in a 250 mL round bottom flask and allowed to stir at room temperature overnight. The reaction mixture was filtered, concentrated and purified via column chromatography

(eluent; diethyl ether: pentane, 4:1, to yield a pale yellow oil. ^{1}H NMR (400 MHz, $CDCl_3$) δ 4.73 – 4.56 (q, 2H), 3.74 (q, 1H), 1.87 – 1.75 (s, 1H), 1.62 – 1.51 (d, 3H), 1.45 – 1.36 (t, 3H).

3-Azido-1,1-diethoxypropane (9): 3-chloro-1,1-diethoxypropane (4.98 g, 29.9 mmol) and NaN_3 (2.45 g, 37.5 mmol) were added to 100 mL round bottom flask with 60 mL DMSO and stirred at 50 °C for 16 hours. The reaction mixture was poured into 50 mL of ice water and extracted with ethyl acetate (3 × 30 mL), saturated with brine (30 mL) and dried over magnesium sulphate. The solvent was evaporated under reduced pressure to yield the product as a yellow oil. Yield = 81 %. ^{1}H NMR (400 MHz, $CDCl_3$) δ 5.05 (t, 1H), 3.30 (q, 2H), 3.17 (t, 2H), 2.08 (q, 2H), 1.41 (t, 3H).

***S*-(1-(1-(3,3-Diethoxypropyl)-1*H*-1,2,3-triazol-4-yl)ethyl) *O*-ethyl carbonodithioate (10):** the compound was synthesised as described by Reader *et al*.[17] A 50 mL round bottom flask was charged with (**8**) (3.71 g, 21.4 mmol) and (**9**) (3.81 g, 21.4 mmol in 10 mL of dry DMF. Argon gas was bubbled through the reaction mixture for 15 minutes. Copper (II) sulphate pentahydrate (0.53 g, 2.14 mmol and sodium ascorbate (1.72 g, 6.43 mmol) were added to another round bottom flask with 5 mL DMF. Argon was bubbled through the solution for 15 minutes. The second solution was then added to the first and the reaction was left to stir overnight at room temperature. The resultant mixture was diluted with 50 mL THF and passed through an alumina column and the solvent was removed under reduced pressure. The product was purified using column chromatography (eluent; diethyl ether: pentane 4:1) to yield the RAFT agent (**10**). ^{1}H NMR (400 MHz,$CDCl_3$) δ 7.50 (s, 1H), 5.06 (q, *J* = 7.2 Hz, 1H), 4.62 (q, *J* = 7.1 Hz, 2H), 4.45 (t, *J* = 5.4 Hz, 1H), 4.40 (t, *J* = 7.1 Hz, 2H), 3.63 (dq, *J* = 9.3, 7.1 Hz, 2H), 3.53 – 3.40 (m, 2H), 2.18 (td, *J* = 7.0, 5.5 Hz, 2H), 1.79 (d, *J* = 7.2 Hz, 3H), 1.38 (t, *J* = 7.1 Hz, 3H), 1.18 (t, *J* = 7.0 Hz, 6H).

General procedure for NVP polymerisation:

Distilled NVP (2.86 g, 0.026 mol), AIBN (11.25 mg, 0.072 mmol and RAFT agent (**2**) (0.1 g, 0.343 mmol) were carefully weighed into a 30 mL Schlenk flask containing a magnetic stirrer. Dioxane was added to make a 1:1 v/v with NVP. Four freeze-pump-thaw cycles were done before filling the flask with argon. The flask was placed in an oil bath at 60 °C. The polymerisation was left to run for a predetermined time. When the polymerisation was finished, the solution was precipitated into diethyl ether and centrifuged. The precipitate was re-dissolved in DCM, precipitated in diethyl ether and centrifuged again. This process was repeated twice. Finally, the polymer was dried under reduced pressure overnight at room temperature. The polymerisation procedure was repeated for RAFT agent **5** and **9**.

General aminolysis procedure: PVP (**6**) (1.00 g 0.312 mmol, M_n = 2774 g/mol, $Đ$ = 1.14) was dissolved in 10 mL of DCM. The solution was heated to 40 °C and 2-aminoethanol (190 mg, 3.13 mmol) was added dropwise. The reaction was left to proceed at room temperature for 14 hours under oxidising conditions. The product was dissolved in minimal DCM, precipitated with di ethyl ether and centrifuged. The process was repeated three times. The aminolysis procedure was the same as for PVP (**3).**

3.6 References

(1) Stace, S. J.; Moad, G.; Fellows, C. M.; Keddie, D. J., *Polym. Chem.* **2015**, 6, 7119.

(2) Johnson, I. J.; Khosravi, E.; Musa, O. M.; Simnett, R. E.; Eissa, A. M., *J. Polym. Sci. A Polym. Chem.* **2015**, 53, 775.

(3) Moad, G.; Rizzardo, E.; Thang, S. H., *Aust. J. Chem* **2012**, 65, 985.

(4) Keddie, D. J.; Moad, G.; Rizzardo, E.; Thang, S. H., *Macromolecules* **2012**, 45, 5321.

(5) Postma, A.; Davis, T. P.; Evans, R. A.; Li, G.; Moad, G.; O'Shea, M. S., *Macromolecules* **2006**, 39, 5293.

(6) Bilalis, P.; Pitsikalis, M.; Hadjichristidis, N., *J. Polym. Sci. A Polym. Chem.* **2006**, 44, 659.

(7) Wan, D.; Satoh, K.; Kamigaito, M.; Okamoto, Y., *Macromolecules* **2005**, 38, 10397.

(8) Nakabayashi, K.; Mori, H., *Eur. Polym. J.* **2013**, 49, 2808.

(9) Pearce, A. K.; Rolfe, B. E.; Russell, P. J.; Tse, B. W. C.; Whittaker, A. K.; Fuchs, A. V.; Thurecht, K. J., *Polym. Chem.* **2014**, 5, 6932.

(10) Willcock, H.; O'Reilly, R. K., *Polym. Chem.* **2010**, 1, 149.

(11) Northrop, B. H.; Frayne, S. H.; Choudhary, U., *Polym. Chem.* **2015**, 6, 3415.

(12) Sun, C.-L.; Xu, J.-F.; Chen, Y.-Z.; Niu, L.-Y.; Wu, L.-Z.; Tung, C.-H.; Yang, Q.-Z., *Polym. Chem.* **2016**, 7, 2057.

(13) Gondi, S. R.; Vogt, A. P.; Sumerlin, B. S., *Macromolecules* **2007**, 40, 474.

(14) Akeroyd, N.; Pfukwa, R.; Klumperman, B., *Macromolecules* **2009**, 42, 3014.

(15) Sayers, C. T.; Mantovani, G.; Ryan, S. M.; Randev, R. K.; Keiper, O.; Leszczyszyn, O. I.; Blindauer, C.; Brayden, D. J.; Haddleton, D. M., *Soft Matter* **2009**, 5, 3038.

(16) Bilgic, T.; Klok, H.-A., *Biomacromolecules* **2015**, 16, 3657.

(17) Reader, P. W.; Pfukwa, R.; Jokonya, S.; Arnott, G. E.; Klumperman, B., *Polym. Chem.* **2016**, 7, 6450.

(18) Bulmus, V., *Polym. Chem.* **2011**, 2, 1463.

(19) Pound, G., PhD thesis, University of Stellenbosch, **2008**.

4 PVP chain end functionalisation, target ligand synthesis and conjugation

4.1 Introduction

Polymeric drug systems with α- and ω-chain end functional moieties have been synthesised in recent years, particularly via RAFT mediated polymerisation. The specific handles that are presented post-polymerisation are necessary for conjugation to drugs and targeting moieties leading to the development of multifunctional drug delivery nano-systems. These nano-systems have been successfully employed for malaria[1] and other infectious diseases as well as for cancer,[2] and other non-communicable diseases.[3] The careful and appropriate employment of robust, orthogonal and efficient chemistries is important in the modification of the formed functional handles.[4] As was mentioned and described in the Chapter 3, RDRP techniques result in the introduction of an array of functional handles that become useful post-polymerisation.

RAFT mediated polymerisation in particular, apart from being tolerant to a wide variety of functionalities, provides heterotelechelic systems with functional handles that can undergo facile post polymerisation transformations necessary for biological applications.[5] A good example is the conjugation to targeting moieties, specifically peptide based therapeutic agents and targeting moieties via the *N*-terminus. Aldehyde terminal polymers have an important role to play in terms of reacting with *N*-termini.[6] RAFT mediated polymerisation has been employed by Pound *et al*. to synthesise ω-aldehyde functional PVP via quantitative post polymerisation conversion of the xanthate moiety. The aldehyde terminated polymer was used for conjugation to lysozyme using the amino groups present in the protein.[7] Xiao and co-workers have also successfully attached proteins on a micellar surface with aldehyde groups via oxime coupling.[8] The same chemistry can also be employed for conjugation to therapeutic agents.

In RAFT mediated polymerisations, two methodologies are normally employed, *i.e.* polymerisation with a chain transfer agent that contains reactive moieties, but are inert towards the reaction conditions,[9] and polymerisation with a chain transfer agent that contains protected functionalities that can be deprotected post polymerisation to yield the desired functionalities for coupling, conjugation or any reactions necessary for building complex, multifunctional nanostructures like polymeric drug delivery systems.[10] The chemistry between aldehydes and amines (Schiff base reaction) via the *N*-

terminus of biomolecules especially peptide based targeting ligands and therapeutic agents has been exploited to good effects in recent studies.[10]

Targeted drug delivery systems in cancer therapy have been designed in many forms, but a lot of research effort has been invested in designing polymer-peptide conjugated systems that combine the therapeutic effect of the normally hydrophobic, cationic anti-cancer peptides with the structural component of the hydrophilic polymers. These constructs often self-assemble into complex nano-structures such as micelles and vesicles.[11] Through robust, efficient and orthogonal chemistry, the drug delivery construct can subsequently be decorated with targeting moieties. In the case of cancer, folic acid derivatives, antibody fragments and small molecule ligands have been used.[12] Optical imaging modalities e.g. fluorescent markers can be added to evaluate the targeting efficiency of the ligands. In addition, the therapeutic agent is hidden from the immune system, until it is released under a physiological trigger, such as a change in pH or temperature.[13]

In the case of prostate cancer, prostate specific membrane antigen (PSMA) has been established as a viable target. It is a type II transmembrane glycoprotein (also called carboxypeptidase glutamate II) that is highly restricted to, and overexpressed in prostate cancer cells at about 100- to 1000-fold higher than in moderately expressed normal tissues, and multiple studies report that normal prostate tissue predominantly expresses a splice variant that does not contain the transmembrane domain. [12, 14-15] The possibility of drug delivery into prostate tissue through the PSMA and other cell markers has recently been explored using a variety of cell marker directed ligands such as aptamers, antibodies and small molecules that bind to the cell surface.[15] These molecules should have high affinity to their cognate receptors and have the natural ability to induce receptor-mediated endocytosis.[16]

In this study, a glutamate urea based small molecule ligand was synthesized and conjugated to the polymer system via reductive amination. The targeting ligand employed is shown in Figure 4.1.

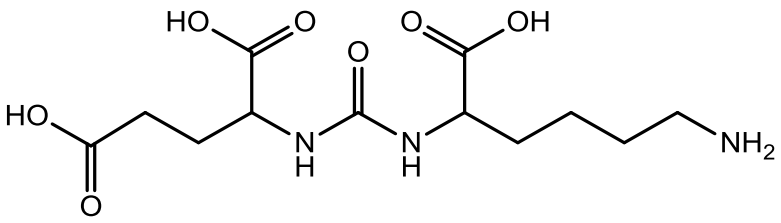

Figure 4.1: Glutamate urea targeting ligand

4.2 Formation of α-aldehyde functional PVP

Polymers **7** and **11** synthesised and reported in Chapter 3 had hydroxyl and acetal alpha chain end functionalities, respectively. It was necessary that these end groups be converted into aldehydes necessary for Schiff base formation with the *N*-terminus of the targeting ligand during conjugation.

4.2.1 Oxidation of α-hydroxyl PVP system

In the case of PVP **7**, the as synthesised polymer was exposed to mild oxidising conditions by stirring in DMSO for 24 h at room temperature before adding acetic anhydride as the activating agent making up a 10:1 (v/v) DMSO: acetic anhydride solution. The reaction was allowed to stir for 48 h under an inert environment according to a method described by Bilgic *et al.*[17] (Scheme 4.1)

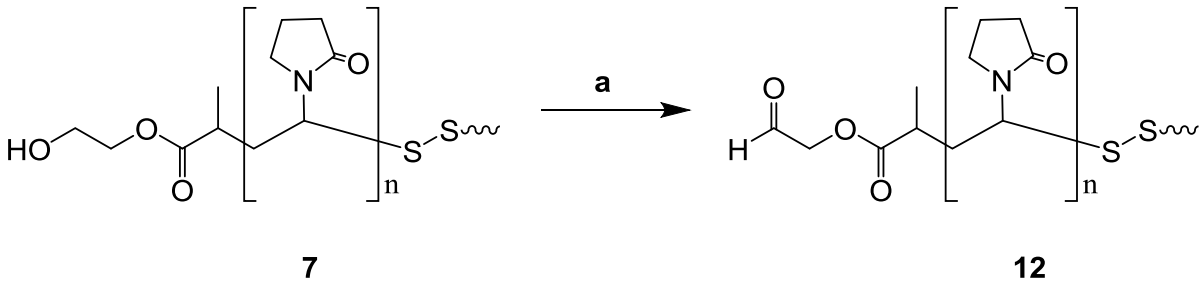

7 **12**

Scheme 4.1: Oxidation of α-hydroxyl functional PVP; (a) DMSO/acetic anhydride 10:1 (v/v), 72 h, r.t.

From the ^{1}H NMR data, only a very weak aldehyde proton peak at around 9.7 ppm could be detected having followed the method described by Bilgic *et al.* on molecular brushes. The reaction was repeated three more times, but the results were consistent. It was concluded that the synthesised polymer system **12** was not functionalised sufficiently enough to proceed to the delicate conjugation reactions. Attention was then switched to the alpha acetal functionalised PVP system **11**.

4.2.2 Deprotection of α-acetal, ω-xanthate heterotelechelic PVP system.

Deprotection of protected bi-functional heterotelechelic systems in an orthogonal fashion is a big challenge in complex systems. Reader *et al.* explored different acetal deprotection strategies before concluding that the acetal functionality was easily deprotected under acidic conditions in a manner that did not affect the integrity of the xanthate moiety. The xanthate moiety itself is well known to be easily cleaved under aminolysis conditions. Based on these two factors, a one pot deprotection strategy was implemented relying on disulphide bridge formation. PVP **11** was treated with 3 times excess of *n*-hexylamine and the reaction was performed in acetone at room temperature in a method described by Reader *et al.*[10] A balloon of oxygen was connected to the neck of the reaction vessel in an attempt to force disulphide bridge formation. Despite the effort it was expected that some thiol

terminated chains would still be present. However, this was not quantified. After a reaction time of 4 hours, HCl in dioxane (4 M) was added dropwise, bringing the overall concentration to 1 M HCl in the reaction mixture. The molar ratio of HCl to PVP (**11**) was 10:1. This was to ensure that there was complete deprotection of the acetal functionality. The excess *n*-hexylamine is expected to be converted into its chloride salt (Scheme 4.2).

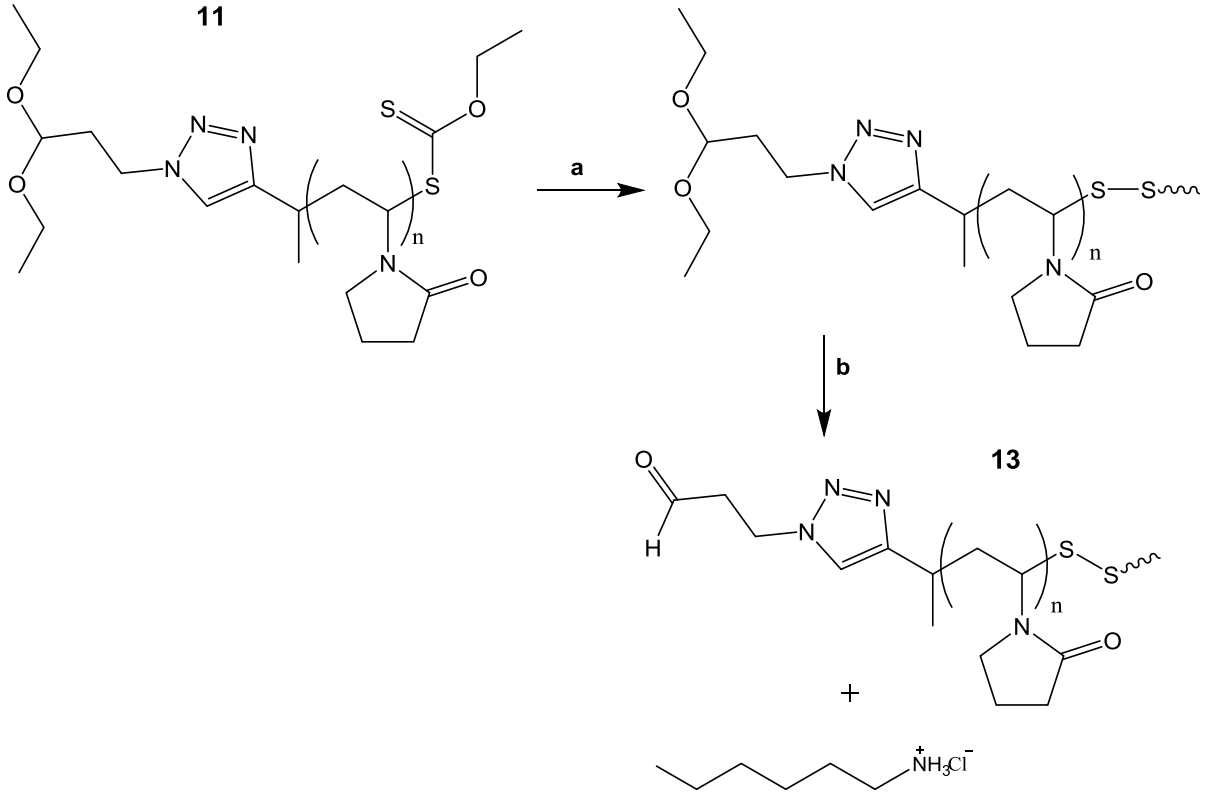

Scheme 4.2: One-pot deprotection of PVP system (11); (a) *n*-hexylamine, acetone, oxygen, r.t.; (b) 4 M HCl in dioxane, acetone, rt

The polymer system was purified via dialysis (2000 Da MWCO) against water/methanol (1:1) for 2 days and pure water for an additional day after which the product was freeze dried to obtain **13**. Formation of the product was confirmed by ^{1}H NMR (Figure 4.2).

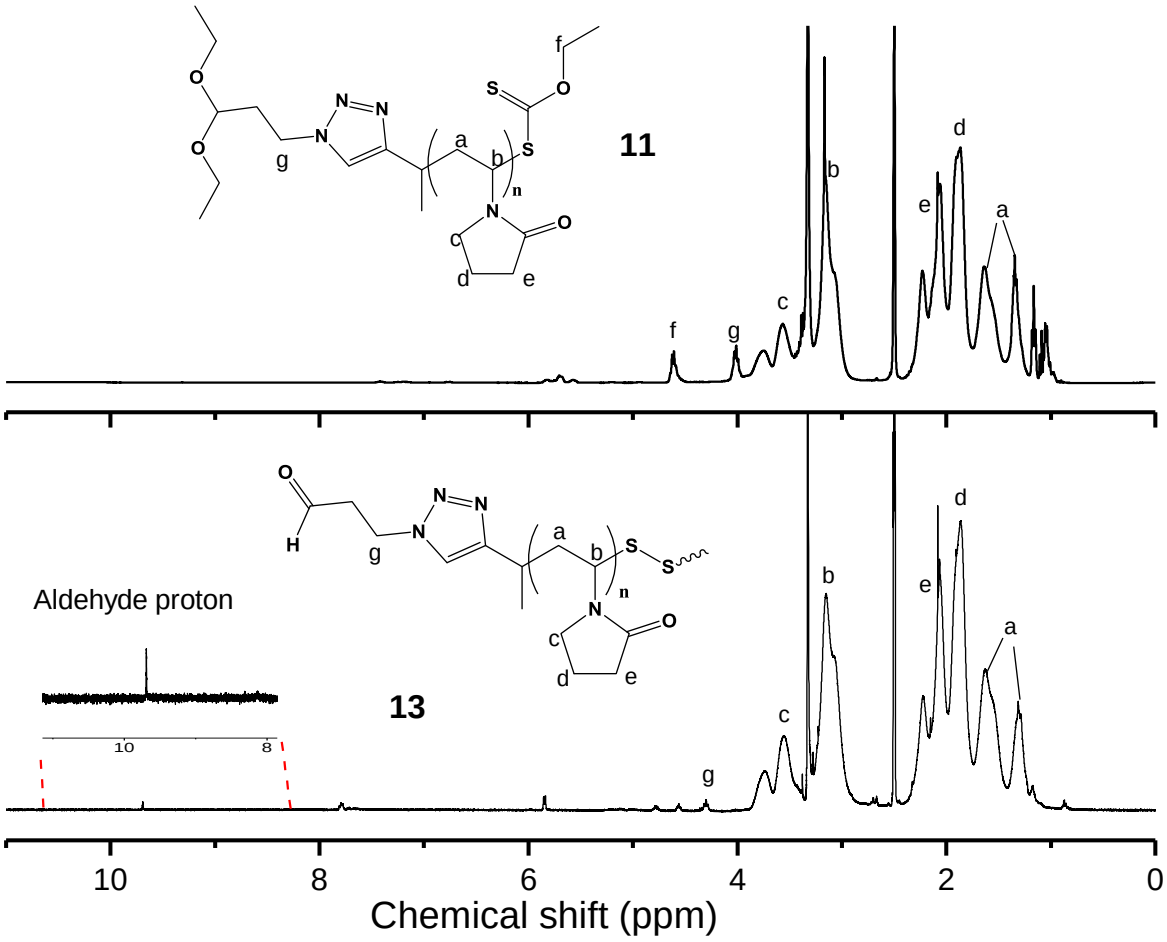

Figure 4.2: ^{1}H NMR spectrum of acetal end-functional (11,top) and aldehyde end-functional PVP (13, bottom).

4.3 Synthesis of targeting ligand

The PSMA targeting ligand was synthesized by a sequence of reactions starting with L-lysine. L-Lysine has two primary amine functional groups, the alpha amino group (N^{α}) adjacent to the carboxyl group and an epsilon amino group (N^{ε}) on the side chain. Chemoselectively reacting one of the two amino groups has turned out to be challenging. The protection of these groups is a vital step in the process of making the corresponding derivatives. In order to prepare the glutamate urea targeting ligand with lysine as the precursor, the Ɛ-amine had to be appropriately protected. The first method that was explored was described by Su *et al.* It is based on the interaction of the alpha amine and carboxylic acid groups on the L-lysine with the inner (hydrophobic) core of β-cyclodextrin.[18] This conveniently leaves the Ɛ-amine available to react with benzyl chloroformate and introduce the benzyl carbonyl group. However, it was difficult to obtain N^{ε}-(benzylcarbonyl) L-lysine using this method. The aforementioned compound was successfully synthesized by using benzyloxycarbonyl (CBz) protecting group as described by Hernández *et al.*[19] The α-amine of the L-lysine was protected by reacting it with basic copper carbonate under reflux conditions resulting in the formation of L-lysine-copper complex. This left the Ɛ-amino group open to react with CBz-Cl. Copper was removed from

the protected L-lysine by washing with a solution of EDTA yielding N^{ε}-(benzyloxycarbonyl) (L-lysine) **14**. The synthetic route is shown in Scheme 4.3.

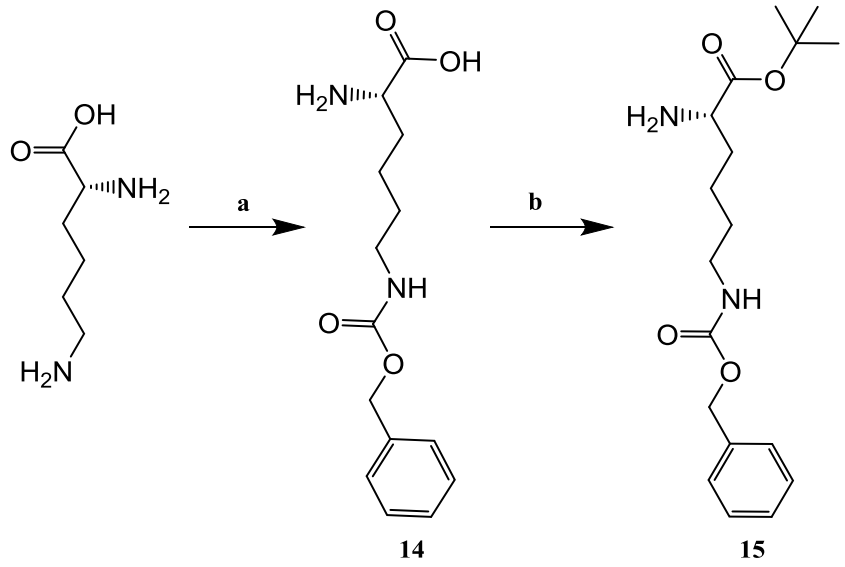

Scheme 4.3: CBz protection of L-lysine; (a) $CuCO_3$ (reflux), benzyl chloroformate, EDTA, 16 h, (b) *tert*-butyl acetate, $HClO_4$, 14 h.

The carboxylic acid group on the α-position of **14** was protected by the *tert*-butyl group by reacting **14** with *tert*-butyl acetate in the presence perchloric acid yielding **15.** The formation of the product was confirmed by ^{1}H NMR and (Figure 4.3).

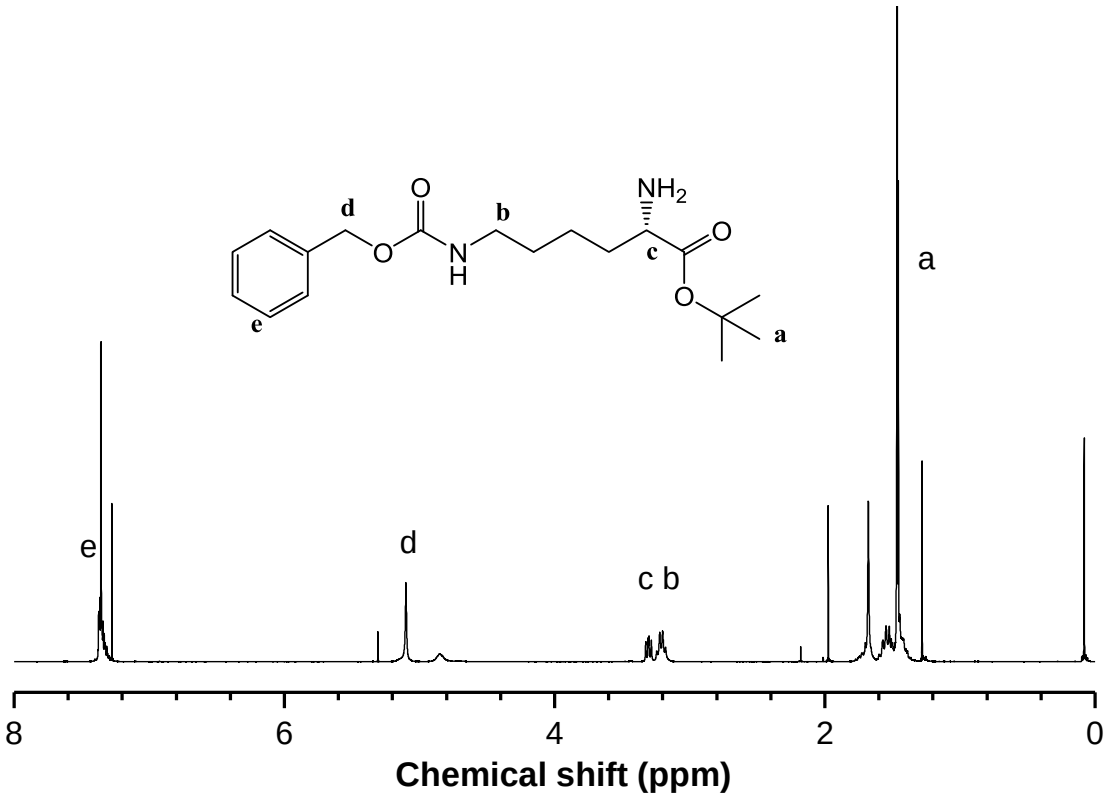

Figure 4.3: ^{1}H NMR spectrum of *tert*-butyl N^{ε}-(benzylcarbonyl) L-lysine (15)

The PSMA ligand with protecting groups on the carboxylic acid moieties was synthesized in two steps based on a method described by Murelli *et al*.[20] The reaction scheme is shown in Scheme 4.4.

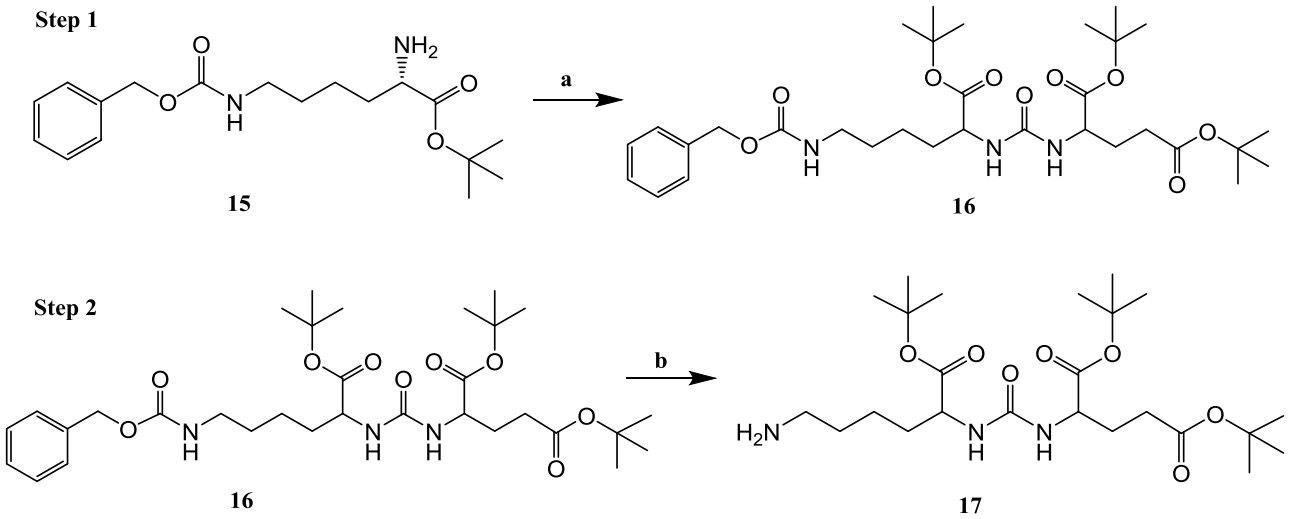

Scheme 4.4: PSMA ligand with *tert*-butyl protecting groups: (a) (Glu–OtBu (OtBu) HCl, triphosgene, triethylamine, argon atmosphere, rt, 16 h, (b) H_2/Pd, methanol, argon atmosphere, rt, 24 h.

Glutamate salt ((Glu–OtBu (OtBu) HCl was coupled to **15** by reacting it with triphosgene in the presence of triethylamine to yield **16**. Formation of the product was confirmed by ESI-MS (Figure 4.4) and ^{1}H NMR.

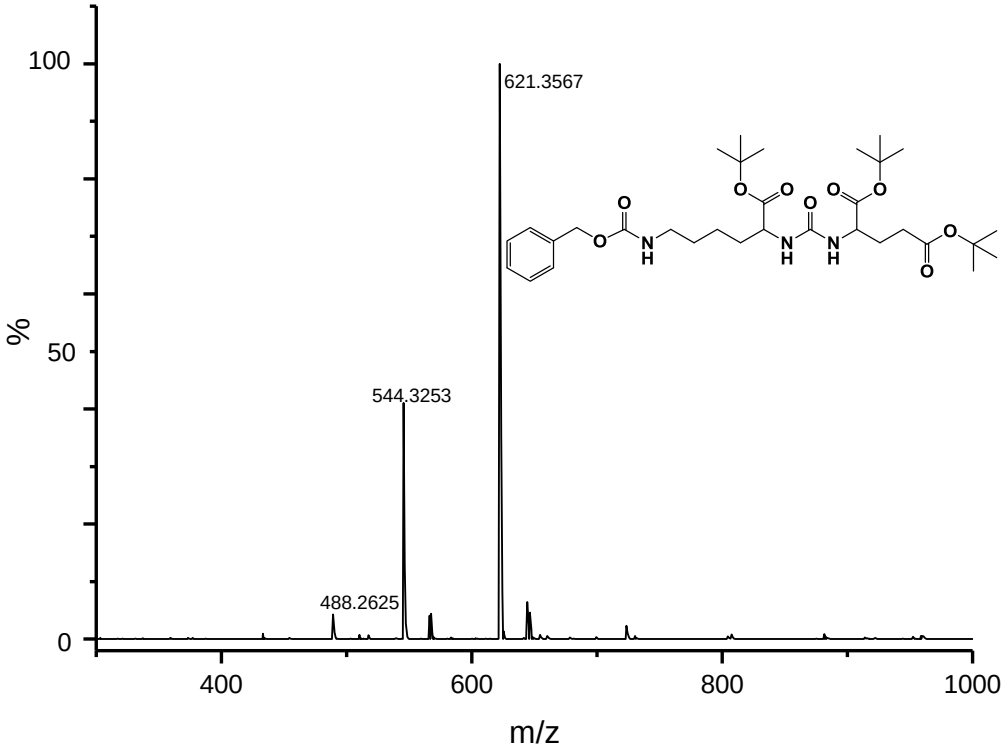

Figure 4.4: ESI-MS spectrum of the formation protected glutamate urea (16).

The molar mass ion peak at m/z 621.36 corresponds with the theoretical molar mass of the synthesised protected glutamate urea which is 621.77 g/mol. After successful coupling, the next step was to remove the benzyl-carbonyl protecting group. The reaction was performed by two methods; hydrobromination (HBr in acetic acid) and hydrogenation with a palladium catalyst on a carbon support. According to ESI-MS and ^{1}H NMR results obtained, hydrogenation was a more effective method in the removal of the benzyl-carbonyl protecting group. The molar mass ion peak at m/z 482.37 corresponds with the theoretical molar mass of compound **17**, which is 482.64 g/mol The ESI-MS results are shown in Figure 4.5.

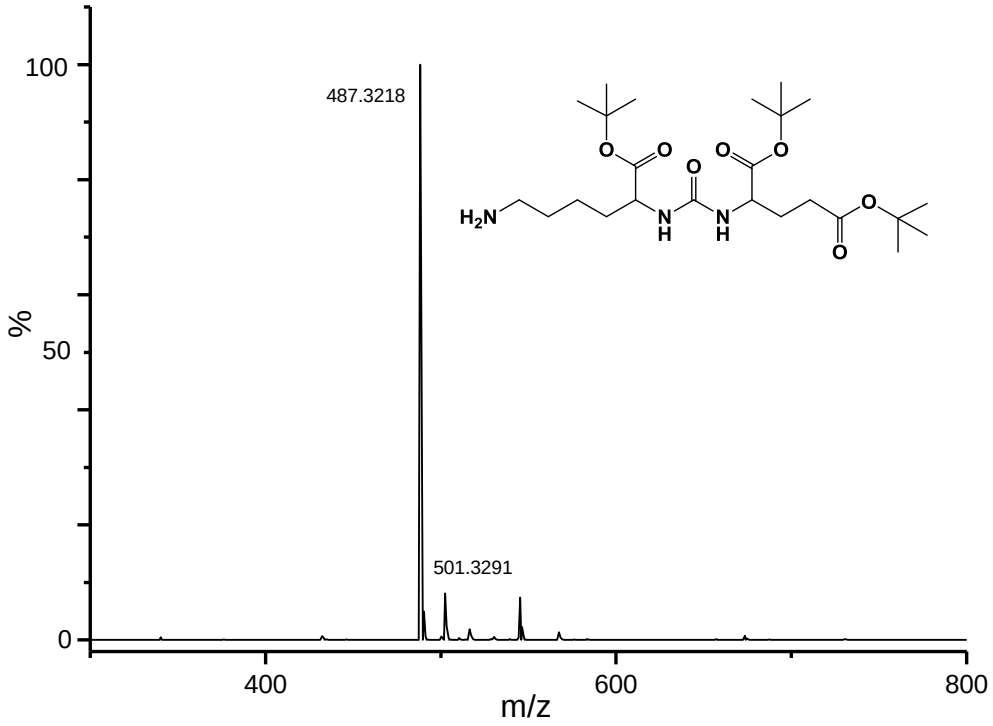

Figure 4.5*:* ESI-MS spectrum of compound (17) after removal of the benzylcarbonyl protecting group.

The final step in the synthesis of the PSMA targeting ligand was the removal of the *tert*-butyl group to afford three carboxylic acid moieties. As mentioned earlier, the carboxylic acid moieties on the ligand are meant to interact with the amino acid on the PSMA and the carbonyl on the urea linkage coordinates with the Zn^{2+} ions on the target [12]. The reaction yielding the PSMA ligand is shown in Scheme 4.5

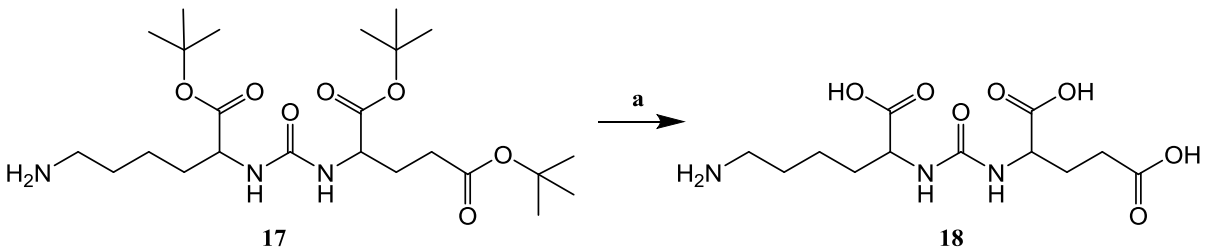

Scheme 4.5: *tert*-Butyl deprotection to form PSMA targeting ligand: (a) KOH, THF, r.t, 4 h.

Deprotection of the *tert*-butyl group was attempted via two methods; acid and base hydrolysis. For acid hydrolysis, **17** was stirred in a solution 1 M HCl in methanol. After isolation of the compound, ^{1}H NMR analysis showed the presence of the methyl protons peak consistent with the *tert*-butyl group. It was concluded that acid hydrolysis was not the best method. Apart from the presence of *tert*-butyl protons peak after the reaction, acid hydrolysis posed the risk of cleaving the urea linkage. Base hydrolysis was achieved by stirring **17** in a suspension of KOH in THF. The reaction was left to run for 4 hours after which residual KOH was filtered off. The filtrate was acidified by HCl in methanol to obtain a neutral pH. The solvent was evaporated under reduced pressure to obtain **18.** Formation of the product was confirmed by ESI-MS (Figure 4.6). The molecular ion mass peak at m/z 319.13 was consistent with the molar mass of our product (319.31 g/mol). ^{1}H NMR analysis also confirmed the formation of the glutamate urea PSMA ligand.

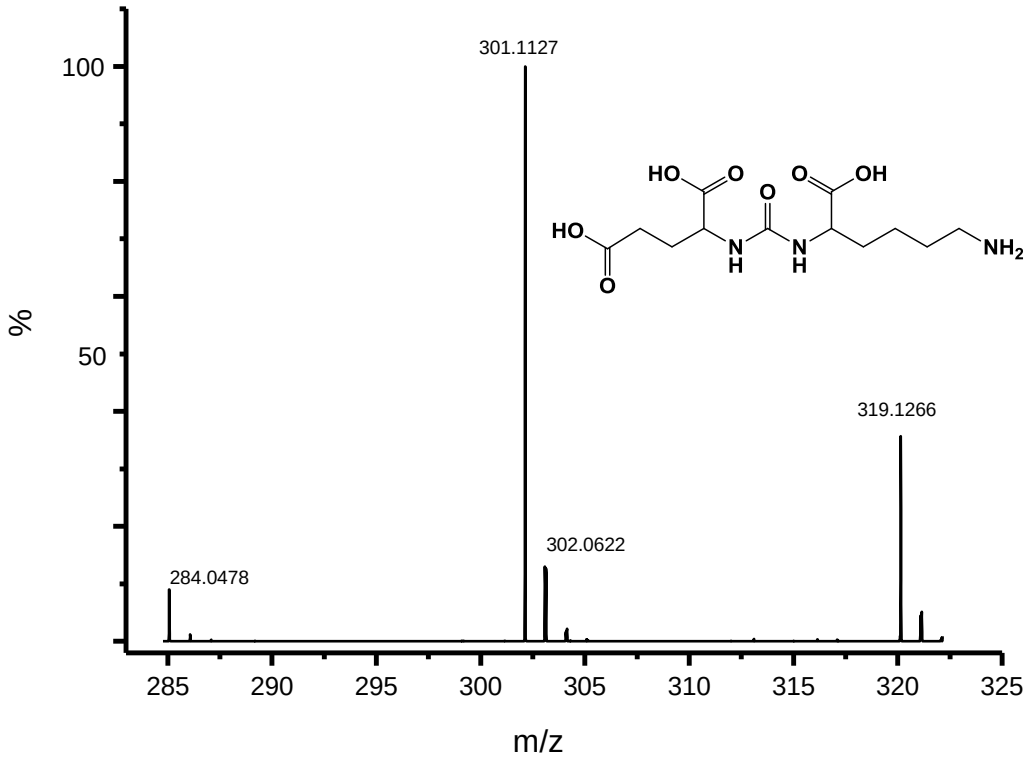

Figure 4.6: ESI-MS spectrum of the glutamate urea PSMA ligand (18).

4.4 Targeting ligand-PVP conjugation

After successful deprotection of the end-groups of the synthesized PVP in a one pot procedure, conjugation strategies were investigated. In order to show its potential as a drug delivery vehicle chain-end conjugation methods were developed, first to a model ligand in order to optimise conditions and then to the synthesised PSMA ligand. Most targeting ligands employed in drug delivery systems

for malaria and cancer (antibodies, small molecule ligands and peptides) contain the *C*- and *N*-terminus. The *N*-terminus, in particular can be exploited by reacting it with carbonyl compounds (aldehyde and ketones) to form imines or Schiff bases.[6] Schiff base reactions normally take place in the presence of an acid or base catalyst. In the case of base catalysis, Schiff base formation is improved around pH 9-10. It is important to note that the bond that is formed is labile until it is converted to a secondary amine structure through reductive amination with sodium cyanoborohydride ($NaBH_3CN$). Schiff base formation and the subsequent reductive amination reaction are illustrated in Scheme 4.6.

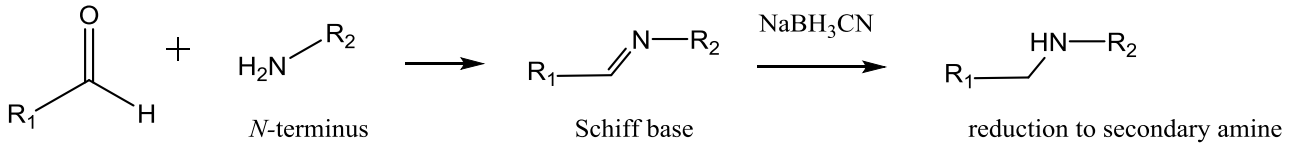

Scheme 4.6: Schiff base formation and subsequent reductive amination

It has been shown that sodium cyanoborohydride reacts selectively in reductive amination reactions of aldehydes and ketones and is also ideal in cases where multiple functionalities are present.[21]

4.4.1 Introduction of model targeting ligand

Glycine-*DL*-Serine (Gly-*DL*-Ser) was chosen as a model compound to serve as an example targeting ligand (Scheme 4.7.)

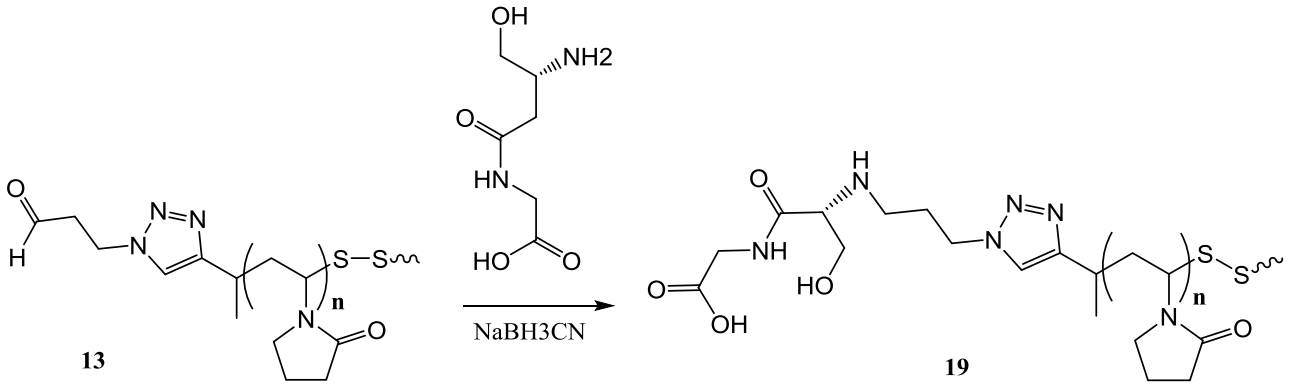

Scheme 4.7 Conjugation of the model ligand Gly-*DL*-Ser to X; (a) sodium borate buffer (pH 9.1), $NaBH_3CN$, r.t

The *N*-terminus of Gly-*DL*-Ser has a pKa of 9.05 hence sodium borate buffer (pH = 9.1) was used to ensure the pH was neutral relative to the *N*-terminus. An excess of Gly-*DL*-Ser (1.5 times) and 10 fold excess of Na BH_3CN were used relative to the end groups of PVP **13**. The reaction was allowed to proceed for 24 hours at room temperature. The resultant solution was purified via dialysis against water for 48 hours and freeze dried to yield the model ligand conjugated PVP **19**. Formation of the conjugate was confirmed by ^1H NMR (Figure 4.7).

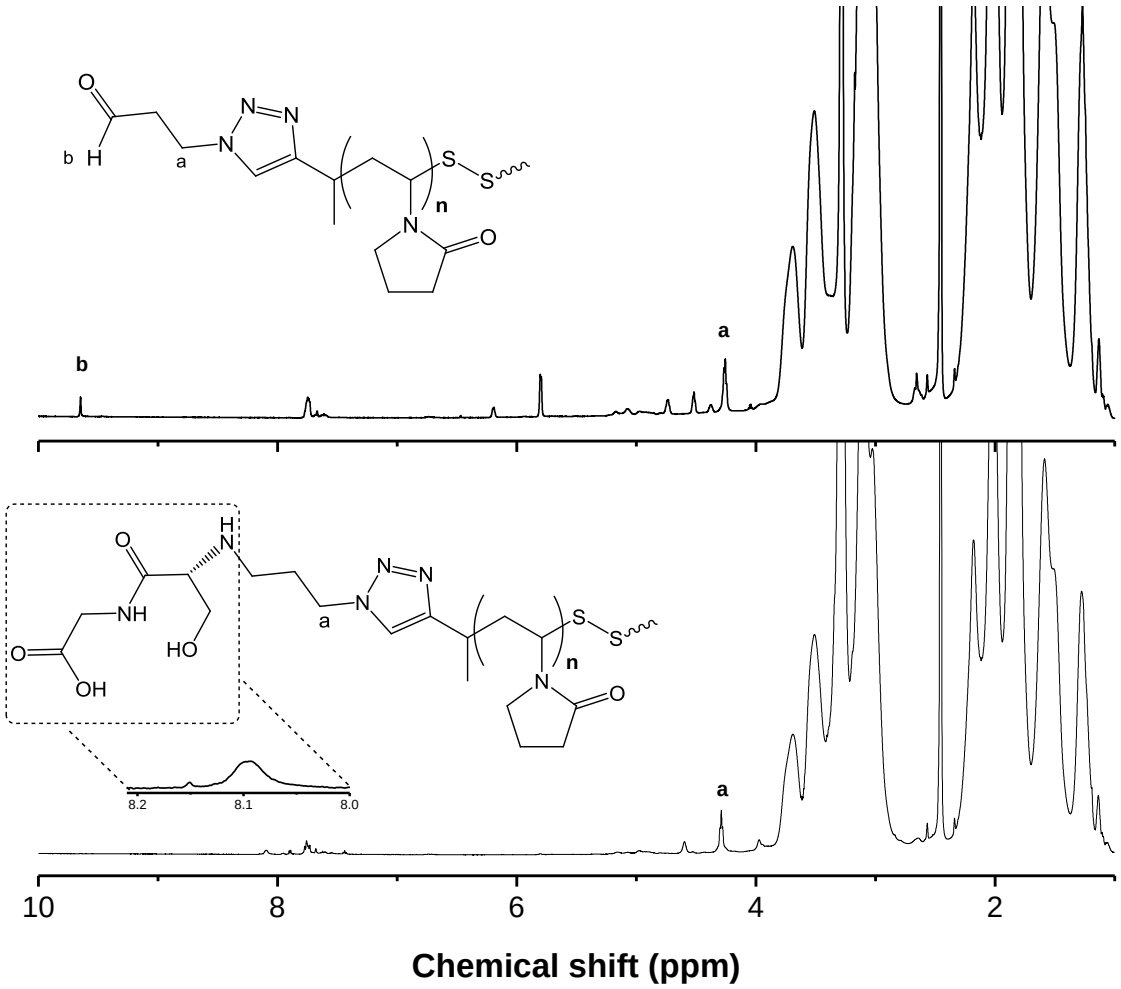

Figure 4.7: ^{1}H NMR spectra showing model ligand conjugation (19)

^{1}H NMR (Figure 4.7) confirmed the disappearance of the aldehyde proton peak at 9.7 ppm and the appearance of new peaks from around 7.5 to 8.3 ppm, which were attributed to the presence of the model ligand (Gly-*DL*-Ser). As a result of the complete loss of the aldehyde protons, we concluded that the model ligand conjugation had occurred in quantitative yield. Although it was not possible to allocate the exact assignment to the model ligand chain end functionality, it is known that in unfolded proteins/peptides, NH chemical shifts are between 7.5-8.5 ppm.[22] Amides in peptide sequences can occur between 7 and 11 ppm.

4.4.2 Introduction of PSMA ligand

After successful conjugation of the model ligand, we proceeded to introduce the PSMA targeting ligand by a more or less similar protocol to that which was employed using the model ligand. Generally for targeting ligands to be effective, they have to be sparsely decorated on the surface of the construct. However, there is not any conclusive information to suggest whether there is an optimal ligand density. This is largely because drug delivery constructs come in many forms. Elias *et al.*

investigated the effect of ligand density and concluded that overcrowding the nanoparticle surface can prevent the targeting ligand binding in the correct orientation with the designated receptor [23]. On this basis it was concluded that 20 mol percent of the PSMA ligand relative to **13** be included into the construct.

For future experiments it was necessary to be able to visualise the drug delivery construct. Therefore, an imaging modality in the form of a fluorescent marker, 6-aminofluorescein (5 mol percent relative to **13** was incorporated into the drug delivery construct. The aldehyde functionality is known to undergo undesirable side reactions. As a result, the remaining 75 % had to be quenched by *n*-propylamine. This particular amine was favourable because di-*n*-propylamine, a close relative to the secondary amine derivative of *n*-propylamine has a pKa of 10.89 [24], in the blood (pH 7.4) it would be protonated, stabilising the 3 dimensional structure [10]. The amine functionalised species were conjugated to **13** as shown in Scheme 4.8.

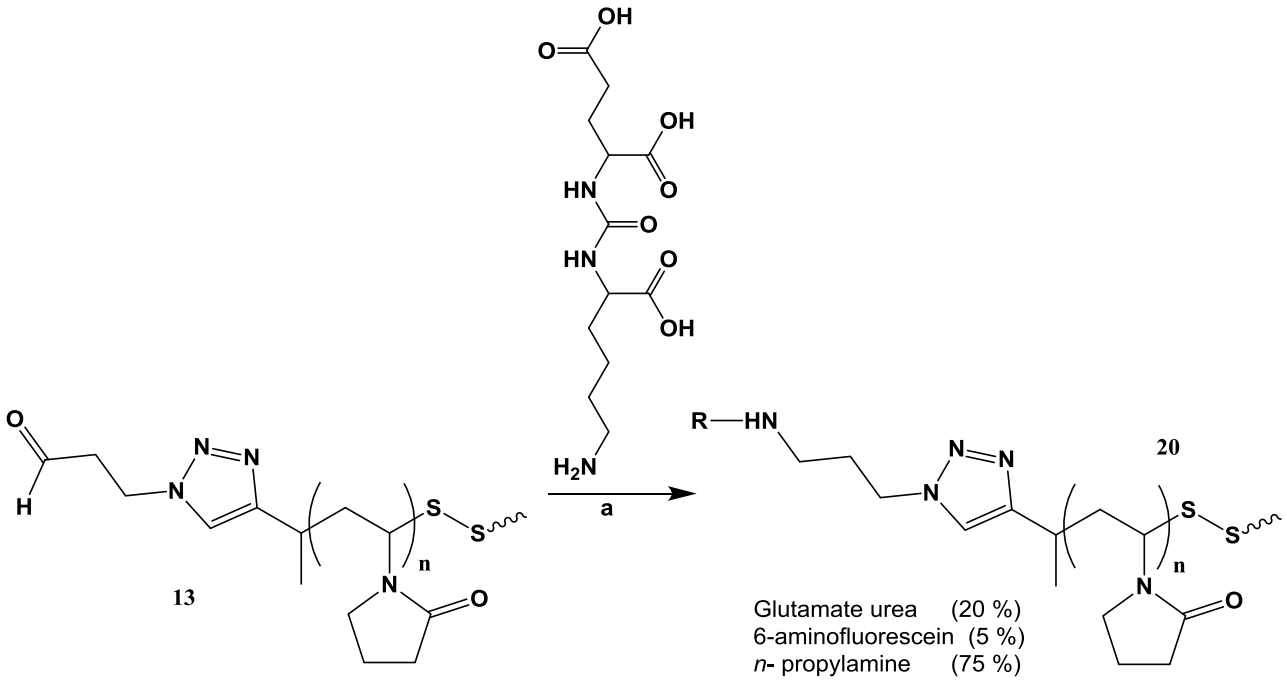

Scheme 4.8: conjugation of targeting ligand to PVP; (a) glutamate urea, 6-aminofluorescein, *n*-propylamine $NaBH_3CN$, sodium borate buffer (pH = 10.8)

13 was reacted with PSMA ligand (40 % mol equivalence), 6-aminofluorescein (10 % mol equivalence) in a sodium borate buffer (pH = 10.8) in the presence of 10 times excess of sodium cyanoborohydride. A higher pH buffer system was used for conjugation to the ligand because the *N*-terminus is comparable to the Ɛ-amine in the L-lysine side chain which has a pKa of 10.79. Thus it ensured that the pH was neutral relative to the *N*-terminus. The reaction was allowed to run overnight at room temperature, after which the remaining aldehydes were quenched with a 2 times excess of *n*-propylamine. The solution was purified via dialysis (2000 Da MWCO) against water for 3 days, after

which freeze-drying yielded a white powder, **20** (PVP – PSMA ligand conjugate). The alpha and omega chain ends were analysed by ^{1}H NMR (Figure 4.8).

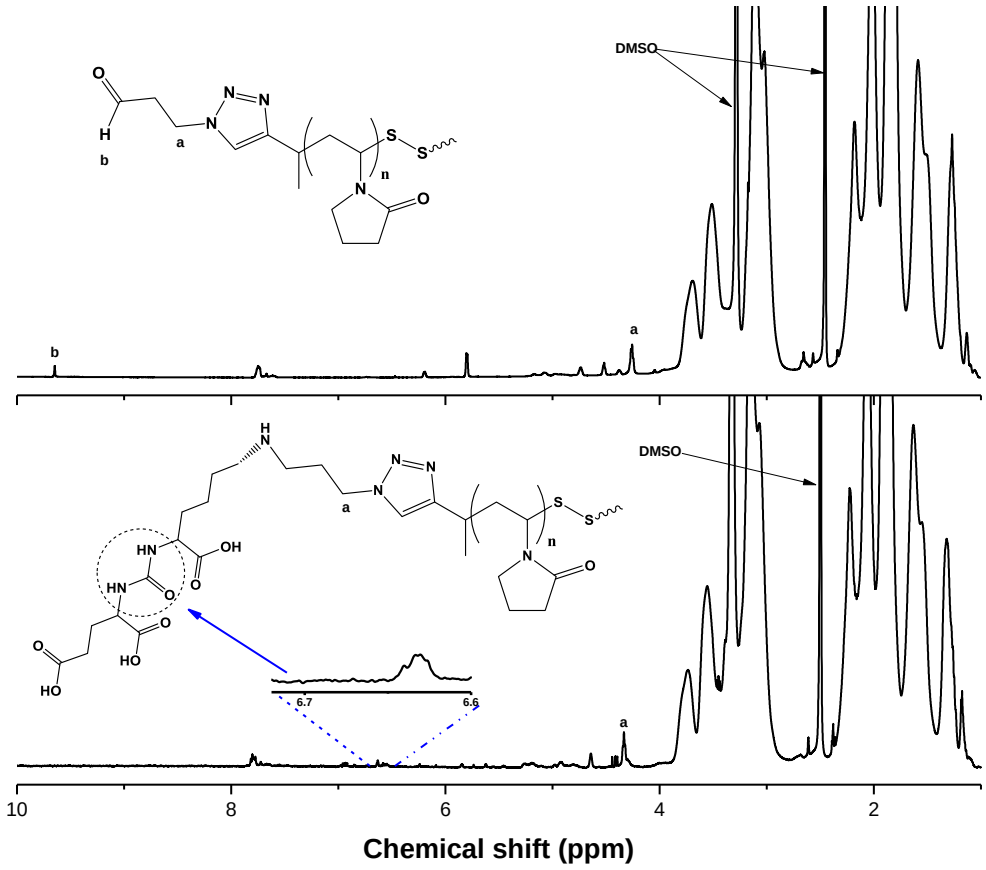

Figure 4.8: ^{1}H NMR spectra of PVP before conjugation (13) and after conjugation with the glutamate urea targeting ligand (20).

The ^{1}H NMR data shows a clear disappearance of the aldehyde proton peak at 9.7 ppm. Furthermore there was formation of new peaks, the most important one being the urea linkage in the targeting ligand. The urea linkage protons are expected around 6.7 ppm.[12] The signal was low as expected and this can be attributed to 20 % mol equivalence that was used to ensure that the drug delivery construct would not be congested.

4.5 Conclusion

The oxidation of the hydroxyl functionality on the alpha chain end of PVP **(7)** to aldehyde, which was necessary for interaction with the *N*-terminus of the targeting ligand through Schiff base formation was not sufficiently effective. Only a very weak aldehyde signal could be detected from ^{1}H NMR. It was deemed insufficient for the conjugation reactions with the *N*-terminus of the targeting moiety and fluorescent marker. The exact reasons for the limited success of the reaction could not be established, however, it could be attributed to the chemical structure of the PVP itself because when the same reaction was run under the same conditions but using hydroxyl functional PMMA, oxidation was successful. However, since our focus was on PVP, the alternative was to use alpha acetal functional PVP (**12**), in which the aldehyde functionality at the alpha chain end could be obtained via a one pot acetal deprotection strategy. The alpha acetal PVP system was successfully deprotected yielding the desired aldehyde functionality. After successful synthesis of the alpha aldehyde end functional PVP, attention was switched to the synthesis of the PSMA ligand, which was successful as confirmed via ^{1}H NMR and ESI-MS. To test the effectiveness of the Schiff base formation and reductive amination during the interaction with the *N*-terminus of the targeting moiety, a model ligand had to be initially employed. Successful conjugation of the model ligand was followed by conjugation of the PSMA ligand and fluorescent marker on to the alpha chain end of the polymer. At this point the PVP system was ready for conjugation to the model drug and to tyrocidine.

4.6 Experimental

4.6.1 General experimental details

Chemicals and solvents used were bought from commercial sources and were generally used without further purification, unless in cases where it was mentioned. Reactions were monitored using TLC, utilising Machery-Nagel Silica gel 60 plates with a UV 254 fluorescent indicator. Dialysis tubing, MWCO 2000, was purchased from Sigma Aldrich. TLC plates were digitised using UN-SCAN-IT software, developed by Silk Industry Inc. An inert argon atmosphere was used for all moisture and oxygen sensitive reactions. ^{1}H-NMR and ^{13}C-NMR spectra were recorded on a Varian VXR-Unity (400 MHz) spectrometer. Samples preparation was done in deuterated solvents obtained from Cambridge Isotope labs. NMR spectra chemicals shifts were reported in parts-per-million (ppm) referenced to the residual solvent protons. Size exclusion chromatography (SEC) was measured on a system that comprised a Shimadzu LC-10AT isocratic pump, a Waters 717+ autosampler, a column system fitted with a PSS guard column (50×8 mm) in series with three PSS GRAM columns (300×8 mm, 10 µm, 2 × 3000 Å and 1 × 100 Å) kept at 40 °C, a Waters 2487 dual wavelength UV detector and a Waters 2414 differential refractive index (DRI) detector. Dimethylacetamide (DMAc) was used as the eluent. The stabilising agents were 0.05 % BHT (*w/v*) and 0.03 % LiCl (*w/v*), at a flow rate of 1 mL·min^{-1}. GHP filters of 0.45 µm pore size were used to filter the polymer samples to facilitate removal of impurities prior to analysis. PMMA standard sets ranging from 690 to 1.2 × 10^{6} g·mol^{-1} obtained from Polymer Laboratories were used to carry out calibration. Data was acquired fromMillennium[32] software, version 4.

4.6.2 Synthetic Procedures

Oxidation of α-hydroxyl functional PVP: **7** (350 mg, 0.126 mmol) was dissolved in 5 mL DMSO and stirred for 24 hours at room temperature. This was followed by addition of acetic anhydride to generate a 10:1 v/v solution. The reaction was allowed to stir at room temperature for 48 hours under an inert atmosphere. The resultant solution was precipitated with diethyl ether, redissolved in minimal DCM and precipitated three more times with di ethyl ether. The product was dried and end group analysis was performed by ^{1}H NMR.

Deprotection of α-acetal, ω-xanthate heterotelechelic PVP system: PVP deprotection proceeded by a method described by Reader *et al.*[10] **11**(2.50 g, 0.926 mmol aldehyde), *n*-hexylamine (0.281 g, 2.78 mmol) and acetone (13.9 mL) were introduced to a 50 mL round bottom flask and stirred for 4 hours at room temperature. HCl (13.9 mL, 4 M in dioxane) was added, to bring the overall HCl

concentration to 1 M, and the reaction was stirred for an additional 4 hours at room temperature. The solution was purified via dialysis (2000 Da MWCO) against water/methanol (1:1) for 2 days and pure water for an additional day, after which the product was freeze-dried to obtain **13** as a white powder. End-group analysis was performed via ^{1}H NMR and molar mass and dispersity were determined via SEC.

Synthesis of N$^{\varepsilon}$-(Benzylcarbonyl) L-Lysine (14): L-lysine monohydrochloride (16.0 g, 0.0876 mol) was dissolved in 150 mL deionized water. Basic copper (II) carbonate ($CuCO_3 \cdot Cu(OH)_2$, 18.5 g, 0.0837 mol) was added and the solution was refluxed for 30 minutes before being cooled down to room temperature and being filtered. Sodium bicarbonate (8.50 g, 0.101 mol) was added and the solution was cooled to 0 °C in a three-neck round bottom flask fitted with a dropping funnel and a mineral oil bubbler. Benzyl chloroformate (10.0 g, 0.0586 mol) was dissolved in 75 mL THF and the solution was charged into the dropping funnel. The benzyl chloroformate solution was then added dropwise to the lysine copper complex solution while maintaining the temperature at 0 °C for two hours. The reaction mixture was then heated at 40 °C overnight. The THF was removed by evaporating under vacuum and the precipitate was filtered and washed with three 100 mL portions of deionized water. EDTA (22.0 g, 0.0591 mol) and sodium carbonate (8.00 g, 0.0755 mol) were dissolved in 300 mL deionized water and added to the precipitate. The mixture was heated at 60 °C with gentle mixing for 1 hour before being cooled to 0 °C and filtered. This procedure was repeated 3 more times to ensure all the copper was removed from the product. The precipitate was washed with three 50 mL portions of deionized water and dried in a vacuum oven at 60 °C overnight. Product Yield: 22.65 g (69%) IR (ATR):20 3334 cm^{-1} (m, N-H secondary urethane), 2599 cm^{-1} (w, br, N-H amine), 2131 cm^{-1} (w, br, N-H amine), 1692 cm^{-1} (s, C=O carbamate), 1522 cm^{-1} (s, C=O acid).

Synthesis of tert-butyl *N*$^{\varepsilon}$-(Benzylcarbonyl) L-Lysine (15)

N$^{\varepsilon}$-benzyloxycarbonyl-L-lysine (**1**, 6.50 g, 23.2 mmol) was stirred in *tert*-butyl acetate (80 mL) followed by addition of $HClO_4$ (3.01 mL). The mixture was stirred at 23 °C overnight before being extracted with H_2O (150 mL) and 0.5 N HCl solution (150 mL). The obtained aqueous solutions were combined before adjusting the pH to 9 with the aid of 10% K_2CO_3 solution. Extraction was done with CH_2Cl_2 (3 × 100 mL). The obtained organic layers were combined and dried over were dried over anhydrous $MgSO_4$, followed by filtration and evaporation under reduced pressure to give **2** as an oil. Product yield: 2.82 g (36%). ^{1}H NMR (400 MHz $CDCl_3$) δ 7.40 – 7.30 (m, 5H), 5.05 – 5.16 (s, 2H), 3.28 – 3.34 (dd, 1H), 3.17 – 3.26 (q, 2H), 1.52 – 1.61 (m, 2H), 1.47 (s, 9H), 1.45 – 1.39 (m, 2H). ^{13}C NMR (75 MHz, $CDCll_3$) δ 175.27, 156.38, 136.38, 128.07 , 127.06, 81.01, 66.59, 54.83, 40.30, 34.45, 31.23, 29.67 , 28.06, 22.67

Synthesis of (9S,13S)-tri-*tert*-butyl 3,11-dioxo-1-phenyl-2-oxa-4,10,12-triazapentadecane-9,13,15-tricarboxylate (16):Glu–OtBu (OtBu) HCl (5.00 g, 16.9 mmol) and triethylamine (TEA) (8.32 mL, 59.7 mmol) were stirred in dry DCM (120 mL) at -78 °C (dry ice/acetone) for 30 minutes. Triphosgene (1.66 g, 5.61 mmol) in 40 mL DCM was added in a dropwise manner through a degassed syringe. The reaction was allowed to warm to room temperature before being purged with nitrogen and stirred for 30 minutes in an inert atmosphere. H-Lys(Z)-Ot-Bu HCl (**2**) (3.79 g, 10.2 mmol) was added, followed by triethylamine (1.42 mL, 10.2 mmol). The reaction was left to proceed at room temperature room temperature overnight in an inert atmosphere. The reaction mixture was diluted with distilled CH_2Cl_2 (150 mL) and washed with water (2 × 250 mL), dried over anhydrous $MgSO_4$ and evaporated under reduced pressure leaving a colourless oil. The oil that was obtained was purified via column chromatography (silica gel, hexane-ethyl acetate (60:40) to yield a colourless oil. Product yield: 5.59 g (77 %). ^{1}H NMR (600 MHz, $CDCl_3$): δ 7.25–7.33 (m, 5 H), 5.08 (s, 2 H), 4.27 – 4.33 (tt,2 H), 3.10 – 3.18 (m, 2 H), 2.27–2.34 (m, 2 H), 2.20 – 2.26 (m, 2H), 1.99 – 2.06 (m, 2 H), 1.79–1.86 (m, 2 H), 1.58–1.70, 1.46–1.54 (m, 2 H), 1.42 (s, 9 H), 1.28–1.34 (m, 2 H). ESI-MS: calculated 621.36, exp 621.66.

Synthesis of (S)-di-*tert*-butyl 2-(3-((S)-6-amino-1-*tert*-butoxy-1-oxohexan-2-yl)ureido) pentanedioate (17)

16 (2.50 g, 4.02 mmol) was dissolved in 15 mL methanol and added to a stirred 3-neck round bottom flask containing 0.20 g of 10 % Pd/C, connected to a hydrogen source, and a balloon fitted to one neck. Argon was bubbled through the reaction vessel before the hydrogen source was opened long enough to allow the hydrogen to inflate the balloon. The reaction was allowed to stir for 24 hours under a balloon of hydrogen at room temperature. The reaction mixture was filtered through a plug of celite and the solvent evaporated. The product was a colourless oil. Product yield: 1.81 g (92 %). Formation of the product was confirmed by ^{1}H NMR and ESI-MS. ^{1}H NMR (600 MHz, $CDCl_3$): δ 5.32 – 5.39 (dd, 2H), 4.26 – 4.32 (m, 2 H), 2.66 – 2.73 (m, 2H), 2.27 – 2.34 (m, 2 H), 2.21 – 2.26 (m, 2 H), 2.00 – 2.05 (m, 2 H), 1.79 – 1.86 (m, 2 H), 1.46 (s, 9 H). ESI-MS: calculated 487.64, exp 487.32.

Synthesis of ((5-amino-1-carboxypentyl) carbamoyl) glutamic acid (18): KOH (12.0 g, 0.214 mol) was dissolved in 50 mL of diethyl ether forming a suspension. **17** (0.150 g, 0.316 mmol) was added to the suspension in a 100 mL round bottom flask. The reaction was allowed to stir for 4 hours under argon. The excess undissolved KOH was left behind in the round bottom flask as the solution was decanted out into an Erlenmeyer flask. The solution was neutralised with minimal 0.1 M HCl in methanol under an ice bath. The resultant solution was evaporated under reduced pressure and dried to yield a brown oil. Product yield: 0.084 g (86 %). Formation of compound was determined by ^{1}H

NMR and ESI-MS. ^{1}H NMR (400 MHz, DMSO): δ 7.90 – 8.10 (d, 2H), 4.37 – 4.43 (m, 1 H), 4.13 – 4.19 (m, 1 H), 2.65 – 2.77 (m, 2 H), 2.28 – 2.36 (t, 2 H), 2.15 – 2.26 (m, 2 H), 1.88 – 2.03 (q, 2H), 1.66 – 1.79 (m, 2 H), 1.49 – 1.62 (m, 2H). ESI-MS: calculated 319.31, exp 319.13.

Model Schiff-base formation and reductive amination: the model ligand – PVP conjugate was synthesized as described by Reader *et al.*[10] A sodium borate buffer (pH = 9.1) was made by dissolving boric acid (6.18 g, 100 mmol) and NaOH (2.00 g, 50.0 mmol) in water, and made up to 1 L, in a volumetric flask. **15** (100 mg, 37.0 nmol), Gly-DL-Ser (9.00 mg, 55.5 nmol), $NaBH_3CN$ (23.3 mg, 0.370 mmol) and sodium borate buffer (5 mL, pH 9.1) were introduced to a 10 mL pear-shaped flask. The reaction was stirred at room temperature overnight, followed by purification via dialysis (2000 Da MWCO) against water for 2 days, after which the solution was freeze-dried to obtain **19** as a white powder. End-group analysis was performed via ^{1}H NMR.

General synthesis of targeting ligand-terminal PVP: NaOH (400 mg, 10 mmol) was dissolved in water and made up to 100 mL, in a volumetric flask (0.1 M, solution A). In parallel, sodium tetraborate decahydrate (0.95 g, 2.50 mmol) was dissolved in water and made up to 100 mL, in a volumetric flask (25.0 mM, solution B). Solution A (48.5 mL) was added to 100 mL of solution B in a separate flask, affording a sodium borate buffer (pH = 10.8). 6-Aminofluorescein (4.13 mg, 11.9 µmol) was dissolved in sodium borate buffer (1 mL, pH = 10.8) to afford a 6-aminofluorescein stock solution (11.9 mM). **19** (0.065 g, 15.1 µmol), glutamate urea (2 mg, 6.05 µmol), 6-aminofluorescein (127 µl, 1.51 µmol), $NaBH_3CN$ (5.7 mg, 151 µmol) and sodium borate buffer (2 mL, pH = 10.8) were introduced into a 10 mL pear shaped flask with a magnetic stirrer. The reaction was left to stir overnight at room temperature. *n*-Propylamine (1.80 mg, 30.2 µmol) was added and the solution was stirred for a further 4 hours after which it was dialysed (2000 Da MWCO) against water for two days and freeze dried to afford **20** as a white powder. The alpha and omega end groups were analysed via ^{1}H NMR.

4.7 References

(1) Nash, M. A.; Waitumbi, J. N.; Hoffman, A. S.; Yager, P.; Stayton, P. S., *ACS Nano* **2012**, 6, 6776-6785.

(2) Kumar Mehra, N.; Jain, K.; Kumar Jain, N., *Curr. Pharm. Des.* **2015**, 21, 6157-6164.

(3) Juillerat-Jeanneret, L.; Schmitt, F., *Med.Res.Rev* **2007**, 27, 574.

(4) Iha, R. K.; Wooley, K. L.; Nyström, A. M.; Burke, D. J.; Kade, M. J.; Hawker, C. J., *Chem. Rev.* **2009**, 109, 5620.

(5) Boyer, C.; Bulmus, V.; Davis, T. P.; Ladmiral, V.; Liu, J.; Perrier, S., *Chem. Rev.* **2009**, 109, 5402.

(6) Sayers, C. T.; Mantovani, G.; Ryan, S. M.; Randev, R. K.; Keiper, O.; Leszczyszyn, O. I.; Blindauer, C.; Brayden, D. J.; Haddleton, D. M., *Soft Matter* **2009**, 5, 3038.

(7) Pound, G.; McKenzie, J. M.; Lange, R. F.; Klumperman, B., *J. Chem. Soc., Chem. Commun.* **2008**, 3193.

(8) Xiao, N.-Y.; Li, A.-L.; Liang, H.; Lu, J., *Macromolecules* **2008**, 41, 2374.

(9) Gauthier, M. A.; Gibson, M. I.; Klok, H. A., *Angew. Chem. Int. Ed.* **2009**, 48, 48.

(10) Reader, P. W.; Pfukwa, R.; Jokonya, S.; Arnott, G. E.; Klumperman, B., *Polym. Chem.* **2016**, 7, 6450.

(11) Shu, J. Y.; Panganiban, B.; Xu, T., *Annu. Rev. Phys. Chem.* **2013**, 64, 631.

(12) Pearce, A. K.; Rolfe, B. E.; Russell, P. J.; Tse, B. W. C.; Whittaker, A. K.; Fuchs, A. V.; Thurecht, K. J., *Polym. Chem.* **2014**, 5, 6932.

(13) Schmaljohann, D., *Adv. Drug Deliv. Rev.* **2006**, 58, 1655.

(14) Ghosh, A.; Heston, W. D., *J. Cell. Biochem.* **2004**, 91, 528.

(15) Huang, B.; Otis, J.; Joice, M.; Kotlyar, A.; Thomas, T. P., *Biomacromolecules* **2014**, 15, 915.

(16) Wang, M.; Thanou, M., *Pharmacol. Res.* **2010**, 62, 90.

(17) Bilgic, T.; Klok, H.-A., *Biomacromolecules* **2015**, 16, 3657.

(18) Su, J.; Sheng, X.; Li, S.; Sun, T.; Liu, G.; Hao, A., *Org. Biomol. Chem.* **2012**, 10, 9319.

(19) Hernández, J. R.; Klok, H. A., *J. Polym. Sci. A Polym. Chem.* **2003**, 41, 1167.

(20) Murelli, R. P.; Zhang, A. X.; Michel, J.; Jorgensen, W. L.; Spiegel, D. A., *J. Am. Chem. Soc.* **2009**, 131, 17090.

(21) Hermanson, G. T., In *Bioconjugate Techniques*,(Third Edition) Hermanson, G. T., Ed. Academic Press: Boston, **2013**.

(22) Mayo, K.; Cavalli, R.; Peters, A.; Boelens, R.; Kaptein, R., *J. Magn. Reson.* **1989**, 257, 197.

(23) Elias, D. R.; Poloukhtine, A.; Popik, V.; Tsourkas, A., *Nanomedicine* **2013**, 9, 194.

(24) Hall, H. K., *J. Am. Chem. Soc.* **1957**, 79, 5441.

5 Tyrocidine PVP PSMA targeting conjugates

5.1 Introduction

Drug delivery systems can be divided into two main classes namely, conventional drug administration and targeted drug delivery. Conventional drug administration involves the therapeutic agent being processed into a suitable carrier, such as an oral tablet or an injectable formulation.[1] Conventional therapeutic approaches come with many shortcomings such as premature drug degradation, low bioavailability along with the occurrence of side effects. Targeted delivery aims to attain high therapeutic indices with as little side effects as humanly possible. This is achieved by allowing the drug to escape immune response from the body,[1-2] leading to improved bio-distribution and localised release.

Targeted drug delivery systems in the form of polymer based nanocarriers have been designed over the years to improve bioavailability, pharmacokinetics and therapeutic properties of the drugs administered parenterally.[3] As drug carriers they enable controlled drug release and thus improvement in drug bioavailability, as well as dosing frequency reduction. Polyethylene glycol (PEG) chains have been mostly employed for attachment to therapeutic agents, which often results in nano drug delivery systems that have masses above that of the renal clearance threshold thus, allowing for longer circulation times.[4]

Targeted drug delivery systems for most infectious diseases and cancer have been designed in many ways based on passive and active targeting. In the case of cancer in particular, passive targeting takes advantage of solid tumours possessing certain pathological characteristics that are not observed in normal tissue.[5] Leaky blood vessels, dysfunctional lymphatic system or lack of it results is size based selection of macromolecules that leads to accumulation of nanocarriers at the tumour sites. The phenomenon is called the enhanced permeability and retention effect and it results in increased localisation.[6-7] Active targeting involves the use of covalently bonded and peripherally conjugated targeting ligands for enhanced delivery of polymeric systems. Active targeting, through the use of small molecule ligands antibody fragments and peptides facilitates binding and subsequent the uptake of nanoparticle systems at precise locations.[8]

Conjugated drug delivery systems that have been tailored to include a therapeutic agent, an imaging modality, a targeting moiety and a mechanism to safely deliver the construct are known to self-assemble.[9] The self-assembled structures are responsible for increased target specificity and therapeutic indices.[10] These micellar nanostructures are especially important in polymer conjugates

with proteins and peptides (therapeutic agents or targeting moieties) that are poorly soluble in aqueous media. Apart from solubility issues, proteins and peptides are susceptible to proteolysis, chemical modifications and denaturation.[11] The hydrophilic polymer chains have a role of solubilising the hydrophobic drugs by shielding them from the aqueous phase. In the process the therapeutic agents are also hidden from the immune system, only for release to be triggered by physiological stimuli such as temperature, salt or pH.[12] These drug delivery systems have proved to be vital when targeting tumours.

Making use of the model ligand, glutamate urea targeting ligands synthesised in Chapter 4, as well the PVP-ligand conjugates that were developed, it was necessary to develop a model theranostic conjugate with a model drug as well as PSMA targeted theranostic device to determine not only the targeting efficiency and the activity but also the feasibility of the conjugation chemistries involved in the conjugation of the drug.

5.2 Introduction of the model drug

After successful conjugation of the model ligand to form conjugate **19** in Chapter 4, it was necessary, as proof of concept to be able to conjugate the model drug via thiol-ene Michael addition. This click type of chemistry has opened new avenues to tailor-made nanoparticles in polymer chemistry.[13] The significance of thiol-ene chemistry in this study was the acid labile linker that results from this type of reaction (Scheme 5.1). Many smart drug delivery systems contain stimuli-responsive release mechanisms.

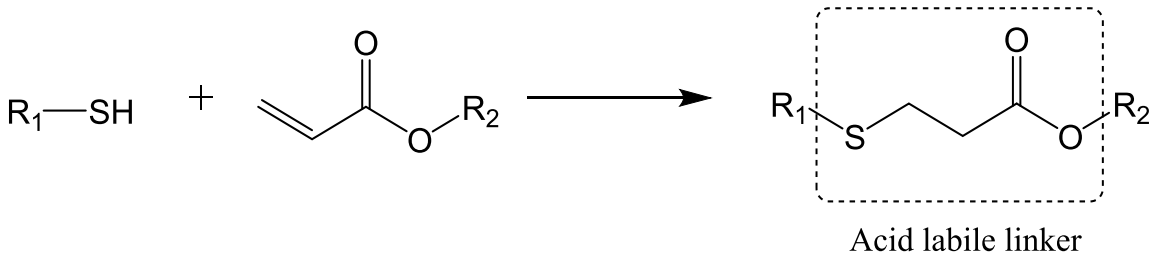

Scheme 5.1: Thiol-ene Michael addition reaction

Normal physiological pH is usually around 7.4. However, the pH in the extracellular tumourous tissue is known to be around 6.8 – 7.0. This is caused by increased rates of aerobic and anaerobic glycolysis that results in elevated concentrations of pyruvic acid. Normal healthy cells generally have lower rates of glycolysis.[14-15] Intracellular compartments, such as endosomes and lysosomes, exhibit even lower pH levels of approximately 5–6.[16] Oishi *et al.*[17] described oligodeoxynucleotide (ODN) conjugated to α-acetal, ω-acrylate PEG via the pH responsive β-thiopropionate ester. The PEG –

ODN conjugates were synthesised via thiol-ene Michael addition and showed cleavage of the ester linkage at endosomal pH of 5 – 6.

The feasibility of introducing acrylates onto therapeutic antimicrobial/anticancer peptides through the hydroxyl moiety or the *N*-terminus can be explored by making use of acryloyl chloride. Alternatively the acryloyl chloride can first be reacted by *N*-hydroxysuccinimide to form the *N*-succinimidyl acrylate ester which can be used to conjugate to the *N*-terminus.

Amino acids threonine, serine and tyrosine are part of the 21 amino acids used for protein synthesis in eukaryotes. Each of these three amino acids contains a hydroxyl functionality. In general aromatic hydroxyl moieties are less reactive towards nucleophilic substitution compared to aliphatic hydroxyl functionalities.[18] Phenol was chosen as the model compound as it is the closest to tyrosine. Phenol was reacted with acryloyl chloride, in the presence of triethylamine (TEA) at room temperature to yield phenyl acrylate (**21**) as shown in Scheme 5.2

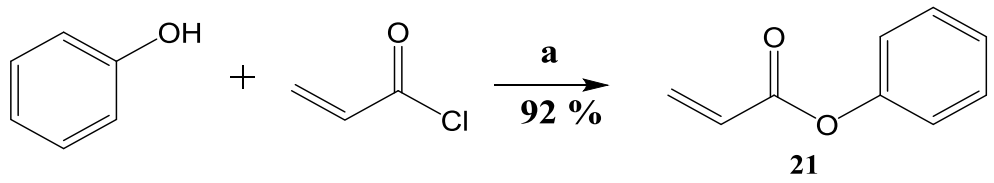

Scheme 5.2: Synthesis of phenyl acrylate (21) as a model drug: (a) TEA, DCM, r.t.

The synthesised phenyl acrylate was ready for conjugation to PVP **20**, however, as a result of aminolysis, the majority of the conjugated PVP **19** and **20** synthesised in Chapter 4 existed as disulphides although a few thiol terminated chains are still expected. In order to have thiol terminated chains necessary for thiol-ene Michael addition, a reducing agent had to be employed. Tris(2-carboxyethyl)phosphine hydrochloride (TCEP) has widely been used for reduction sensitive biodegradable polymers with disulphide bridges but sodium borohydride is also a good reducing agent for this purpose (Scheme 5.3).

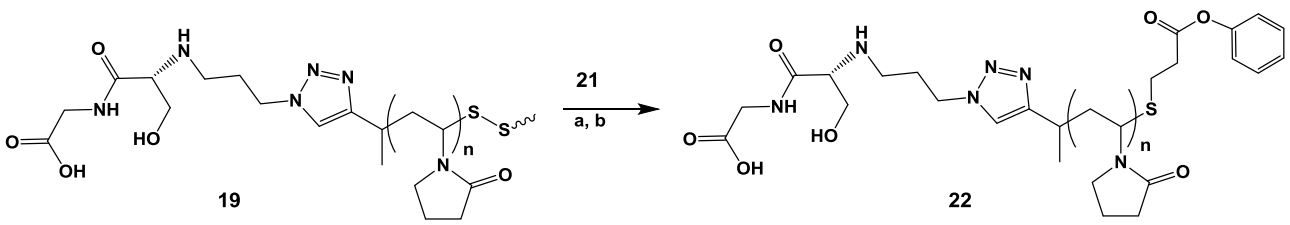

Scheme 5.3: Thiol-ene Michael addition between 19 and 21; (a) TCEP, ethylene diamine, DMF, rt, 24 h, (b) $NaBH_4$, triethylamine, DMF, rt 24 h

According to Scales *et al.*, it was possible to use as much as 150 times excess of the reducing agent TCEP in the conjugation of maleimide functionalised pyrene to poly(*N*-isopropyl-acrylamide)

disulphide chains.[19] In order to catalyse the Michael addition, they added ethylene diamine. Similar conditions were applied to conjugate PVP **19** to phenyl acrylate **21**.

After employing TCEP as the reducing agent and ethylene diamine as the catalyst for the thiol-ene Michael addition, ^{1}H NMR analysis (not shown) indicated the appearance of peaks that could not be accounted for suggesting that there were side reactions involved. Li *et al.* reported that phosphine based compounds are very reactive catalysts for thiol-ene Michael addition reactions. Moreover, in the presence of phosphine based compounds, there is nucleophilic addition of phosphine to the vinyl group.[20] Li *et al.* again showed the thiol-ene Michael addition reaction involving 3-mercaptopropionic acid (3-MPA) did not exceed 50 % conversion even after 4 days of reaction. This was attributed to the presence of the carboxylic acid functionality that resulted in potential enolate quenching and subsequent non-generation of the thiolate. According to Chan *et al.* as a very strong base, with a relatively high pK_a the enolate can abstract a proton from any acidic species in the reaction medium including the thiol, conjugate acid, or protic solvent if present.[21] The above mentioned phenomena could have been responsible for an inefficient thiol-ene Michael addition reaction.

Li *et al.* concluded from their studies of the effects of catalysts that when triethylamine was used as catalyst even in excess amounts, it did not result in any noticeable side reactions. This was because it mechanistically operates differently to primary amines and phosphine based catalysts. Primary amines were found to be appropriate catalysts although they react with the vinyl group and phosphine catalysts provided the fastest rates with the highest amount of side reactions.[20]

Based on these literature findings it was important that TCEP be replaced as the reducing agent since it ultimately served as a reducing agent for the disulphide bridges as well as a catalyst for the thiol-ene Michael addition reaction. It was also important that ethylene diamine be replaced as a catalyst because of the tendency of primary amines to react with the vinyl group. Moreover conjugates **19** and **20** had carboxylic acid species with the potential of quenching the enolate ion. It was envisioned that the use of triethylamine would solve this problem in two ways; a large excess of triethylamine is not expected to result in the formation of side products and at the same time it would facilitate the capturing of the protons from the carboxylic acid species in the targeting moieties preventing the quenching of the enolate ion in the process.

The introduction of the model ligand proceeded by a method described by Reader *et al.*[18] in which conjugate **19** was reacted with 18 times excess of the catalyst, triethylamine, 10 times excess of reducing agent $NaBH_4$, and 2 times excess of the model drug, phenyl acrylate. The reaction proceeded for 24 hours at room temperature in DMF: water 1:1.The resultant solution was purified via dialysis (2000 Da MWCO) against water/methanol (1:1) for 2 days and water for an additional day and

subsequently freeze dried to obtain a white powder. Formation of the product was confirmed by ^{1}H NMR and is shown in Figure 5.1.

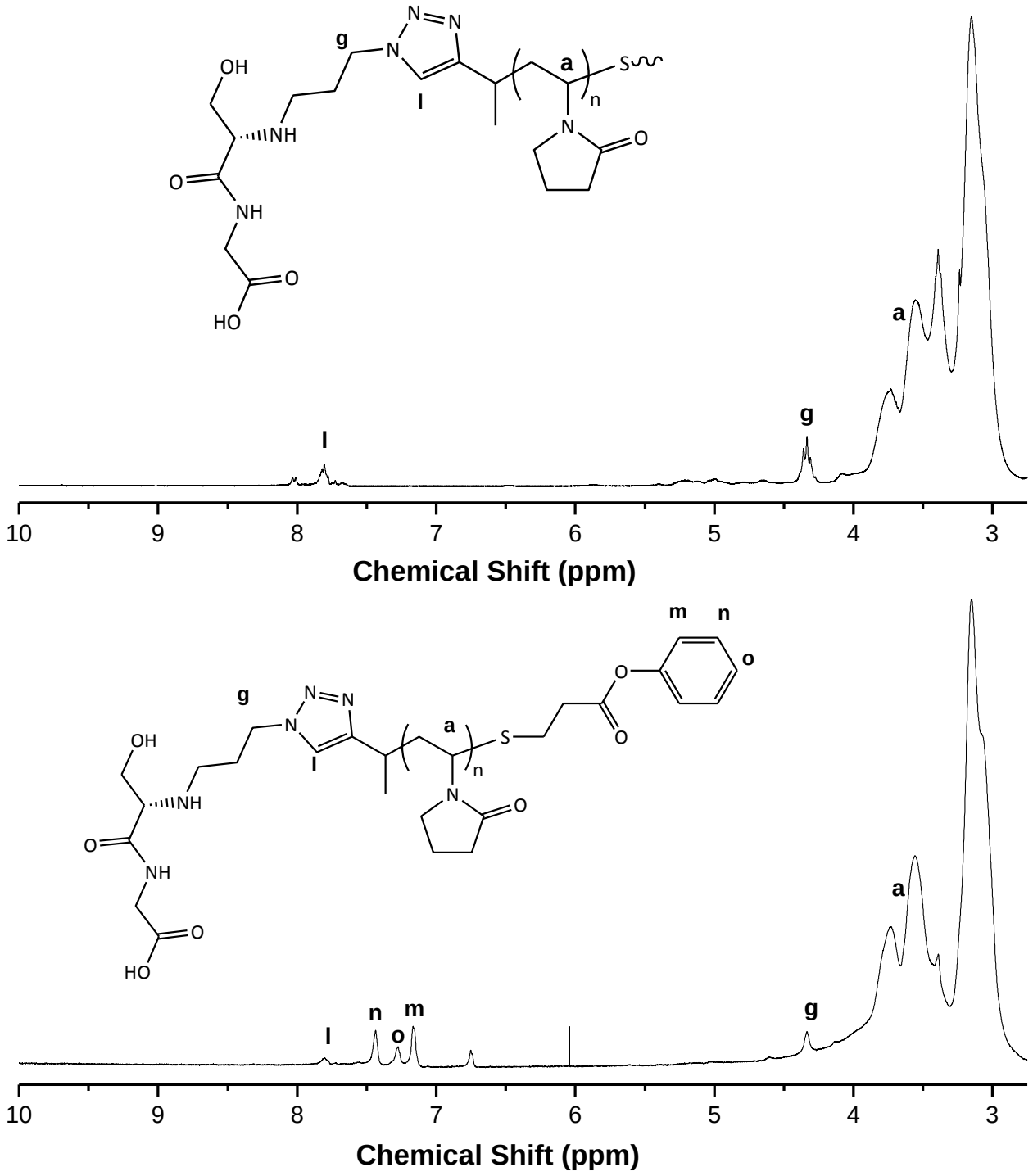

Figure 5.1: Thiol-ene Michael addition between 19 and 21 yielding conjugate 22.

Generally, it is acceptable practice to add a 5 times excess of the acrylate to the thiol to obtain a quantitative ester linkage.[22] However, 2 times excess of **21** was added with respect to **22** to simulate conjugation to an expensive therapeutic payload in which it would be uneconomical to use 5 times excess. Protons **m**, **o** and **n** due to the aromatic functionality integrated at almost 1:1 with respect to

the methylene protons peak **g**. The conversion was deemed acceptable even though a slight excess of phenyl acrylate was used. This was because the excess of the model drug would be removed by dialysis eliminating the possibility of having unconjugated free drug that can result in potential toxicity towards healthy mammalian tissue.

5.3 Tyrothricin and antimicrobial/anticancer peptide

Tyrothricin is a mixture of 28 different cyclic non-ribosomal produced tyrocidines (Trcs) and tryptocidines (Tpcs) and 9 ribosomal produced linear gramicidines (gramicidin D)[23] produced by *Brevibacillus parabrevis*, now known as *Bacillus aneurinolyticus and B. Brevis*, a Gram-positive bacterium found in soil.[24] In the mid-20th century during the Second World War, a peptide complex, tyrothricin containing the Trcs and gramicidins, were prepared from bacterial cultures and were found to be antagonistic against a selection of microorganisms.[25] Since then a number of studies on the tyrocidines have shown that they exhibit activity against various other organisms such as the food pathogen *Listeria monocytogenes*,[26-27] filamentous fungi[28] and the pathogenic biofilm forming yeast *Candida albicans*.[29]

Rautenbach *et al.*[30] established that the six major Trcs exhibit potent and selective antimalarial activity against *Plasmodium falciparum*, one of the causative parasites in malaria that is linked to high mortality. The IC_{50}s (peptide concentration resulting in 50 % inhibition) of the tyrocidines were found to between 5 and 500 nM, which is on par with drugs like chloroquine and like. From these studies it was observed that the Trc caused an inhibition of the intracellular parasite development and a stunted life cycle. Recent studies have shown that some of the Trcs are potent against cancerous cells in particular against prostate cancer immortal cell lines (personal communication M. Rautenbach).

In working with tyrothricin it was necessary to be able to differentiate between the chemical structures/composition of the major peptides and their analogues. Tyrocidines (Trc) and tryptocidine (Trp) are a mixture of cyclic decapeptides that differ from each other in the 3, 4, and 7 position (Figure 5.2). Tyrocidine B (TrcB) is shown as an example with its variable positions coloured.

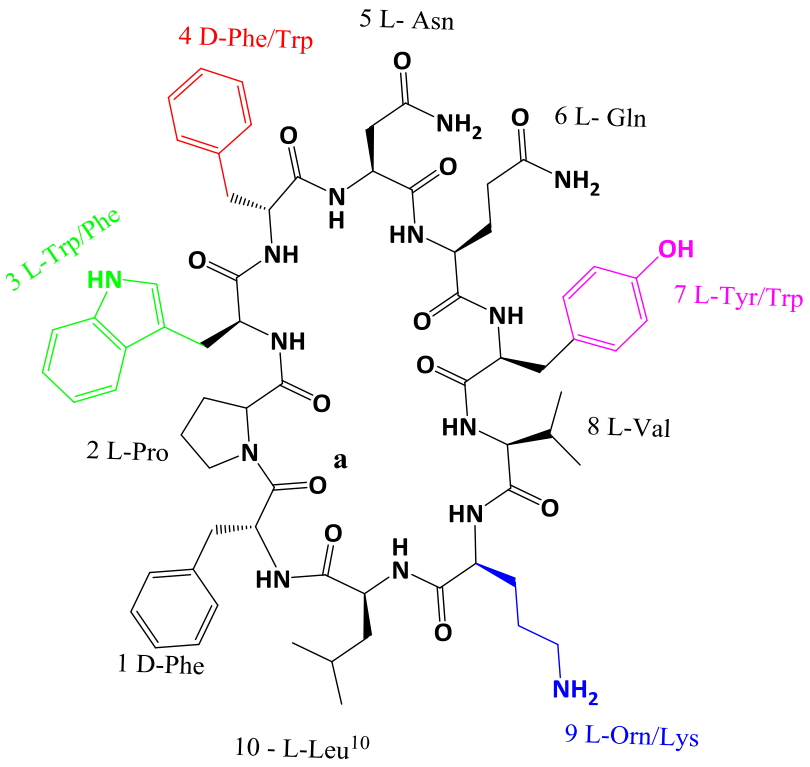

Figure 5.2: Primary structure for Trc B, one of the cyclic decapetide in the tyrothricin complex. The variable positions 3, 4, 7 and 9, with the alternative amino acid residues found in the Trc and Tpc analogues. These analogues are summarised in Table 5.1.

Table 5.1: Summary of the tyrocidines and tryptocidines and their analogues

Name	Abbreviation	Position 3	Position 4	Position 7	Position 9
Tyrocidine A	Trc A	L -Phe	L-Phe	L-Tyr	L-Orn
Tyrocidine B	Trc B	L -Trp	L-Phe	L-Tyr	L-Orn
Tyrocidine C	Trc C	L -Trp	L-Trp	L-Tyr	L-Orn
Tyrocidine A_1	Trc A_1	L -Phe	L-Phe	L-Tyr	L-Lys
Tyrocidine B_1	Trc B_1	L -Trp	L-Phe	L-Tyr	L-Lys
Tyrocidine C_1	Trc C_1	L -Trp	L-Trp	L-Tyr	L-Lys
Tryptocidine A	Trp A	L -Phe	L-Phe	L-Trp	L-Orn
Tryptocidine B	Trp B	L -Trp	L-Phe	L-Trp	L-Orn
Tryptocidine C	Trp C	L -Trp	L-Trp	L-Trp	L-Orn
Tryptocidine A_1	Trp A_1	L -Phe	L-Phe	L-Trp	L-Lys
Tryptocidine B_1	Trp B_1	L -Trp	L-Phe	L-Trp	L-Lys
Tryptocidine C_1	Trp C_1	L -Trp	L-Trp	L-Trp	L-Lys

Conventional three-letter abbreviations for amino acids are used, except Orn for ornithine

5.3.1 Tyrothricin analysis and tyrocidine extraction

A tyrothricin extract was obtained from the BIOPEP® peptide group, Stellenbosch University. The tyrocidines were extracted from the commercial tyrothricin peptide complex by washing with a 10 mg/mL acetone-ether (1:1 *v/v*) solvent mixture. This was done to obtain linear gramicidin-free (VGA) cyclic decapeptide preparation. Although it has been shown to be a potent antimalarial agent,[31] VGA is known to have a haemolytic effect on erythrocytes. Ultra-performance liquid chromatography linked to electrospray mass spectrometry (UPLC-MS), was used to analyse the tyrothricin extract as well as the purified decapeptide preparation, in order to determine the decapeptide profile. (Figure 5.3).

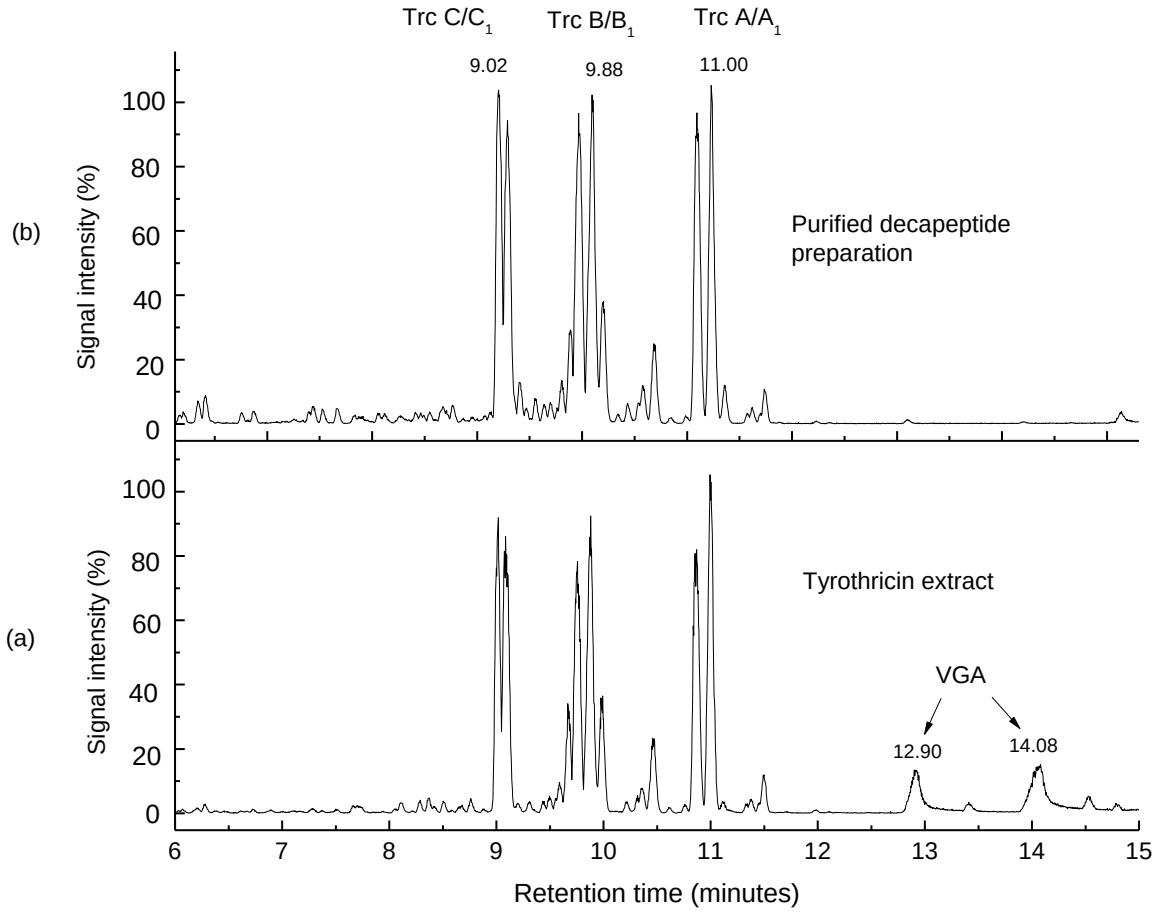

Figure 5.3: UPLC-MS chromatograms depicting tyrothricin extract (a) and the resultant tyrothricin after purification (b)

The chromatographic peaks for Trc C/C_1, B/B_1 and A/A_1 elute closely together as pairs. This is attributed to the Trc analogues containing either an L-Orn or L-Lys on position 9. The second group of pairs appearing in between three major peak pairs is attributed to the Tpcs that result from the presence of Trp instead of Tyr on position number 7 of the cyclic decapeptides.

Table 5.2: Retention times, and molecular weights of the tyrocidines (C, B and A)

Abbreviation	Retention time (minutes)	Major m/z detected	M_r experimental (M_r theoretical)
Trc C	9.02	673.8293	1347.6716 (1347.6764)
Trc B	9.88	661.3304	1308.6533 (1308.6554)
Trc A	11.00	641.8210	1270.6436 (1269.6546)
VGA	12.90	929.5186	1881.0051 (1881.0784)

5.3.2 Acrylate modification of tyrocidine

It was decided that the cyclic decapeptide preparation would be conjugated to the polymer drug delivery system using the same chemistry developed during the model drug conjugations. In order to selectively couple the tyrocidines to the PVP system, it was necessary to introduce an acrylate functionality onto the peptides. It is well known that acrylates can be introduced on to hydroxyl and amine functionalities. The hydroxyl functionality of L-Tyr is present only in the Trcs and not Tpcs. However, a primary amine functionality is present in both Trcs and Tpcs on residue 9 which is either an L-Orn or L-Lys residue in the respective analogues (refer to Table 5.1).

Taking into account that the reaction could take place on two points, two methods were employed to target the hydroxyl on tyrosine and the primary amines of L-Lys and L-Orn. Acryloyl chloride was chosen to introduce acrylate on to the Tyr. In the case of modification of the primary amines, acryloyl chloride was initially reacted with *N*-hydroxysuccinimide to yield *N*-succinimidyl acrylate. The resultant activated ester was reacted with the purified tyrothricin extract to target the primary amines (Scheme 5.4).

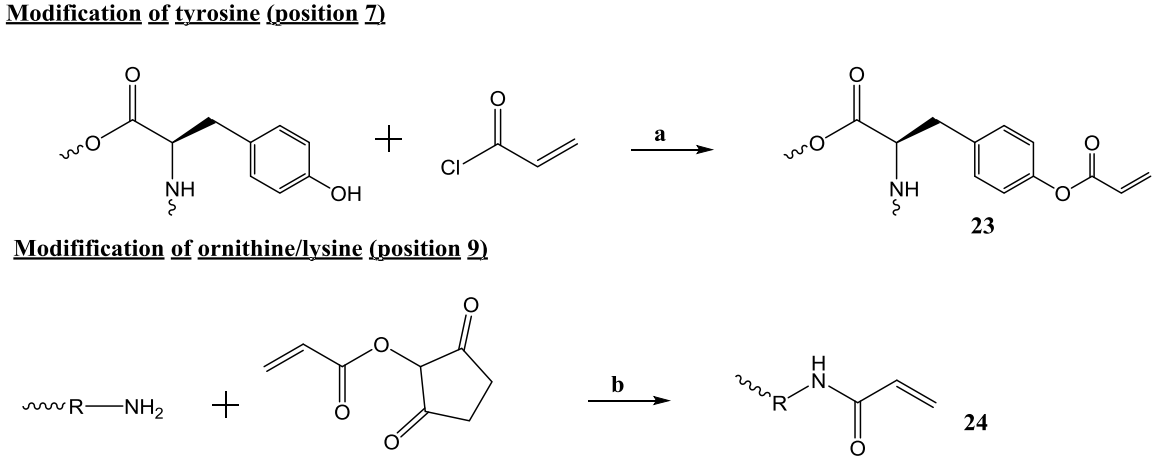

Scheme 5.4: Synthesis of modified tyrocidines; (a) DIPEA, DMF, 0 °C – r.t 48 h, (b) TEA, DMF, 0 °C – r.t, 24 h.

Tyrocidines are known to aggregate in solution even though the molecular interactions during this process are not fully understood.[32-33] It is important that this phenomenon be suppressed during the acrylate modification reactions since it would limit the number of available reaction sites. To prevent this from happening, freshly distilled DMF that was confirmed to be amine free by the Sanger test,[34] was used as the solvent because it is known to be a good solvent for tyrocidines. Twenty times excess of organic base *N*,*N*-diisopropylethylamine (DIPEA) was used in both reactions. A solution of DIPEA and tyrocidine in DMF was added dropwise over 30 minutes to the acrylate bearing compound dissolved in a large excess of DMF at 0 °C. The reaction was allowed to warm to room temperature on its own accord and left to run for 24 hours. DMF was removed by evaporation under reduced pressure. The residue was dissolved in minimal ethanol, precipitated in diethyl ether and centrifuged to obtain a pellet. The precipitation was repeated three times. The resultant pellet was subsequently redissolved in acetonitrile (MeCN) : water (1:1) and freeze dried to obtain acrylate modified tyrocidines, **23**. UPLC-MS was used to analyse compound **23** and **24** Modification using acryloyl chloride targeting tyrosine to synthesize **23** showed very little success and in other instances there was no modification at all. The results that are summarised in Figure 5.4 are for the modification that targeted L-Orn and L-Lys to synthesize **24**.

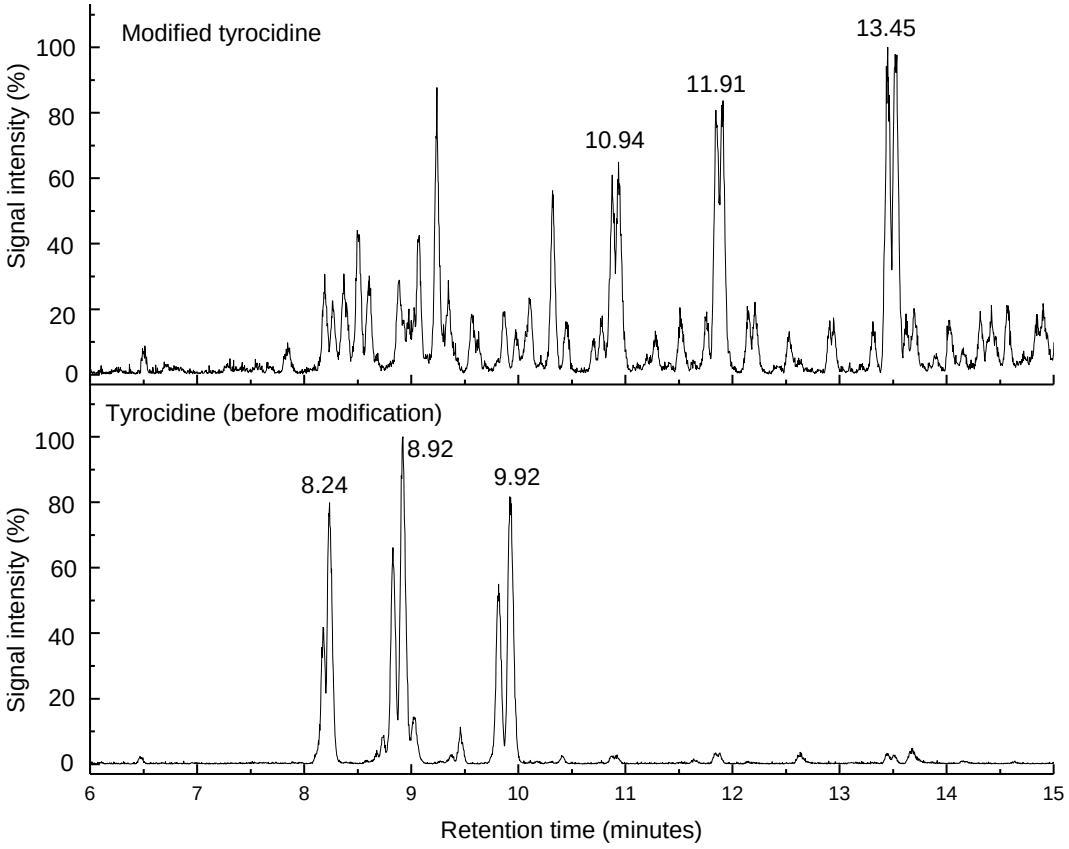

Figure 5.4: Chromatograms showing the tyrocidines before and after acrylate modification.

The elution peaks of the tyrocidines post modification shifted towards higher retention times, due to the formation of acrylamide on L-Orn/ L-Lys. The modified tyrocidine analogues peaks were visible as fronting peaks on each of the 3 main signals at 10.94, 11.91 and 13.45. No gramicidin was present in the modified sample. The retention times, corresponding m/z values and experimentally determined molar masses for the modified tyrocidines and the analogues are summarised in Table 5.3

Table 5.3: Modified tyrocidines and analogues data obtained from UPLC-MS

Abbreviation	Retention time (minutes)	Major m/z detected	M_r experimental (M_r theoretical)
Mod-Trc C_1	10.88	707.8354	1416.6864 (1416.7152)
Mod-Trc C	10.94	700.8303	1402.6803 (1402.6995)
Mod-Trc B_1	11.85	688.3354	1378.6854 (1377.7043)
Mod-Trc B	11.91	681.3254	1363.6748 (1363.6886)
Mod-Trc A_1	13.45	669.3334	1338.6743 (1338.6934)
Mod-Trc A	13.54	662.3198	1324.6625 (1324.6777)

5.3.3 Aggregation of tyrocidines

The concept of dimer formation and aggregation in tyrocidines has been widely reported.[32-33] Having successfully modified the peptides, it was important that this property be retained in the acrylate modified peptides. This is because it is thought to drive self-assembly, which is crucial in the case of polymeric drug delivery systems. To confirm the dimer formation properties of the tyrocidines, the maximum entropy (MaxEnt) calculation was performed on Trc B as well as on modified Trc B. The results are represented in Figure 5.5.

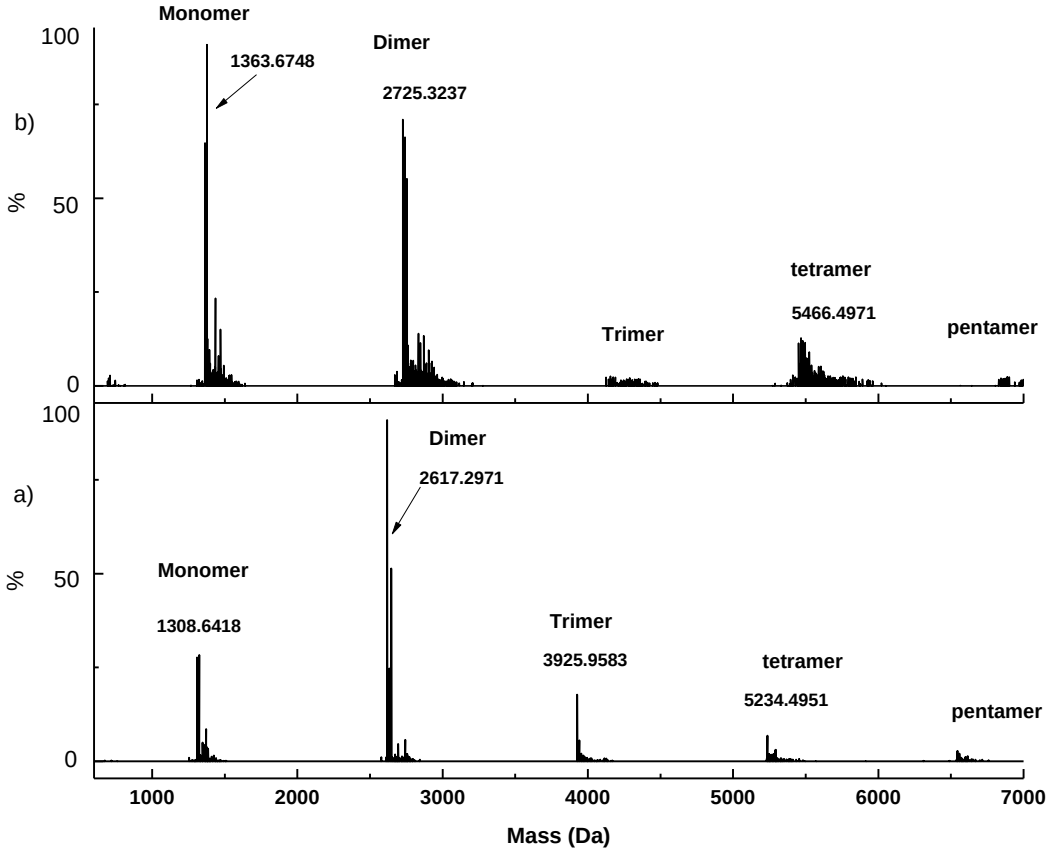

Figure 5.5: Dimer formation of Tyr B as observed via mass spectrometry: (a) calculated mass spectrum for acrylamide modified Tyr B, (b) calculated mass spectrum for Tyr B.

From the MaxEnt data mono-, di-, tri-, and tetrameric species of Trc B were detected before and after acrylate modification. The dimers were distinct however, a small amount of trimers and tetramers was observed. The conclusion was that although less aggregation was observed for the acrylamide modified Trc B the presence of multiply charged species showed that self-assembly would still be favoured. Similar aggregation trends were observed in Trc A and Trc C.

5.4 Conjugation of tyrocidine to PVP-ligand

PVP-PSMA ligand, **19** was conjugated to acrylate modified tyrocidine using the conditions that were developed during the model conjugations (Scheme 5.5).

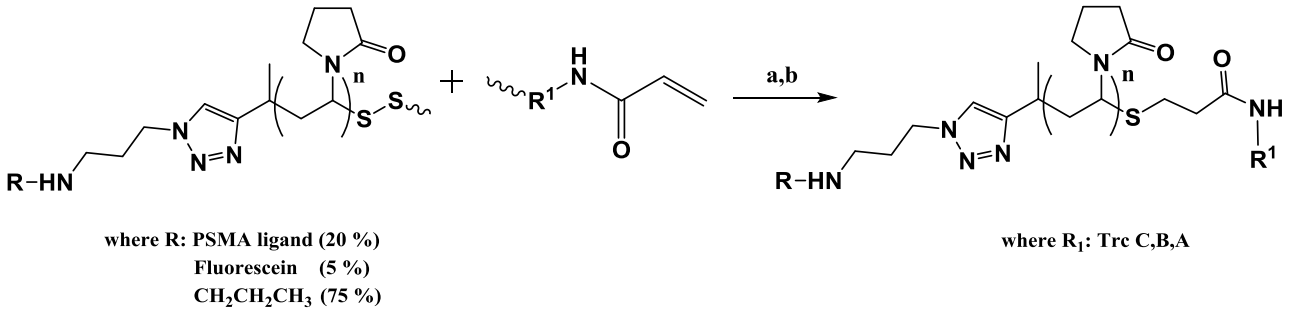

Scheme 5.5: Synthesis of targeting ligand – PVP – tyrocidine conjugate; (a) TCEP, triethylamine, DMF/H_2O, r.t, 24 h, (b) $NaBH_4$, triethylamine, DMF, r.t, 24 h.

19 was dissolved in a minimal amount of DMF/ water (1:1) when TCEP was used as the reducing agent (a) and in 100 % DMF when sodium borohydride was used as the reducing agent (b). Tyrocidines normally aggregate in the presence of water, hence, DMF would be the best solvent. However, TCEP that was meant to be the reducing agent for the disulphide bridges is insoluble in DMF. As a result a DMF/H_2O (1:1) solvent mixture had to be used. A 10 times excess of TCEP solution (0.5 M, pH 7.0) and 20 times excess of triethylamine were added and the solution was placed on a shaker at room temperature for 24 hours. The same ratios were applied when sodium borohydride was employed as the reducing agent.

The huge excess of triethylamine that was used had a twofold purpose. The first, being as a catalyst and the second, to capture protons from all the acidic species in the reaction medium. Unlike in the model conjugation studies where the ligand had one carboxylic acid species, the PSMA ligand has three carboxylic acid functionalities that could have easily affected the thiol-ene Michael addition reaction by quenching the enolate ion (intermediate carbanion). This is because the enolate ion is a strong base and can abstract protons from acidic species in the reaction medium.[21] Furthermore according to Li *et al.* an excess of triethylamine does not necessarily accelerate the rate of reaction but at the same time it does not result in the formation of side products.[20] In the same study, the authors concluded that a huge excess of primary amine resulted in the formation of side products. Hence, for the conjugation, acrylamide modified tyrocidine to PVP – PSMA ligand, it was necessary to employ a large excess of TEA but at the same time allow the reaction to run for a long time. After 24 hours, the solution was dialysed (2000 Da MWCO) against water for two days to remove DMF and unreacted peptide. The resultant solution was freeze dried and conjugate formation was confirmed by ^{1}HNMR analysis (Figure 5.6).

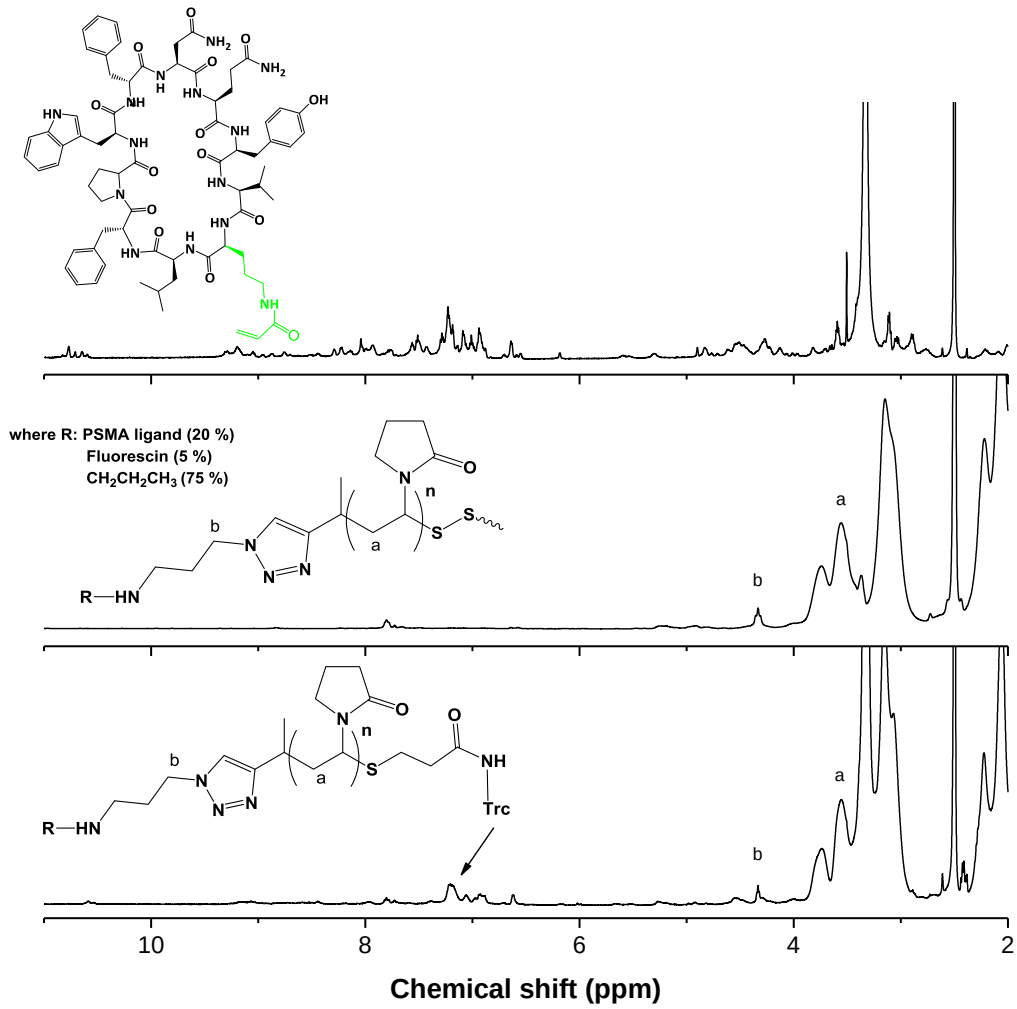

Figure 5.6: ^{1}H NMR spectra comparison of acrylamide modified tyrocidine, PVP – ligand and PVP – ligand – tyrocidine conjugate.

The NMR spectrum of **24** was not assigned, but the polypeptide proton peaks from 6.5 to 11 ppm show that the acrylamide modified tyrocidine was incorporated into **25**. There was a clear distinction between the spectra 19 and 24 in the aromatic region around 7.1 ppm. This again served as evidence of conjugation.

5.5 Particle size analysis

After successful conjugation it was important to do the particle size studies to determine the success of self-assembly and micelle formation. **25** was dissolved in minimal DMF before water was added slowly over 60 minutes through a syringe pump while stirring. The resultant solution was dialysed (2000 Da MWCO) against water for a day. In general micelle sizes could range anywhere between 20 to 200 nm provided there is little aggregation and good size distributions. Dynamic light scattering (DLS) was used to determine the particle size distribution (Figure 5.7).

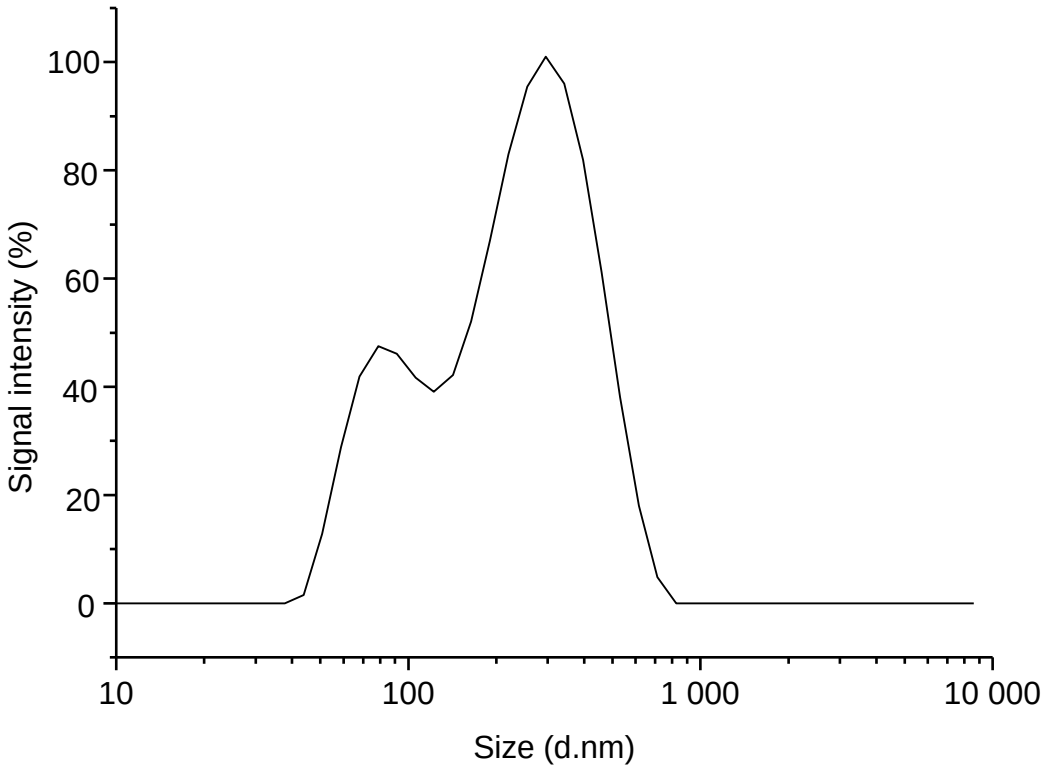

Figure 5.7: DLS size distributions of conjugate 25 (200 µg/mL)

From the DLS results two peaks were observed. This suggested that more than one size distribution was present. Peak 2 had a relative intensity of 25 % with a diameter of 86.4 d.nm and peak 1, with 75 % intensity had a diameter of 298 d.nm. The Z average was determined to be 151 d.nm with a polydispersity index of 0.431. The Z average value was not outside of the expected range, however, a PDI value of 0.431 suggests multiple size distributions. This can be attributed to the high tendency of the tyrocidines to aggregate.

Scanning transmission electron microscopy (STEM) in bright field mode (BF) was used to visualise the distribution of particle sizes. Most particles had sizes slightly above 200 nm. This confirmed the DLS results in which peak 2 an average diameter of 298 d.nm at 75 % intensity with a standard deviation of 124 d.nm. In general it showed the presence of multiple size distributions, as was the case with the DLS results. It was once again attributed to the aggregation of tyrocidines.

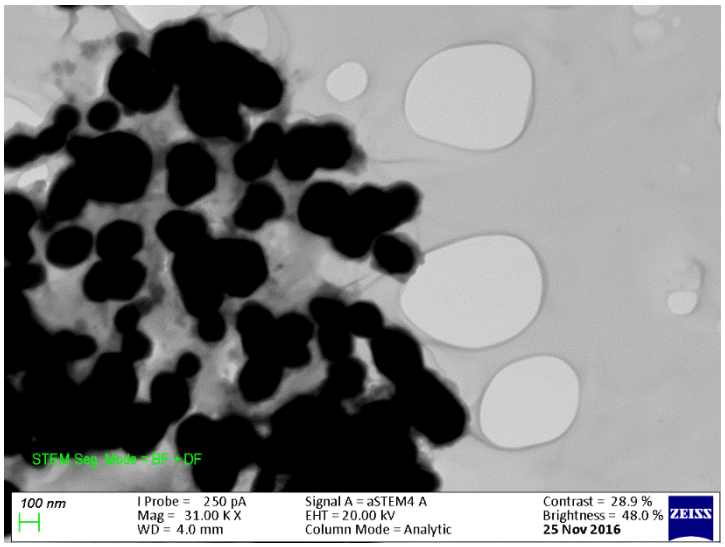

A

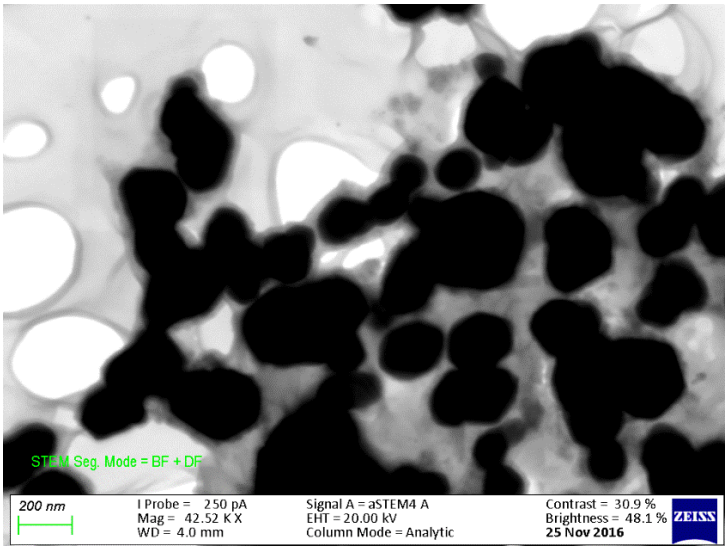

B

Figure 5.8: STEM images of conjugate 25; (A) scale bar is100 nm, (B) scale bar is 200 nm.

5.6 Tyrocidine release studies

Reader *et al.* [18] showed that the β – thiopropionate ester linkage between a model drug and PVP was unstable under acidic conditions and cleaved over 24 hours. This is largely because the thiol destabilises the ester. The initially proposed protocol for the study was to modify the Tyr on position 7 of the Trc with acrylate and subsequently form a β – thiopropionate ester linkage after Michael addition. However, Tyr modification proved to be more challenging than had been anticipated. Since acrylate modification was easily achieved on the L-Lys and L-Orn positions it meant that an amide linkage rather than an ester linkage would be formed. After Michael addition, it was expected that the thiol would destabilise the amide in a similar way that it destabilises the ester linkage in acidic media. This formed the basis of the release studies.

A quantitative study was, therefore, performed on the release of tyrocidine over time via UPLC-MS. A freeze dried sample of conjugate, **25** was dissolved in two formic acid solutions of pH 5.5 and pH 3.0 at 1.2 mg/mL. The solutions were analysed at 40 minute intervals for the first 4 time points before being analysed again after 24 hours via UPLC-MS.

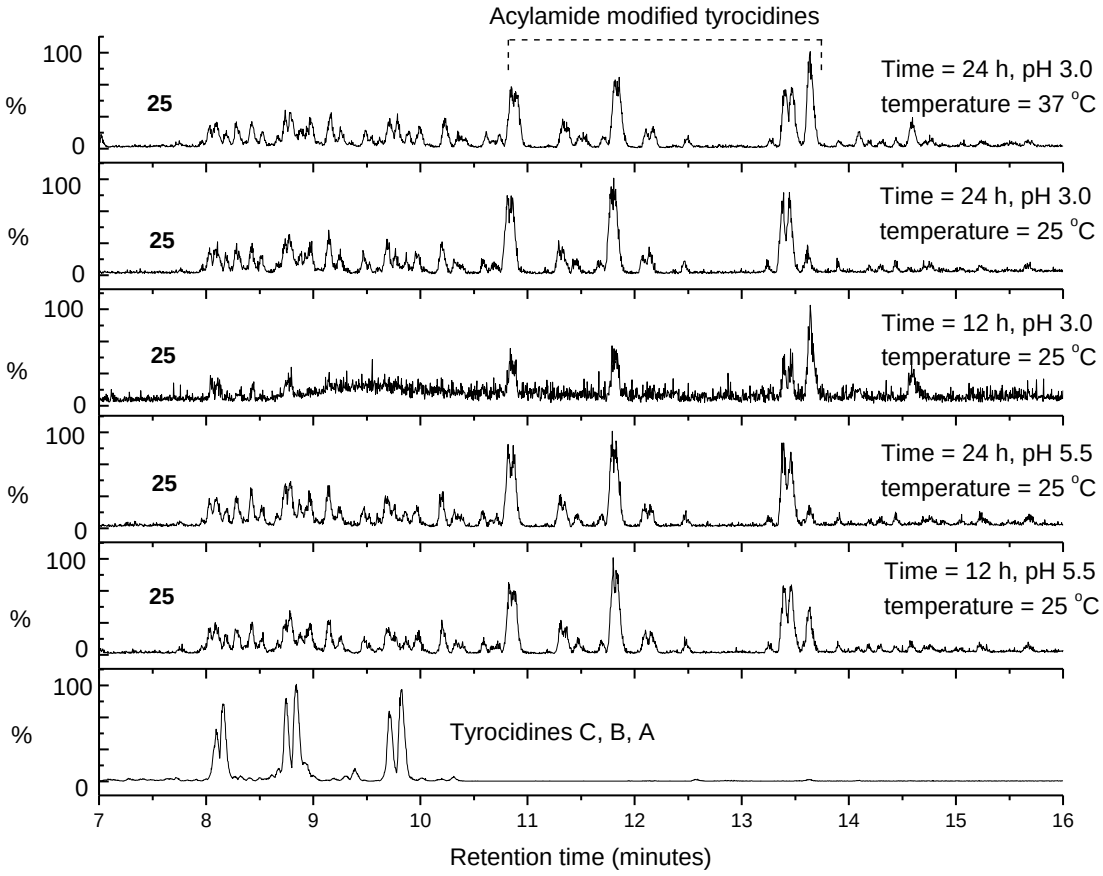

Figure 5.9: Release of tyrocidine from conjugate 24 over time in formic acid solutions (pH = 5.5, pH = 3.0)

Five chromatograms were chosen representing conjugate **25** after 12 and 24 hours of exposure to the formic acid solutions. In all cases, the tyrocidine was not released. Elevating the temperature during exposure to the acid, to 37 °C (physiological temperature) did not aid the release of the drug. The only Trcs that were detected were the acrylamide modified tyrocidines that could have been trapped in micelles and aggregates during conjugation studies. It was concluded that the amide was a much more stable bond. The original hypothesis that the thiol would destabilise the amide in a similar manner it destabilises the ester did not hold. Thus it might be useful to revisit the Tyr modification, as well as explore other avenues around L-Lys and L-Orn modification.

5.7 Conclusion

The conditions for conjugating the model drug to PVP via thiol-ene Michael addition to form a β –thiopropionamide linkage were studied and optimised. Different reducing agents targeting the disulphide bridges and different catalysts for thiol-ene Michael addition were employed before settling on sodium borohydride and triethylamine as reducing agent and catalyst respectively. The acrylamide modification of the tyrocidines was achieved by targeting the L-Lys and L-Orn groups because Tyr modification to synthesize the β–thiopropionate proved to be much more challenging.

Polymer peptide conjugates with the potential to actively target PSMA on prostate cancer cells were successfully synthesised by the protocol developed in the model studies and successful conjugation was confirmed by ^{1}H NMR. The polymer chains were decorated with 20 % of the targeting ligand and 5 % of a fluorescent marker. The resultant conjugates were self-assembled into proposed micellar like structures. The size of the nanoparticles determined by DLS and STEM, showed that the average diameter was ±200 nm, but there were also populations of multiple size distributions that could have been as a result of the aggregation tendencies of the modified Trcs that were trapped and not conjugated.

The release of the Trcs from the conjugate was unfortunately not achieved. It is an area of the drug delivery system that will require further optimisation. After successful synthesis of the conjugate, the release of the drug was not achieved in different acidic solutions. Increasing the temperature did not facilitate the release either. The failure to release was attributed to the stability of the amide linkage compared to the ester which can be destabilised by a β–thioether at low pH. It is important that other mechanisms of drug release from the amide be explored. It is also be vital to achieve the Tyr acrylate modification to yield the acid labile β–thiopropionate ester linkage, as this has previously been found to be a feasible option in delivery of the Trcs into the red blood cell to target the malaria parasite.

5.8 Experimental

5.8.1 General experimental details

Chemicals and solvents used were bought from commercial sources and were generally used without further purification, unless in cases where it was mentioned. Distilled deionised water was obtained from the Millipore Milli-Q purification system and used in all experiments. ^{1}H-NMR and ^{13}C-NMR spectra were recorded on a Varian VXR-Unity (400 MHz) spectrometer. Samples were prepared in deuterated solvents obtained from Cambridge Isotope labs. Chemicals shifts were reported in parts-per-million (ppm), referenced to the residual solvent protons.

Ultra-performance liquid chromatography coupled to electrospray mass spectroscopy (UPLC-MS) was measured on a system that comprised a Waters Acquity Ultra Performance Liquid Chromatograph coupled to a Waters Q-Tof Ultima mass spectrometer fitted with a Z-spray electrospray ionisation source. The system was designed with a Waters UPLC BEH C_{18} column (2.1 × 50 mm, 1.7 µm spherical particles, Millipore-Waters, La Jolla, USA). For experiments that required direct injections and ESMS analysis, 3 µL of the sample solution (±50 ng peptide in 50 % acetonitrile) were injected each time. For UPLC, 1-3 µL of the sample solution (±50 ng peptide in 50 % acetonitrile) was injected each time. Separation was achieved using either 1 % or 0.1 % formic acid (A) to acetonitrile (B) gradient (100 % A for 30 seconds, 0 to 30 % B from 30 to 60 seconds, 30 to 60 % B from 1 to 10 minutes, 60 to 80 % B from 10 to 15 minutes at a flow rate of 300 µL/min), followed by re-equilibration of the column to initial conditions.

Dynamic light scattering (DLS) was performed on a Malvern Instruments ZetaSizer 1000HSa equipped with a He-Ne laser operating at a wavelength of 633 nm and the scattered light was detected at an angle of 90 °. The particle size and distribution was obtained from 3 measurements, each comprising 10 sub-runs. The particle size and distribution were determined using CONTIN analysis and presented as the Z-average particle size.

5.8.2 Synthetic procedures

Phenyl acrylate (**21**): Phenol (3.00 g, 31.9 mmol), triethylamine (3.87 g, 38.3 mmol) and DCM (15 mL) were introduced into a 50 mL round bottom flask and the solution was cooled to 0 °C in an ice bath. Acryloyl chloride (3.46 g, 38.3 mmol) dissolved in DCM (5 mL) was added dropwise over 30 minutes after which the solution was allowed to warm to room temperature and stirred overnight. The solution was washed with water (10 mL × 2), brine (10 mL × 2), dried over magnesium sulphate and concentrated to afford **21** as a dark yellow oil. 4.37 g, 93 %. ^{1}H NMR (400 MHz, $CDCl_3$) δ 7.43 –

7.34 (m, 2H), 7.27 – 7.20 (m, 1H), 7.16 – 7.10 (m, 2H), 6.65 – 6.56 (m, 1H), 6.38 – 6.27 (m, 1H), 6.03 – 5.97 (m, 1H).

General synthesis of model targeting ligand-PVP-drug conjugate (22): A stock solution of triethylamine (83.0 mM) was prepared by dissolving triethylamine (16.0 mg, 166 µmol) in water (20 mL). **20** (22.0 mg, 8.10 µmol), $NaBH_4$ (3.00 mg, 81.0 µmol), triethylamine stock solution (1.75 mL, 146 µmol), **21** (1.2 mg, 8.10 nmol), DMF (1 mL) and H_2O (1 mL) were introduced to a 5 mL pear-shaped flask and the reaction was allowed to stir for 24 hours at room temperature. The solution was purified via dialysis (2000 Da MWCO) against water/MeOH (1:1) for 2 days and water for an additional day. The solution was subsequently freeze-dried and the α- and ω-end-groups were analysed via ^{1}H NMR.

Synthesis of acrylamide-modified tyrocidine (24): A 50 mL round bottom flask was charged with *N*-succinimidyl acrylate (93.7 mg, 0.554 mmol) and DMF (5 mL) and cooled in an ice bath. Tyrocidine (36.0 mg, 27.7 µmol) was dissolved in 45 mL of DMF. To the solution DIPEA (96.8 µL, 0.554 mmol) was added. Tyrocidine and DIPEA in DMF were added dropwise over 30 minutes to the cooled solution of acryloyl chloride in DMF. The reaction was allowed to warm to room temperature on its own accord and allowed to stir for 24 hours at room temperature after which the solution was concentrated. The remaining residue was redissolved in ethanol (500 µL) and precipitated with diethyl ether. The resultant pellet was centrifuged and rewashed twice with diethyl ether. The pellet was dried over nitrogen, dissolved in MeCN : water (1:1) and freeze dried to afford **24** (28.5 mg, 76 %).

General synthesis of PSMA ligand-PVP-tyrocidine conjugate (25): Triethylamine (16.0 mg, 166 µmol) was dissolved in water (20 mL). PVP **20** (13.0 mg, 3.02 µmol), tyrocidine mixture (3.90 mg, 3.02 µmol), TCEP solution (6.0 µL, 30.2 µmol, 0.5 M, pH = 7.0), triethylamine stock solution (0.7 mL, 60.5 µl) and DMF 1.0 mL were introduced into a 50 mL round bottom flask and placed on a shaker at room temperature for 24 hours. The solution was freeze dried. 1.00 mg of the freeze dried sample was dissolved in 200 µL DMF to which 4.8 mL water was introduced over 60 minutes via a syringe pump to drive self-assembly. The solution was purified by dialysis (2000 Da MWCO) against water for two days to afford a milky dispersion, **25**

5.9 References

(1) Mills, J. K.; Needham, D., *Expert Opin. Ther. Pat.* **1999**, 9, 1499.

(2) Kumar, N.; Kumar, P.; Kumar, P.; Kumar, M.; Kumar, R., *J.Drug.Deliv* **2011**, 3, 25.

(3) Allen, T. M.; Cullis, P. R., *Science* **2004**, 303, 1818.

(4) Knop, K.; Hoogenboom, R.; Fischer, D.; Schubert, U. S., *Angew. Chem. Int. Ed.* **2010**, 49, 6288.

(5) Bertrand, N.; Wu, J.; Xu, X.; Kamaly, N.; Farokhzad, O. C., *Adv. Drug Deliv. Rev.* **2014**, 66, 2.

(6) Maeda, H.; Bharate, G. Y.; Daruwalla, J., *Eur. J. Pharm. Biopharm.* **2009**, 71, 409.

(7) Maeda, H.; Wu, J.; Sawa, T.; Matsumura, Y.; Hori, K., *J. Control. Release* **2000**, 65, 271.

(8) Pearce, A. K.; Rolfe, B. E.; Russell, P. J.; Tse, B. W. C.; Whittaker, A. K.; Fuchs, A. V.; Thurecht, K. J., *Polym. Chem.* **2014**, 5, 6932.

(9) Fang, C.; Zhang, M., *J. Control. Release* **2010**, 146, 2.

(10) Cho, K.; Wang, X. U.; Nie, S.; Shin, D. M., *Clin. Cancer Res.* **2008**, 14, 1310.

(11) Wang, Y.-C. J.; Hanson, M. A., *Parenteral formulations of proteins and peptides: stability and stabilizers*. Parenteral Drug Association: **1988**.

(12) Schmaljohann, D., *Adv. Drug Deliv. Rev.* **2006**, 58, 1655.

(13) Kade, M. J.; Burke, D. J.; Hawker, C. J., *Sci., Part A: Polym. Chem.* **2010**, 743.

(14) Gaucher, G.; Dufresne, M.-H.; Sant, V. P.; Kang, N.; Maysinger, D.; Leroux, J.-C., *J. Control. Release* **2005**, 109, 169.

(15) Lee, E. S.; Na, K.; Bae, Y. H., *J. Control. Release* **2003**, 91, 103.

(16) Schmaljohann, D., *Adv. Drug Deliv. Rev.* **2006**, 58, 1655.

(17) Oishi, M.; Sasaki, S.; Nagasaki, Y.; Kataoka, K., *Biomacromolecules* **2003**, 4, 1426.

(18) Reader, P. W.; Pfukwa, R.; Jokonya, S.; Arnott, G. E.; Klumperman, B., *Polym. Chem.* **2016**, 7, 6450.

(19) Scales, C. W.; Convertine, A. J.; McCormick, C. L., *Biomacromolecules* **2006**, 7, 1389.

(20) Li, G.-Z.; Randev, R. K.; Soeriyadi, A. H.; Rees, G.; Boyer, C.; Tong, Z.; Davis, T. P.; Becer, C. R.; Haddleton, D. M., *Polym. Chem.* **2010**, 1, 1196.

(21) Chan, J. W.; Hoyle, C. E.; Lowe, A. B.; Bowman, M., *Macromolecules* **2010**, 43, 6381.

(22) Warren, N. J.; Muise, C.; Stephens, A.; Armes, S. P.; Lewis, A. L., *Langmuir* **2012**, 28, 2928.

(23) Samuelsson, G., In *Stockholm, Sweden*,(5th Edition) Swidish Pharmaceutical press: Stokholm, **2004**; p 620.

(24) Tang, X.-J.; Thibault, P.; Boyd, R. K., *Int. J. Mass Spectrom* **1992**, 122, 153.

(25) Hotchkiss, R. D.; Dubos, R. J., *J. Biol. Chem.* **1941**, 141, 155.

(26) Leussa, A. N. N.; Rautenbach, M., *Chem. Biol. Drug. Des* **2014**, 84, 543.

(27) Spathelf, B. M.; Rautenbach, M., *Bioorg. Med. Chem. Lett.* **2009**, 17, 5541.

(28) Troskie, A. M.; de Beer, A.; Vosloo, J. A.; Jacobs, K.; Rautenbach, M., *Microbiology* **2014**, 160, 2089.

(29) Troskie, A. M.; Rautenbach, M.; Delattin, N.; Vosloo, J. A.; Dathe, M.; Cammue, B. P. A.; Thevissen, K., *Antimicrob. Agents Chemother.* **2014**, 58, 3697.

(30) Rautenbach, M.; Vlok, N. M.; Stander, M.; Hoppe, H. C., *Biochim. Biophys. Acta* **2007**, 1768, 1488.

(31) Otten-Kuipers, M. A.; Franssen, F. F.; Nieuwenhuijs, H.; Overdulve, J. P.; Roelofsen, B.; den Kamp, J. A. O., *Antimicrob. Agents Chemother.* **1997**, 41, 1778.

(32) Munyuki, G.; Jackson, G. E.; Venter, G. A.; Kövér, K. E.; Szilágyi, L.; Rautenbach, M.; Spathelf, B. M.; Bhattacharya, B.; van der Spoel, D., *Biochem. J.* **2013**, 52, 7798.

(33) Ruttenberg, M. A.; King, T. P.; Craig, L. C., *J. Am. Chem. Soc.* **1965**, 87, 4196.

(34) Bhushan, R.; Tanwar, S., *J. Chromatogr. A* **2009**, 1216, 5769.

6 Epilogue

6.1 General conclusions

This thesis is centred on the design of a polymeric drug delivery system targeting prostate cancer. In the work that was previously done in the group, tyrothricin (cyclic decapeptides) conjugated to PVP was shown to actively target *P. falciparum* infected erythrocytes. As a follow up to this work, PVP and tyrothricin drug delivery conjugates targeting PSMA were synthesised. PVP and PSMA ligand were successfully synthesised and conjugated to tyrothricin. The details of the thesis and results of the work are summarised along with some recommended future work.

In **Chapter 1**, the incidence and mortality rates related to cancer were discussed. The shortcomings of current treatment regimens were highlighted and emergence of polymer peptide conjugates as a potential long term solution to cancer therapy was stated. The primary objective of this study was to develop a polymeric drug delivery system targeting prostate cancer by incorporating a targeting moiety, the therapeutic agent (tyrothricin) and a fluorescent marker. In **Chapter 2,** RDRP techniques were introduced and discussed with specific literature examples. Special emphasis was placed on RAFT mediated polymerisation. Different chemistries in the post polymerisation modification of RAFT synthesised polymers were explained. The chapter introduced polymer-protein/peptide conjugates, first by looking into PEG, and then exploring its alternatives, particularly PVP.

Chapter 3 was the first experimental chapter. It presented RAFT mediated polymerisation of *N*VP by employing three RAFT agents. The RAFT agents were evaluated with respect to their control of molecular weight and molecular weight distribution, chain end retention as well the ease of the post-polymerisation modification reactions that followed. α-Acetal, ω-xanthate and α-hydroxyl, ω-xanthate PVP chains were deemed the most suitable to proceed with to further post-polymerisation modifications that were necessary in the development of the prostate cancer theranostic.[1] The third polymer system, α-succinimide, ω-xanthate PVP was deemed unsuitable since there was orthogonality of the chain ends of the system after aminolysis.

Chapter 4 presented results of the study on various means for modification of the alpha chain ends of the two polymer systems, in particular, Schiff base and reductive amination. The alpha-hydroxyl PVP system was oxidised to form the aldehyde. However, the aldehyde signal was deemed too weak, indicative of a low yield of the chain end modification. As a consequence, the polymer was deemed

unsuitable to carry out the Schiff base and reductive amination reaction. The alpha-acetal PVP system was deprotected successfully yielding the required aldehyde functionality. Using this system, the Schiff base and reductive amination reaction were carried out, initially with a model ligand via a suitable *N*-terminus, based on pKa values. Having successfully introduced the model ligand, the synthesis of the PSMA ligand was described in this chapter. It proceeded in a multi-step process that started with L-lysine. The synthesised PSMA ligand was successfully conjugated to the alpha aldehyde PVP system using the conditions that had been described in the model conjugation.

Chapter 5 started by describing the conjugation of the model drug to the model ligand-PVP system. This was done by initially reducing the disulphide bridges on the PVP system followed by thiol-ene Michael addition. The significance of Michael addition was the acid labile β – thiopropionate ester that resulted from this reaction. The different conditions that were employed to optimise the conjugation conditions were clearly outlined in the chapter. After successful conjugation to yield the model drug delivery system, the chapter goes on to describe acrylate modification of tyrothricin (therapeutic agent). The modification was carried out on the tyrosine and ornithine/lysine positions using different conditions that were outlined. However, tyrosine modification was not successful. This meant that the β – thiopropionate ester was not formed. Ornithine/Lysine modification was successful and resulted in a β – thiopropionamide, which was also expected to be acid labile. The conjugation of the tyrothricin to the PVP – PSMA ligand system was carried out by the conditions that had been earlier described during the model conjugations. Successful conjugation was reported by ^{1}H NMR. A description of the self-assembly studies that followed conjugation was given. The resultant micelles were analysed and the particle size was reported by DLS data. The formed micelles were visualised as STEM images. The last part of the chapter described tyrocidine release studies. The release procedure was described, but following analysis, it was concluded that the drug release did not take place. This was tentatively attributed to the stability of amide bond although other factors are still being investigated.

6.2 Perspectives

The results in this thesis highlight the feasibility of developing drug delivery systems through incorporating multiple functionalities into a single unit. However, more work still needs to be done on the conjugates to facilitate good release. As far as the conjugates that were prepared are concerned the following work still needs to be done.

- **Release studies**

The conjugate's failure to release was tentatively attributed to the stability of the amide bond. More work might have to be done to introduce the acrylate through an appropriate β – thiol ester like 2-bromoethyl acrylate (Scheme 6.1).

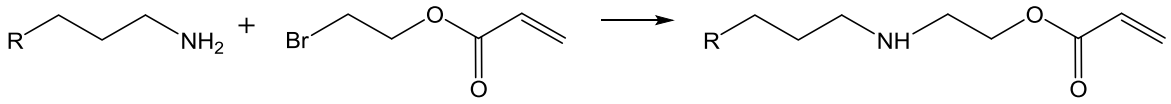

where R: tyrocidines

Scheme 6.1: Proposed modification of the L-Lysine and L-Ornithine residues of tyrocidine

Such a modification strategy would allow for a more destabilised structure that could aid in drug release. The disadvantage of this strategy however is that the released compound will present a modest modification of the active peptide, which need to be assessed in terms of its therapeutic efficacy.

- **Conjugation**

  More characterisation with regards to separation techniques has to be done after the conjugation experiments. The obtained conjugate has to be free of any unmodified peptide before proceeding to do the release studies.

- **Targeting efficiency**

  Having optimised conjugation and release, it would be necessary to determine the targeting efficiency of the PSMA ligand that was synthesised. It has been reported that glutamate urea based ligands are capable of specifically binding to PSMA.[2]

6.3 References

(1) Pearce, A. K.; Rolfe, B. E.; Russell, P. J.; Tse, B. W. C.; Whittaker, A. K.; Fuchs, A. V.; Thurecht, K. J., *Polym. Chem.* **2014**, 5, 6932.

(2) Huang, B.; Otis, J.; Joice, M.; Kotlyar, A.; Thomas, T. P., *Biomacromolecules* **2014**, 15, 915.